INVESTIGATION OF THE CO-PYROLYSIS BETWEEN *SARGASSUM* MACROALGAE AND POLYSTYRENE

by

KETWALEE KOSITKANAWUTH

Presented to the Faculty of the Graduate School of

The University of Texas at Arlington in Partial Fulfillment

of the Requirements

for the Degree of

DOCTOR OF PHILOSOPHY

THE UNIVERSITY OF TEXAS AT ARLINGTON

MAY 2012

ACKNOWLEDGEMENTS

With years at the University of Texas at Arlington, I would like to acknowledge and extend my sincere gratitude to the following people who have assisted and supported me to successfully complete this dissertation. I would like to express my deep appreciation to my supervising professors, Dr. Melanie L. Sattler and Dr. Brian H. Dennis, who guided me on the direction of my research as well as always encouraged and granted me helpful suggestions. Their patience, motivation, and advice is invaluable and unforgettable. My grateful thanks also go to all the committee members: Dr. Chien-Pai Han who instructed on statistic field through his course work and also on my dissertation, and also Dr. Siamak Ardekani, Dr. Hyeok Choi, and Dr. James P. Grover who provided valuable comments.

In addition, this work would not have been possible without a handful colleagues including Siusan Choi for technical support, Dr. Rachaneewan Charoenwat, Dr. Wilaiwan Chanmanee, and Mahir Alrashdan for their time and patient training me in the lab, and all the Crest Lab friends. Also, a special thanks to Mr. Norman Hall, and Mr. Michael Westerfield from Dart Container Corporation as well as Mr. Kevin Koster, Mr. Jim, Mr. Derek Herzog, and Ms. Stacie Talbert from the City of Corpus Christi, Texas, who were willing to assist and provide the materials for this research. I also would like to extend my great appreciation to Wat Buddhamahamunee, Arlington, Texas which provided an area for preparing the sample.

My time during pursuing the Ph.D. degree is fulfilled with warmth and happiness from Dr. Thornchaya Wejrungsikul, Drs. Sulak and Paline Sumitsawan, Pinit and Yajai Ruttanaporamakul, Dr. Suratsavadee Korkua, Dr. Davis Kirachaiwanich, Dr. Surachai

Charoensri, and all friends. With their enthusiasm, encouragement, and valuable friendship, I have been enjoyed the time working toward my degree.

Last but not least I would like to dedicate my gratitude to my beloved family: my dad, Wuttipong, my mom, Wanida, both sisters, Narissara and Chayakan Kositkanawuth, and my dearest grandpa and grandma, Dang and Anong Mala. It would never be enough to demonstrate my heartfelt thanks for their patience, love and understanding during my time spending in school. Their endless support and care is precious and inspires me to pursue a successful path.

April 20, 2012

ABSTRACT

INVESTIGATION OF THE CO-PYROLYSIS BETWEEN

SARGASSUM MACROALGAE AND

POLYSTYRENE

Ketwalee Kositkanawuth, PhD

The University of Texas at Arlington, 2012

Supervising Professors: Melanie L. Sattler and Brian H. Dennis

Biomass is one source of renewable energy which helps minimize greenhouse gas (GHG) emissions, specifically carbon dioxide (CO_2), since biomass utilizes CO_2 via photosynthesis. Various conversion processes are applied to utilize energy from biomass, including pyrolysis. Pyrolysis is a thermal route of decomposing biomass at high temperature without the presence of oxygen. The process generates three main products including bio-oil, residue, and non-condensable gases; however, the most promising product is the biomass oil, which is in liquid form and convenient for handle and transport. Numerous studies on pyrolysis of terrestrial biomass reveal that the crude bio-oil cannot be directly used since it contains high oxygen, resulting in low heating value of the fuel. Consequently, co-pyrolysis between biomass and polymers has been investigated in order to enhance the oil quantity as well as improve its quality.

Not only land biomass can be converted into liquid fuel, but also aquatic species such as macroalgae have recently gained attention since the algae reproduces faster, has a shorter life cycle, and requires less land area. Furthermore, the components in the seaweed are less complex than the land crops, leading to lower thermal stability. However, only a few studies

have been conducted on pyrolysis of macroalgae, and no observations of co-pyrolysis between the algae and polymers have been conducted. Thus, in this study the thermal characteristics of a species of brown macroalgae, *Sargassum*, are first examined by thermogravimetric analysis; then pyrolysis experiment is carried out to evaluate the product distribution and characterization. Moreover, co-pyrolysis of the seaweed and polystyrene (PS) resin is observed to determine advantages of a synergistic effect in the final product.

The pyrolysis and co-pyrolysis were conducted by using a stainless steel pipe reactor with a PID temperature controller with 10^{o}C/min heating rate. Initially, the macroalgae was pyroized under 400-700^{o}C temperature to identify the optimum temperature for the co-pyrolysis, which was 600^{o}C. Then, four different mixture ratios (5%, 15%, 25%, and 33% plastic weight) were subjected to co-pyrolysis under nitrogen. Products were further characterized using various methods. Gas chromatography was applied for both oil and gas products, while elemental analysis was used for oil and solid residue. In addition, the surface area and adsorption capacity of the residue were determined to investigate the potential of using the residue a pollutant adsorbent.

Co-pyrolysis of seaweed and polystyrene improved oil quality by lowering the oxygen content from 9% to 0.3%, while increasing the carbon content from 74% to 89%, compared with oil from seaweed alone, . The interaction between the seaweed and polymer, however, increased water phase product instead of an oil phase. Water elimination of the hydroxyl group in the biomass was a main reaction likely responsible for the higher amount of water and lower oxygen in the oil product. The synergistic effect between the seaweed and PS produces more methane gas, which is beneficial in terms of energy use of the gas. The residue exhibits a low surface area and adsorption capacity; thus, its use as a pollutant adsorbent is not promising. However, it may be able to be used as a fertilizer or soil amendment since it contains significant nitrogen. The lab-scale process provides low overall energy recovery (14-33%) due to heat loss to the effluent gas, phase changes, and a large reactor surface area per volume ratio. Suitable

design of a pilot-scale system could reduce these losses.

TABLE OF CONTENTS

LIST OF ILLUSTRATIONS

LIST OF TABLES

CHAPTER 1

INTRODUCTION

1.1 Introduction

Due to the current energy crisis and increasing fossil fuel prices, renewable energy sources such as wind, solar, hydro, and biomass have gained more attention from researchers and scientists. In addition to increasing sustainability in terms of resources, switching from fossil fuels to renewable energy sources also helps reduce emissions, therefore improving air quality. Specifically, biomass neutralizes carbon dioxide (CO_2) in the atmosphere because it consumes CO_2 via photosynthesis. Several land biomass and fuel crops have been studied as potential sources for sustainable energy. However, the main drawback of fuel crops such as corn, soybean, palm, and sunflower is competition with the food market. Therefore, researchers have started targeting aquatic biomass, especially algae, as a renewable energy source instead of terrestrial biomass. Aquatic biomass poses several advantages in addition to no competition with land needed for food crops. For example, the higher growth rate for many forms of aquatic biomass results in faster mass production. Besides, algae grow in water instead of land; thus, problems associated with land use, such as fertilizer and pesticide pollution of stormwater, are reduced.

Both micro and macro algae can be converted to liquid fuel through pyrolysis, which occurs in the absence of oxygen at high temperature and yields three final products: liquid oil, gas, and solid residue. A main challenge in producing pyrolysis oil from biomass is the high oxygen content of the oil, which results in low calorific value. Consequently, a combination of biomass with synthetic polymers is an option to improve oil quantity and quality, since the polymers are petroleum products, contain less oxygen, and provide comparable high heating value to conventional fossil fuels. In this study, a macroalgae named "*Sargassum*" is initially

pyrolyzed at different temperatures to determine an optimum condition. Later, the algae is mixed with polystyrene resin in various ratios; then “co-pyrolysis” is performed to investigate an interaction or “synergistic effect” between the two materials through product characterizations.

1.2 Research Objectives

A number of studies on biomass pyrolysis have been conducted but mostly concentrated on terrestrial plants such as pine cone, nut shell, agricultural residues, and forest residues. Algae is considered a new generation of biofuel feedstock but not much research has been done in order to analyze bio-oil from algae via pyrolysis. Consequently, the purpose of this research is to study the products from pyrolysis of algae including bio-oil, solid residues, and non-condensable gases. Another interesting feedstock in this study is plastic waste. There is an evidence of a beneficial interaction between terrestrial biomass and polymers in terms of oil quality; thus, it should be worth investigating whether this beneficial interaction also occurs between aquatic biomass and polymers. The research objectives are classified into two parts, based on two main experiments, as discussed below.

1.2.1 Thermogravimetric Analysis (TGA)

1. To investigate thermal characteristics and stability of pyrolysis feedstocks, and determine feedstock composition, including moisture content, volatile organic carbon content, and fixed carbon content.
2. To compare decomposition temperature of feedstocks, including mixtures with various proportions, to determine the influence of mixing ratios on decomposition temperature. Use this information to determine an optimum temperature for pyrolysis.

1.2.2 Pyrolysis

1. To investigate the influence of temperature on pyrolysis product distribution for algae.
2. To observe whether a beneficial interaction between mixed feedstocks exists, in terms of oil quality and quantity.

3. To analyze products from the pyrolysis process including bio-oil, char, and gases. Different methods are applied in this part such as gas chromatography, elemental analysis, and adsorption.
4. To evaluate energy recovery from raw feedstocks to final products by comparing energy input to total energy output.

1.3 Organization of the Dissertation

The organization of the remaining dissertation chapters is as follows:

Chapter 2 reviews previous literature concerning pyrolysis and co-pyrolysis of various biomass and polymers. Moreover, fundamental information associated with thermal behavior and chemical composition is discussed in order to understand the nature of each feedstock.

Chapter 3 describes procedures, instruments, and experimental parameters applied in this study. Initially, feedstock analysis is explained. Next, pyrolysis experiments are described. Finally, details of product analysis for oil, gas, and residue are provided.

Chapter 4 provides results and discussion.

Chapter 5 provides a calculation of energy recovery from the process based on heating value of the feedstocks and products.

Chapter 6 summarizes important results and main conclusions associated with the research objectives. In addition, further studies and recommendations are suggested.

CHAPTER 2

LITERATURE REVIEW

2.1 Introduction

Climate change recently has become a serious issue since it affects the environment in different ways. According to the Intergovernmental Panel on Climate Change (IPCC, 2008), increasing evidence of climate change such as changes in precipitation patterns, increased glacier melting, and rising sea levels has been observed around the world. Due to changes in the hydrologic cycle associated with climate change, increased flash and severe floods occur in some areas, while others experience increased droughts. The main cause of climate change is increased amounts of greenhouse gases (GHGs), such as methane (CH_4), carbon dioxide (CO_2), and nitrous oxide (N_2O), in the atmosphere. These gases have the ability to trap outgoing long-wave radiation from the Earth, leading to increased temperatures. Fossil fuel consumption, including coal, natural gas, and petroleum, in particular releases a significant amount of greenhouse gases into the atmosphere. According to U.S. Energy Information and Administration (EIA, 2011b), the main contributor of GHGs is the industrial sector, contributing approximately 34%, followed by the transportation, commercial, and residential sectors, which contribute 28%, 20%, and 18%, respectively. However, if particularly considering CO_2 emissions, the transportation sector emits the largest portion of CO_2, followed by the industrial and residential sectors, while the commercial sector ranks last. Even though a number of air pollution control technologies such as wet scrubbers have been developed to reduce emissions of GHGs, these are costly end-of-pipe solutions. Consequently, scientists and researchers have been developing innovative technologies for producing renewable energy to replace conventional fossil fuels in order to minimize GHGs emissions from the source.

At present, a number of renewable energy sources, such as wind, solar, tidal, biomass, and waste, have gained attention due to environmental benefits. Renewable energy often emits fewer air pollutants and greenhouse gases, compared to fossil fuels. Energy recovery from biomass and waste in particular helps reduce the amount of waste ending up in landfills and incinerators. Renewable energy resources are sustainable for future generations, while fossil fuels will be depleted at some point in the future. Renewable energy also provides both national and local economic benefits. Countries that switch from using conventional fossil fuels to alternative fuels will rely less on imported foreign oil, which helps reduce the nation's financial burden, while improving national security. For local economies, renewable energy helps create job opportunities, especially for researchers and workers to develop technologies and build facilities, respectively (Lev-On, 2009).

Biomass resources include agricultural crops and waste, forest residues, animal manure, aquatic plants, and municipal solid waste (MSW). Energy from biomass can be achieved by direct combustion, which requires no advanced technologies, compared with other alternative energy resources such as solar, wind, and tidal energy. According to Demirbas (2005), use of biomass energy around the world is approximately 14%, which is comparable to gas, electricity, and coal consumption. Especially in developing countries such as Africa and Asia, regional biomass energy consumption is accounted for 35%. Therefore, Demirbas addressed the potential of biomass as a cost-effective and sustainable energy resource in the future based on availability and environmental benefit. Based on U.S. EIA (2011a), renewable energy consumption has increased from 6.6% in 2006 to 8% in 2010. Biomass is the largest renewable energy resource in the U.S., contributing 50% of the renewable power. Utilizing energy from biomass provides benefits related to environmental impacts. Biomass balances the amount of CO_2 release into the atmosphere with CO_2 consumed via photosynthesis. Therefore, it produces no net increase of CO_2 (Demirbas, 2005). According to the U.S. Department of Energy (2010), GHG emissions can be reduced by as much as 80% by using biofuels from

cellulosic feedstocks, compared to petroleum based fuels. Moreover, sulfur content in biomass is considered negligible, resulting in less sulfur dioxide emissions, which contribute to acid rain problem. Compared to fossil fuels like coal, biomass generates a lesser amount of ash during the combustion process (Demirbas, 2001). As a result, several types of biomass have been extensively studied as potential fuel sources.

2.2 Conversion of Biomass/Waste to Energy

Either biological or thermal conversion is normally used to convert biomass or waste into useful energy sources. For biological conversion, microorganisms have an important role in breaking down complex compounds into smaller fragments. Anaerobic digestion and fermentation are popular processes used to convert biomass into methane and ethanol, respectively. However, biological conversion has several disadvantages. For instance, since microorganisms are quite responsive to environmental conditions such as temperature, pH, and nutrients, the reactor might fail if the operating conditions are suddenly changed. Moreover, biological processes require long conversion times, from several months up to years. McKendry (2002) mentioned that biomass is composed of cellulose, hemicellulose, and lignin, which are all long chain polysaccharides; as a result, fermentation of biomass into ethanol is more complex. Therefore, pretreatment processes using acid or enzymes are required to primarily break down the chains. Shields and Boopathy (2011) used leaves from sugar cane to produce ethanol. In their experiment, 3 grams of the feedstock was initially soaked 24 hours in acid, and then rinsed with distilled water for 3 hours. After that, it was maintained for 15 days for fermentation before they collected the samples. Lin and Tanaka (2006) pointed out challenges in biomass fermentation, mostly involving technologies and enzymes.

Thermal conversion has recently gained more attention because it is much faster than biological processes. In addition, thermal processes can be used to obtain energy from certain wastes, like plastics, which microbes cannot break down. Several thermal conversion processes are carried out to generate energy, such as direct combustion, gasification, pyrolysis, and

liquefaction. Even though all thermal conversions have the same basic concept - using heat input to obtain useful energy/fuel output - the amount of air supply and the form of output energy/fuel for each process are quite different. For direct combustion, an excess amount of air is provided to the process, and then energy is produced in the form of heat. A partial amount of air is fed to gasification, while pyrolysis occurs in an absence of air. Syngas and bio-oil are fuel outputs obtained via gasification and pyrolysis, respectively. The liquefaction process is quite different from the others. Liquefaction can be achieved under wet condition; thus, the feedstock does not have to be dried prior to the process. Similar to pyrolysis, liquefaction also produces a liquid product (Demirbas, 2001).

Among the different thermal conversion processes, Demirbas (2002) illustrated that pyrolysis is the most efficient one, producing energy with high fuel-to-feed ratios. Unlike the gas-phase products of direct combustion and gasification, bio-oil from pyrolysis is in the liquid phase; therefore, it is more convenient to store and transport. In contrast, heat from combustion should be use instantaneously. Pyrolysis takes places in the absence of oxygen, resulting in higher net calorific value gas-phase products (10-20 MJ/Nm^3) than gasification and combustion (4-15 MJ/Nm^3) (Fichtner Consulting Engineers Ltd, 2004). Additionally, pyrolysis can be achieved at lower temperature than combustion and gasification, resulting in less trace heavy metals and dioxin emissions in the gas stream (Astrup and Bilitewski, 2011). Compared to pyrolysis, liquefaction occurs at lower temperature but higher pressure (Demirbas, 2001). However, McKendry (2002) noted that not much attention has been paid to liquefaction due to high cost of liquefaction reactors and fuel-feeding systems. Besides, Zhang et al. (2010) mentioned the need for a catalyst for liquefaction, while a catalyst is unnecessary for pyrolysis. Figure 2.1 depicts different biomass conversion processes.

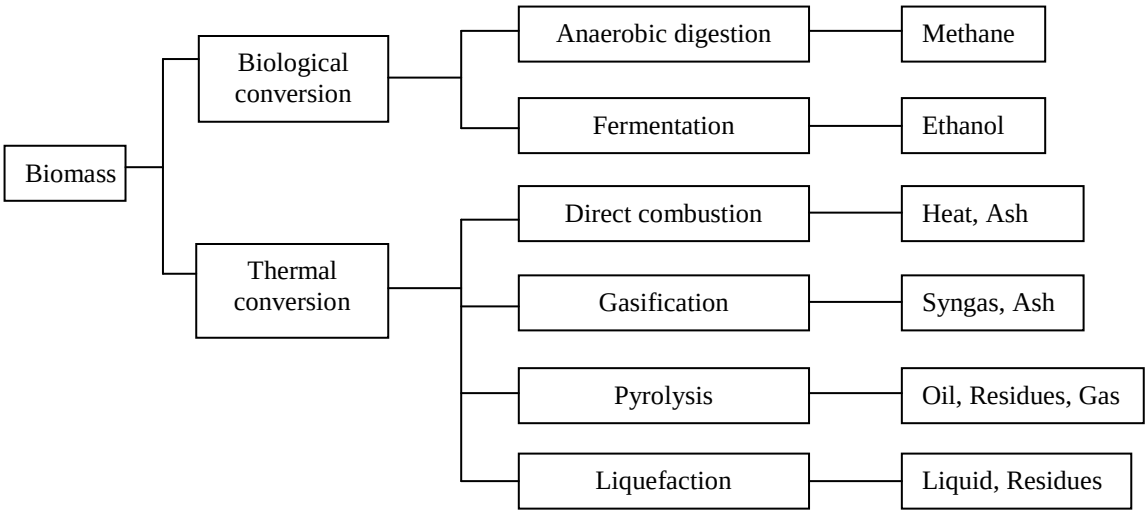

Figure 2.1 Conversion processes for biomass

2.3 Pyrolysis

Pyrolysis is a thermo-degradation process of biomass or waste in the absence of oxygen. It occurs from 400-700oC, and yields three final products: bio-oil (30-75%), residues or char (10-35%), and non-condensable gases (10-35%) such as CO, CO_2, H2, and light hydrocarbons (Balat et al., 2009). From an energy stand point, bio-oil is the most attractive product from pyrolysis, since it can be used as liquid fuel for different purposes, such as combustion in stationary diesel engines and gasification. Nevertheless, bio-oil is still inappropriate for direct transportation use due to its characteristics. Compared to gasoline and diesel fuels, bio-oil has quite a low pH and high viscosity, which can lead to corrosion and severe engine deposition, respectively. Furthermore, the high oxygen content makes its heating value lower than conventional fuels, as shown in Table 2.1. As a result, further upgrading and refining processes such as deoxygenation and hydrotreating are needed to improve the quality of bio-oil (Bridgwater et al., 2002).

Table 2.1 Comparison between bio-oil and heavy fuel properties (Bridgewater et al., 2002 and Walsh, 2004-2006)

Properties	Bio-oil	Gasoline	No.2 Diesel
C (%)	55-58	85-88	84-87
H (%)	5.5-7.0	12-15	16-33
O (%)	35-40	0	0
HHV (MJ/kg)	16-19	43-47	44-46
pH	2.5	N/A	N/A

Bio-oil is also a source of useful chemicals, since the oil contains different compounds, mostly oxygenated, such as carboxylic acids, aldehydes, phenols, alcohols, ketones, and furfurals. These compounds result from degradation of the three main biomass constituents: hemicelluloses, cellulose, and lignin (Bridgewater et al., 2002). Ates and Isikdag (2008) also found a significant amount of aromatics, esters, alkenes, and alkanes existing in bio-oil product. Blasi et al. (2010) observed furfural yield from beech, fir wood, and several agro-industrial residues via pyrolysis; furfural can be used as a binding agent, selective solvent, and adhesive in resin production and petroleum production. The study found a high yield of furfural from feedstocks containing a significant amount of cellulose and pentose, like agro-industrial residues. Levoglucosan and hydroxyacetaldehyde, which can be used for preservation purposes, were notably produced from fir wood feedstock.

Residues and non-condensable gases from pyrolysis are also useful. Moreno-Pirajan et al. (2010) created activated carbon from cow bone residues via pyrolysis, and then studied its adsorption capacity for copper (Cu^{2+}) and lead (Pb^{2+}) ions. The results indicated that cow bone adsorbents could remove metal ions from water. Mullen et al. (2010) also confirmed the use of residues for metal removal from drinking and wastewater. They found that adsorbents made from corn cob and corn stover residues could adsorb up to 50 and 80%, respectively of Cu^{2+}

from solution. The authors also discussed two other options of using pyrolysis residues for soil amendment purposes or renewable solid fuel. Gas products can be circulated back to the process, and thus serve as an additional heating source or fluidizing gas in reactors. Park et al. (2008) suggested that recirculating gas product back to the process helps enhance oil yield, compared with using only inert gas in the system. This agreed with results found by Jung et al. (2008).

2.3.1 Pyrolysis Technologies

National Renewable Energy Laboratory (NREL, 2006) discussed different pyrolysis technologies used in large scale production including fluidized bed, transported bed, rotating cone, ablative, and vacuum, as shown in Figure 2.2. Among those technologies, fluidized bed is considered the most reliable technology, since it has been applied in chemical and petroleum manufacturing for many years. National Energy Technology Laboratory (NETL, 2006) gave examples of various fossil fuel utilization processes achieved by fluidized bed technologies, including transport coal gasification, gasification of low rank coals, sulfur sorbent regeneration, hydrogasification, oxycombustion, and CO_2 capture. Consequently, fluidized bed technology is well understood in operation. Moreover, design and construction are simple, and the technology can be easily scaled up for both experimental and commercial use. A number of pyrolysis research studies have been carried out using this technology with different dimensions and feeding capacities.

Kang et al. (2006) and Lee et al. (2005) conducted pyrolysis of radiata pine and rice straw using a fluidized bed reactor with 154 mm diameter, 616 mm length, and capacity of up to 3 kg/h. Garcia-Perez et al. (2008) designed a smaller reactor with 102 mm internal diameter, 320 mm length, 198 mm conical part for pyrolysis of mallee eucalyptus, and a capacity of 2 kg/h. A bench scale reactor with a capacity of 1 kg/h was applied for pyrolysis of mixed plastic wastes and forest and agricultural residues by Cho et al. (2010) and Oasmaa et al. (2010), respectively. Furthermore, Luo et al. (2004) used a fluidized bed reactor to conduct pyrolysis of

three species of wood biomass and rice straw, using an experimental scale of 80 mm diameter, with varying height between 700-1200 mm, and a capacity of 3 kg/h. Later, they used a larger scale pyrolysis unit, 20kg/h capacity, and considered technology which would be economical at an industrial scale. Finally, they concluded that a larger scale pyrolysis provides a better benefit because the production cost will be decreased.

Similar to fluidized bed, transported bed is also a well understood technology. However, this technology requires additional operation in moving bed media around, since the particle solid media are reheated and recycled back into the process. Moreover, separation of the media and char particles is required, since both are moving together out of the reactor, but only the media will be recirculated back to the process (Bridgewate et al., 1999). Besides, the transported bed reactor requires smaller biomass feed size than the fluidized bed because the circulating system of the media leads to less contact time between the biomass and the media; consequently, size reduction helps enhance heat transfer (NREL, 2006). Therefore, the operating cost is rather high.

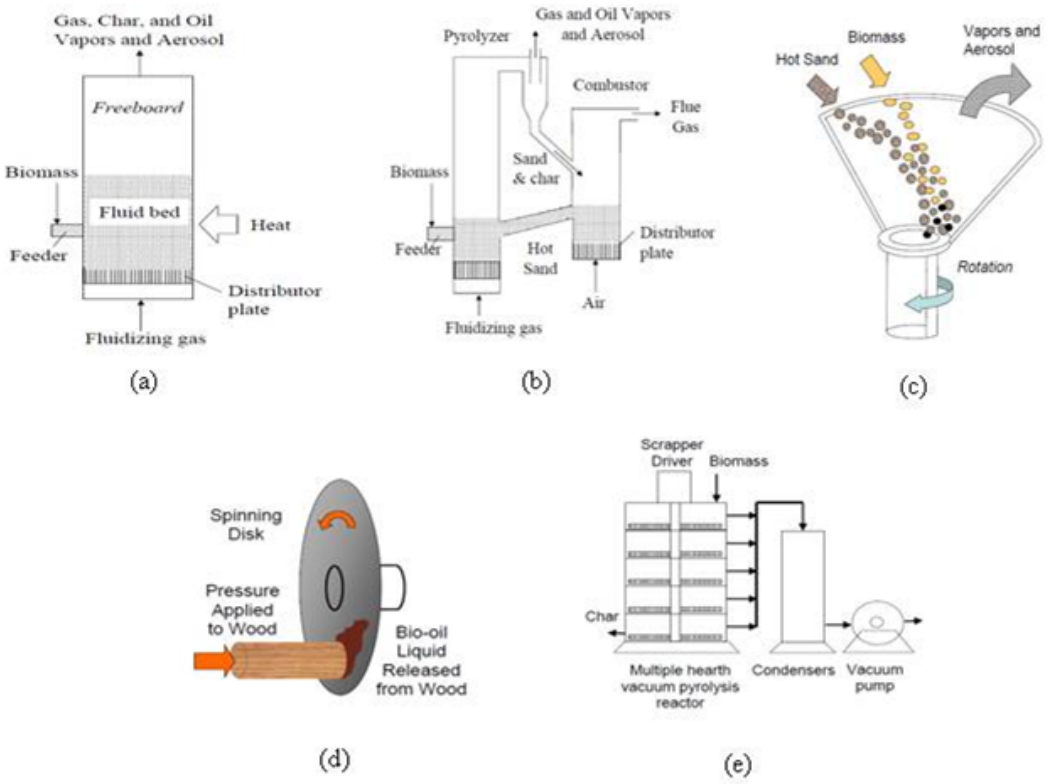

Figure 2.2 Pyrolysis Technologies: (a) Fluidized bed (b) Transported bed (c) Rotating cone (d) Ablative process (e) Vacuum process (Brown and Holmgren, 2000)

In contrast, rotating cone and ablative processes are more complicated than the previous reactors, since these two technologies use centrifugal force as a key driver of the process. The desired velocity of particles must be maintained to achieve optimum centrifugal force for the reactors. Therefore, they are hard to control and design, resulting in high scaling costs (Bridgwater et al., 2002). Westerhout et al. (1998) conducted pyrolysis of mixed plastic waste to evaluate the technology of three different reactor types - fluidized bed, transported bed, and rotating cone - at the same process condition, considering economics. They chose these three reactors based on the following criteria: good heat transfer, high throughput/volume ratio, uniform reactor temperature, and feasibility to scale up. Among these three reactor types, the cost of rotating cone reactor was the most expensive, followed by transported bed, while

fluidized bed reactor was the cheapest. They further compared capital investment for separation units of each process, and again rotating cone showed the highest cost in capital investment. The last technology is vacuum, which has quite high capital and maintenance costs due to vacuum devices. Vacuum conditions should be maintained at all times during the process; thus, a good sealing system is required (NREL, 2006).

In this study, the reactor will be a modified form of fluidized bed technology, with the reactor heated externally. However, the flue gas will not be applied in this study since the system needs to be secured as much as possible to prevent leakage caused by fittings. Additionally, heat loss related to gas convection will also be minimized.

Not only is technology important for pyrolysis, but operating parameters such as temperature, feed size, feed rate, heating rate and residence time also influence the process. These parameters are discussed below.

2.3.2 Pyrolysis Parameters

Numerous studies have been conducted to investigate the effect of pyrolysis parameters on the products' quantity and quality. Heo et al. (2010) studied pyrolysis of waste furniture sawdust under various conditions of temperature, feed size, feed rate, and gas flow rate. The authors found maximum bio-oil yield at 450^{o}C. The yield decreased when the temperature was too low or high since incomplete or secondary decomposition occurred, respectively. For feed size, larger or smaller size could contribute to less oil product due to less heat transfer or overheating of the particles. Both feed rate and gas flow rate affected the vapor residence time inside the reactor. A lower rate provided a longer residence time for oil vapors, allowing them to react further and change into non-condensable gases, resulting in less oil yield. The same conclusions can be found in Park et al. (2008) and Jung et al. (2008), which included experiments to observe the effect of temperature, feed size, and feed rate on pyrolysis of Japanese larch sawdust, rice straw and bamboo sawdust.

Among the above parameters, Heo et al. (2010) and Park et al. (2008) indicated that the most significant parameter affecting characteristics of pyrolysis products is temperature. Garcia-Perez et al. (2008) also stated the importance of temperature on yield and compositions of bio-oil, char, and gases. Additionally, Sensoz and Kaynar (2006) studied the effect of temperature, heating rate, and particle size on pyrolysis of soybean cake. The results showed that particle size had an insignificant effect on product yield, while temperature and heating rate did influence product yields. Similarly, Aguiar et al. (2008) examined the influence of temperature and particle size on pyrolysis of orange peel residues and concluded that temperature has a greater effect on product yields than particle size. Since temperature is a major operating parameter influencing both yield and properties of the products, it is chosen as a factor in this study.

2.4 Feedstocks

Feedstock is a key factor that influences product characteristics because composition varies from one feedstock to another. In this research, two feedstocks, algae and plastic waste, will be studied individually. In addition, co-pyrolysis between both feedstocks will be observed through various mixing ratios and under desired pyrolysis temperatures. Details about feedstocks are discussed below.

2.4.1 Algae

In recent years, algae has become more attractive in terms of alternative fuel sources because it provides several advantages compared to terrestrial plants. Like other land crops, algae derive energy and produces oxygen (O_2) via photosynthesis, using mainly CO_2 and sunlight. Consequently, CO_2 emitted from algal fuel is considered CO_2 neutral since it balances with CO_2 uptake during the algae growing stage. Algae mostly are non food crops; therefore, they will not compete with other uses in the market like other biofuel feedstocks such as corn, palm, and peanut. Unlike other land crops, land availability is not a problem for algae cultivation because algae can grow in marine water, freshwater, or even in wastewater treatment ponds

(Demirbas, 2010). Wang et al. (2010) investigated the feasibility of growing a species of green algae on four wastewater types, including wastewater before primary settling tank, wastewater, after primary settling tank, after activated sludge tank, and from sludge centrifuge. The results showed that the algae could be well adapted in all wastewaters, especially in the fourth wastewater type, due to rich concentrations of nutrient such as nitrogen and phosphorus.

According to Clarens et al. (2010), algae would use at least 3 times less farming area than corn, canola, and switchgrass to meet the annual US energy consumption. Algae grow faster and yield higher oil production per area than seed plants such as corn, soybeans, and peanuts, as shown in Figure 2.3 (Gao et al., 2009). Demirbas (2010) noted that energy produced per hectare from algae can be 30-100 times greater than land crops. Weiss et al. (2010) and Devarenne (2010) studied molecular biology and genetics of a green algae species; they noticed the same chemical components of liquid hydrocarbons derived from the algae as found in gasoline, diesel, and kerosene from petroleum. They suggested that algae are probably a main source of coal and petroleum deposits.

In addition to yielding more oil per acre, algae helps reduce impacts from agricultural activities related to chemical uses such as fertilizers and pesticides. Lardon et al. (2009) compared life cycle impacts of biodiesel from various feedstocks including algae, rapeseed, soybean, and palm. Algae biodiesel showed the lowest impacts on eutrophication and land use because of lesser amounts of pesticide and fertilizer use. Due to the ability of algae to consume nutrients such as nitrogen (N) and phosphorus (P), which are primary reasons for the eutrophication problem, Mahakhant et al. (2010) studied 6 different species of microalgae and found that the algae reduced up to 50% and 90% of nitrogen and phosphorus, respectively, from the water after 14 days. Similar to Wang et al. (2010)'s experiment on growing algae in wastewater, up to 80% and 90% of total nitrogen and phosphorus removal were recorded , respectively.

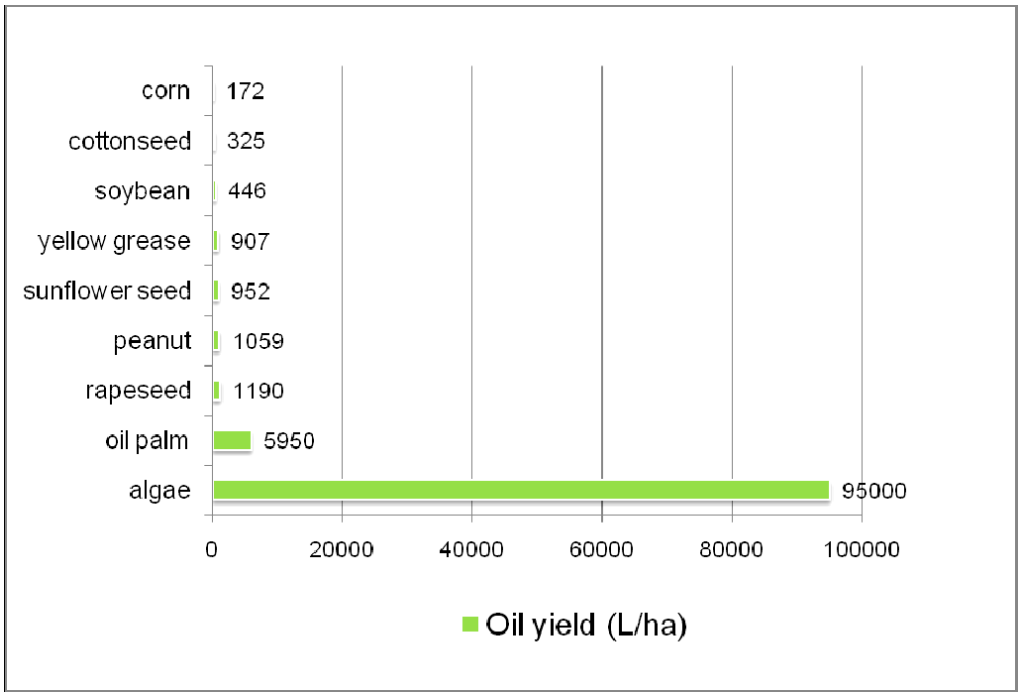

Figure 2.3 Oil Yields of Feedstocks for Biofuel from EarthTrends, 2008 (Gao et al., 2009)

In term of pyrolysis, algae provide some advantages over terrestrial biomass, including lower required temperature and better quality oil. Ross et al. (2008) stated that algae require a lower decomposition temperature compared to woody biomass because of differences in chemical structures. Algae contains mainly protein (30-70%), carbohydrate (10-30%), and lipid (5-20%) (Demirbas, 2010), while the main components of woody biomass are cellulose (40-50%), hemicellulose (25-35%), and lignin (10-40%) (Balat et al., 2009). Peng et al. (2001) investigated pyrolysis characteristics of microalgae under N_2 atmosphere with 15-80^{o}C/min heating rates, and found that the main pyrolysis occurred over the range of 150-560^{o}C. Gani and Naruse (2007) examined pyrolysis behavior of various types of agricultural under N_2 atmosphere with 20^{o}C/min heating rate, and found that pyrolysis started about 200^{o}C and continued until 650^{o}C. Based on these experiments, pyrolysis of biomass starts and finishes later than algae. Demao et al. (2010) also compared decomposition temperatures of different

biomass and algae and confirmed that land plants require higher pyrolysis temperatures than algae.

Table 2.2 Comparison of bio-oil properties from various feedstocks

Properties	Wood	Waste paper	Forest residues/ Straw/Grasses	Microalgae	Microalgae residues
C (%)	55-58	40.80	40-42	61.52	56.13
H (%)	5.5-7.0	6.29	7.5-9.0	8.50	7.63
O (%)	35-40	52.91	50-62	20.19	30.09
Density (kg/L)	1.20	1.20	1.15-1.25	1.16	N/A
Viscosity (kg/m.s)	0.04-0.10	N/A	N/A	0.10	N/A
HHV (MJ/kg)	16-19	13.10	11-17	29	24.4
Authors	Bridgewater et al.	Islam et al.	Oasmaa et al.	Miao et al.	Pan et al.
Year	2002	2005	2010	2004	2010

There is evidence that algae oil has better quality than lignocellulosic biomass oil. As shown in Table 2, the oxygen content of oil produced from algae is lower than that from wood, leading to a higher heating value. Additionally, Miao et al. (2004) noted lower viscosity and density of algae oil, making it more suitable for use.

Not only can fresh algae be used as a feedstock, but algae cake is also a possible feedstock for pyrolysis. Algae cake is algae residue after lipid content is extracted, normally for biodiesel production. Usually, the residue can be further used for farming purposes due to high protein content still in the cells. However, Pan et al. (2010) studied algae oil from microalgae residues after lipid was extracted to produce biodiesel. Still 70% dry weight was left and used in pyrolysis experiments, which yielded up to 31% bio-oil product.

Most research has focused on microalgae pyrolysis due to its faster growth rate and productivity and higher lipid content. However, significant barriers to using microalgae for biofuel exist regarding harvesting and cultivation. Since microalgae are small scale biomass, normally 3-30 μm diameter, they require highly efficient harvesting methods, which depend on species, cell density, and culture conditions, resulting in high capital and operating costs (Carlsson et al., 2007). Demirbas (2010) also pointed out two main drawbacks of biofuel production using microalgae: low biomass concentration and small cell size, both of which increase the cost of harvesting. Besides, it is quite impractical to harvest microalgae from natural sources since it will be time consuming and difficult to distinguish pure species. Consequently, macroalgae, including seaweed, can be another potential choice in biofuel production. Yu et al. (2008) mentioned seaweed, including red, green, and brown kinds, as a possible energy source, especially for coastal areas, due to their benefits of short life cycle and high productivity rate, like other algae. Some studies have been conducted on thermal characteristics of different macroalgae.

Wang et al. (2007) studied pyrolysis behavior of a species of seaweed from China using 20-50^{o}C/min heating rate under N_2 from room temperature to 1200^{o}C. The seaweed started to release volatile materials earlier than wood biomass since the composition of the seaweed is more preferable for pyrolysis than wood. Besides, the seaweed released some heat (exothermic) during the process, which means that the seaweed requires less energy input; wood pyrolysis normally absorbs heat (endothermic). The authors therefore concluded the seaweed can be another energy resource due to its fast growth rate and good thermal behavior. These results agreed with Hui et al. (2011), who investigated pyrolysis characteristics and kinetics of seven marine macroalgae, finding that the good combustion characteristics of the algae make it suitable for use as a pyrolysis feedstock. Moreover, Ross et al. (2008) investigated the thermal behavior of five species of brown seaweed compared to three forms of terrestrial biomass. In characterizing the products, the authors a found lower proportion of

phenolic compounds compared to terrestrial biomass; this could be advantageous, since phenolic compounds pose difficulty in the deoxygenation process needed to upgrade the oil. Most of the previously mentioned studies were conducted by thermogravimetric analysis (TGA) using about 10 mg of sample, but only a few studies have conducted actual pyrolysis on marine macroalgae. Bae et al. (2011) conducted pyrolysis of two brown and one red macroalgae between 300-600^{o}C using 6-8 g of samples; the oil yields were comparable to conventional pyrolysis of land biomass. The oil was characterized by GC-MS and elemental analysis, showing variation of compounds among three algae species. The authors also calculated the heating value of the oil excluding water content, which proved to be comparable to the heating value of oil from wood biomass.

Thus, due to its advantages in terms of productivity and thermal stability, macroalgae is chosen as one feedstock in this study.

2.4.2 Sargassum

Sargassum is a genus of marine brown macroalgae (Phaeophyceae), which is generally found in different parts of the world, including Asia, North America, Australia, and Europe.

Sargassum contains an air bladders structure, which enables it to float. Therefore, the seaweed can quickly travel across oceans and spread out in different regions. Moreover, *Sargassum* can survive in both intertidal and subtidal zones, and in most climate ranges including temperate, subtropical, and tropical (Graham and Wilcox, 2000). Thomas (2002) noted that *Sargassum muticum*, originated in Japan, but can be found widespread from British Columbia to Baja in California, and along the coasts of Britain, France, Scandinavia, and Iberian Peninsula. Davis et al. (2003b) used various *Sargassum* species to observe their metal selectivity, including *Sargassum fluitans* collected at Guanabo Beach of Cuba; *Sargassum siliquosu* and *Sargassum oligocystum* from Goold Island and along the shore of Great Barrier Reef of Australia; and *Sargassum thunbergii* found in Pusan Bay, Korea. Furthermore, Hanta

Andriamanantoanina, and Rinaudo (2010) studied alginate composition of five different brown algae, including two species of *Sargassum* collected from the coasts of Madagascar.

Figure 2.4 *Sargassum* seaweed

Chlorophyll a is a common pigment in all algae including red, green, and brown. For brown algae; carotenoids such as fucoxanthin and β-carotene are also found as pigments which yield yellow-brownish color (Levinton, 1995 and Thomas, 2002). These pigments are useful for photosynthesis since they can capture energy from sunlight at different absorption spectrum ranges. Apart from pigments, seaweed is mainly composed of carbohydrates or proteins, with low amounts of lipid, varying with species and environment. In 2008, Manivannan et al. observed the composition of 12 species of seaweed from the southeast coast of India: 4 species of green, 5 species of brown, and 3 species of red algae. Protein and carbohydrate varied from 3-17% and 20-25%, respectively, while only 1-5% lipid was found. Similarly, Banerjee et al. (2009) examined the biochemical composition of three seaweed species from the Bay of Bengal, India, at six different sampling sites. The authors demonstrated that lipid was the lowest content, ranging from 0.07-1%; next is protein, ranging from 4-14%, while

carbohydrate was the highest, ranging from 20-57%, depending on species and location. Murakami et al. (2011) particularly studied on chemical composition of *Sargassum horneri*; they found carbohydrate to be the primary component in the seaweed, excluding moisture. Carbohydrate is a source of volatile matter that is able to be converted into the fuel.

According to Anastasakis et al. (2011), brown macroalgae is composed of four main carbohydrates, which are alginate, fucoidan laminarin, and mannitol. Alginate and fucoidan are parts of brown algae cell wall, while laminarin and mannitol are storage products (Davis et al., 2003a). Graham and Wilcox (2000) summarized three main components of the algae cell wall are cellulose, alginate, and fucoidan. Like higher plants, cellulose provides structural support, but it is not a major component in the algae, accounting for 1-10% only. In contrast, alginate and its salts are a main component, comprising up to 35-40% of algae. Alginate plays important roles in ion exchange and desiccation prevention (Graham and Wilcox, 2000). Davis et al. (2003b) recorded the yield of alginate extracted from *Sargassum fluitans* and *Sargassum oligocystum* to be 45% and 37%, respectively. In addition, Andriamanantoanina, and Rinaudo (2010) also extracted alginate from five different brown algae including two *Sargassum* species; the results showed that *Sargassum* contain 23-27% alginate, which is 2-3 times higher than other species.

Fucoidan is a sulfated polysaccharide, which can range from 5-20% of algae dry weight; however, there is still no clear explanation of its function (Davis et al., 2003a; Graham and Wilcox, 2000). The other two of carbohydrate forms are mannitol and laminarin, which are products of photosynthesis. Bold and Wynne (1978) and Lewis and Smith (1967) found a wide range of laminarin and mannitol in brown algae: typically 2-34% and 5-25%, respectively. Avad et al. (2009) extracted laminarin and mannitol from two brown seaweed species from Egypt, and recorded that the seaweeds contained about 2-4% laminarin and low mannitol (approximately 1-3%). However, Rioux et al. (2007) detected an extremely low level of laminarin (<0.004%) in their study of three different brown algae from Quebec, Canada. They suggested this might be

due to harvest season as well as the extraction method, which can cause significant differences. Macroalgae also contains a significant amount of halogens, approximately 2-5 %, which is higher than in terrestrial biomass due to the marine environment (A.B. Ross et al., 2009).

Composition of seaweed can vary with season due to changes in the environment. Marinho-Soriano et al. (2006) studied a relationship between composition and environment of red and brown seaweeds from the northwest part of Brazil through one whole year (July 2000 to June 2001). In the study, they analyzed protein, carbohydrate, lipid, fiber, nitrogen, and ash content, as well as recorded rainfall, solar radiation, salinity, and water temperature at the time they collected the samples. The results showed that an increase in light intensity, salinity, and water temperature favors carbohydrate product because sunlight helps promote photosynthetic activity, while the inverse relationship found in protein and ash content. Besides, they noticed a correlation between protein and nitrogen content in both seaweeds. The same conclusion was described in another study conducted by Banerjee et al. (2009) in order to specify the influence of surface water temperature, salinity, and nitrate content on carbohydrate, protein, and lipid contents of two green and one red macroalgae species from Bay of Bengal, India. Marinho-Soriano et al. (2006), however, mentioned that there was no significant variation found in lipid content throughout the year of study, which agrees with the result from Murakami et al. (2011), who investigated the change of composition of *Sargassum horneri* from Fukuoka, Japan, collected from November 2004 to May 2005.

Additionally, Adams et al. (2011) studied the changes of carbohydrate, volatile, metal, and elemental contents (C, H, O, N, and S) of a species of brown macroalgae from United Kingdom through the year of 2008. They found that volatile, carbon, and hydrogen contents had followed the same trend as carbohydrate, which reached a maximum during the summer and began to decrease at the beginning of fall until late spring. On the other hand, they noticed the opposite trend for alkali metal contents: the concentration of Ba, Ca, K, Mg, Na was lowest

during the summer and peaked during spring. Murugaiyan and Sivakumar (2008), however, observed high concentrations of elements such as Na, K, Ca, and Mg during summer due to the high salinity environment when they were studying a correlation between elemental composition and salinity of two brown seaweeds from Gulf of Mannar, India over a year period. Murakami et al. (2011), in contrast, did not observed any significant changes of minerals, including Ca, Mg, and Zn, in *Sargassum horneri* through the year of study. There is no obvious trend for metal contents since other factors can also influence the concentrations. For example, Adams et al. (2011) mentioned that not only environments can shift the metal concentration, but the bioaccumulation capability of seaweed also affects the concentrations.

In general, there are different benefits from macroalgae based on chemical composition. Pena-Rodriguez et al. (2011) cultivated a species of green macroalgae from Mexico, and then conducted chemical analysis for different components such as crude protein, ash, dietary fibers, sugars, amino acids, lipid and fatty acids, carotenoids, and mineral content. They concluded that the algae contains significant amount of high-quality polyunsaturated fatty acids, soluble dietary fiber, carotenoids, and some minerals, which can potentially be used as an ingredient for food or dietary supplement. Anantharaman et al.'s study (2010) also supports this conclusion. The authors studied the mineral contents of 4 green, 2 brown, and 3 red seaweeds from India. Various minerals such as Cr, Fe, Mg, Mn, and Zn were found in levels which are valuable for the food and supplement industries. Moreover, Thomas (2002) talked about pharmaceutical uses of seaweed in cosmetic products and medicines. Brown seaweed in particular has high alginate content, which helps enhance thickening, gelling, and stabilizing process. Therefore, it is very useful in gel industries (Andriamanantoanina and Rinaudo, 2010).

Unfortunately, macroalgae can sometimes cause problems due to their rapid growth rate and reproductive cycle. For example, *Sargassum* deposits along the shoreline of Gulf Mexico, including at Whitecap Beach of the city of Corpus Christi, Texas as depicted in Figure 2.5. The seaweed originally travels with the current ocean but then is trapped inside the Gulf

Mexico. Tons of seaweed are deposited on the shoreline from the early spring until late summer. The seaweed can serve as a food source for native birds; however, with a large amount of seaweed, when it starts to decompose, it releases an unpleasant smell as well as destroys the beach aesthetic for visitors. Moreover, it can block the sea turtles from nesting and impact their egg hatching (Fox, 2008). The city of Corpus Christi has started a beach maintenance program to manage the beach during seaweed season. The current solution is scooping the seaweed and dumping in onto the nearby sand dune; later the seaweed decomposes and becomes fertilizer. However, energy recovery would be a more efficient use of this seaweed. Consequently, this study is conducted to investigate the possibility of utilizing brown seaweed as a renewable energy source.

Figure 2.5 *Sargassum* along Whitecap Beach, the City of Corpus Christi, Texas

The *Sargassum* in this study was collected in early May, and possibly grew in winter to early spring season. Therefore, it likely contains less carbohydrate due to limited sunlight intensity and cold water temperature. As a result, volatile matter would be lower compared to

seaweed that grew in summer. Additionally, a high mineral content is expected in this sample since the seaweed naturally absorbs alkali and alkali earth metals from the sea.

2.4.3 Plastic

Plastic waste is the other feedstock that will be studied. According to the U.S. Environmental Protection Agency (EPA, 2010), plastic waste represents about 12% of municipal solid waste (MSW) and the consumption rate has been increasing rapidly. Recycling programs divide plastic waste into 7 categories, including HDPE (High Density Polyethylene), LDPE (Low Density Polyethylene), PP (Polypropylene), PVC (Polyvinyl Chloride), PET (Polyethylene Terephthalate), PS (Polystyrene), and others. Examples of each resin type are shown in the below table.

Table 2.3 Different categories of plastic resins (Clean Up Australia Ltd., 2009)

#	Resins	Products
1	PET (Polyethylene Terephthalate)	Soft drink, juice and water bottles plus some plastic jars.
2	HDPE (High Density Polyethylene)	Milk bottles, juice bottles, cream containers, bottles for shampoo and cleaners.
3	PVC (Polyvinyl Chloride)	Detergent, shampoo and cordial bottles.
4	LDPE (Low Density Polyethylene)	Garbage bags, garbage bins and recycle bins.
5	PP (Polypropylene)	Straws, microwave ware, plastic-hinged lunch boxes.
6	PS (Polystyrene)	Yogurt Containers, plastic cutlery, foam hot drink cups.
7	Others	All other resins and multiple blend plastic materials.

However, only 7% of the plastic waste was recycled in the US in 2008 (EPA, 2009), while the rest was discarded. In Western Europe, even though up to 50% of plastic waste was collected, only 15% of that was recycled, while the rest was either incinerated or disposed in landfill; that means that overall, only 7.5% of plastic waste was recycled (Williams, 2005). Azapagic et al. (2003) discussed the technical, economical, and quality challenges in recycling plastic waste. Many sorting and recycling technologies are still under development. To scale up the commercial recycling plants, the recovery rate of the wastes should be sufficient to continuously supply the plants; otherwise, the plants will not be cost-effective. Moreover, recycled plastic is considered lower quality compared to virgin materials. It is rather hard to control the quality of recycled materials to meet customers' specifications and requirements because the waste comes from various sources and is possibly contaminated in different ways. Consequently, the recycled plastic can only be used in limited industries. Another difficulty in recycling plastic waste is additive components, including pigments and stabilizers, which may contain heavy metals and harmful substances. Those components will either contaminate the rest of the materials during the recycling process or require advanced processing, resulting in higher capital and operating costs (Azapagic et al., 2003).

Normally, discarded waste ends up either in a landfill or incinerator. Plastic waste is seldom biodegraded; therefore, it would permanently remain in a landfill and may cause groundwater contamination due to chemical and additive components. Lazarevic et al. (2010) pointed out that landfilling is the least preferable method for plastic waste management. Specifically, polystyrene is lightweight and has a low density; therefore, it will occupy large volume in a landfill. Additionally, Gu Ricky et al. (2010) mentioned that polystyrene waste creates a large carbon footprint in being transported to a landfill due to its low density. Polystyrene products mostly contain air; only about 5% of the volume of polystyrene that is loaded onto trucks is actual polystrene. Plastic is originally made from polymers which are petroleum products; hence, it has quite a high heating value, comparable to fossil fuels.

Consequently, energy recovery can be another option for managing discarded plastic waste. Normally, incineration is the traditional thermal treatment used to manage municipal solid waste; however, the process releases a significant amount of emissions, including polycyclic aromatic hydrocarbons (PAH) and dioxins due to oxidizing conditions. Therefore, it requires flue gas cleaning, which can be either wet or dry, using technologies such as fabric filters, scrubbers, and electrostatic precipitators (ESP) (Vehlow and Dalager, 2011). Similarly to incineration, gasification also occurs in the presence of oxygen, which results in emissions. As mentioned earlier, compared to combustion and gasification, pyrolysis yields liquid product, which is more convenient for handling, and less emissions since less oxygen is present during the process.

A number of pyrolysis studies have been conducted using plastic waste as a feedstock and have shown quite high yields of bio-oil with high heating value. Williams and Williams (1999) studied pyrolysis of individual plastics and a plastic mixture simulated from the plastic fraction in MSW of western Europe at 700^{o}C; oil yields of 80, 84, 83, 84 and 75% were reported for HDPE, LDPE, PS, PP and the mixture, respectively. Furthermore, the authors analyzed oil products from all plastic resins and noticed both aliphatic and aromatic compounds in oil products, which have potential use as either fuel or chemical feedstock. Pinto et al. (1999) distilled pyrolysis oil from PS, PP, and PE, and their mixtures, and found that the distillation curves of the oil lie between standard gasoline and gas oil curves; this likely indicates a similarity in oil composition between plastic pyrolysis oil and standard fuels. Onwudili et al. (2009) estimated the heating value of oil products from pyrolysis of LDPE at 450 and 500^{o}C to be 40.4, and 40.2 MJ/kg, respectively, comparable to medium fuel oil. Similarly, Lopez et al. (2010) studied pyrolysis of municipal plastic wastes at 500^{o}C; the authors noted that the oil produced had a high heating value comparable to fossil fuel, which means it would be valuable to use as an alternative fuel.

According to the United Nations Environmental Programme (UNEP, 2009), only PE, PP, and PS are preferred for conversion into liquid fuel, based on following criteria: “feeding

difficulty to conversion equipment, effective conversion into fuel products, and well-controlled combustion and clean flue gas in fuel user facilities". Among those three plastics, PS resin will be used in this study since it has the least percent recycled based on MSW records (EPA, 2008). Most recycling stations do not accept PS waste due to uneconomical recycling cost, and the difficulty in finding markets. Especially, PS containers which have been used for food are more complicated to recycle due to contamination. Interestingly, PS has quite high energy content - approximately 16,000 BTUs per pound, which is twice that of coals (American Chemistry Council, Inc. 2010-2011). Besides, Pinto et al. (1999) found that pyrolysis of PS yielded the highest liquid product and the lowest gas yield compared to PP, PE, and PS under the same optimum conditions. Siddiqui and Redhwi (2009) conducted pyrolysis of individual LDPE, HDPE, PP, PET, and PS at different temperatures (300-500^{o}C). The results showed maximum conversion of PS, which was almost complete, followed by PP and PET; while LDPE and HDPE were the lowest. Moreover, PS pyrolysis produced low gas and no insoluble organic matter. As a result, they applied PS as a plastic base in further study to investigate pyrolysis of mixed plastics at different ratios. Onwudili et al. (2009) studied PS and LDPE pyrolysis between 300-500^{o}C. The results showed that PS produced an insignificant amount of gas, while LDPE produced higher quantities of gas. Moreover, they found that in pyrolysis of a mixture of LDPE and PS, PS influenced LDPE conversion by lowering degradation temperature and increasing oil product compared to either individual plastic. Therefore, PS is chosen as another feedstock in this study.

PS comes from building block of styrene monomer (CH2=CHC6H5) (Biron, 2007) binding together as a long chain polymer as shown in Figure 2.6. PS has been frequently used as packaging or containers in all sectors including residential, commercial, and industrial levels due to several benefits. PS is easy to handle and transport due to its light weight. Moreover, PS is quite durable and hardly decomposes since plastic is water resistant and flame retardant (European Manufacturers of Expanded Polystyrene (EUMEPS), 2002). Biron (2007) also

mentioned the good stability and stress resistance of PS at room temperature, which makes PS able to be used in any occasion.

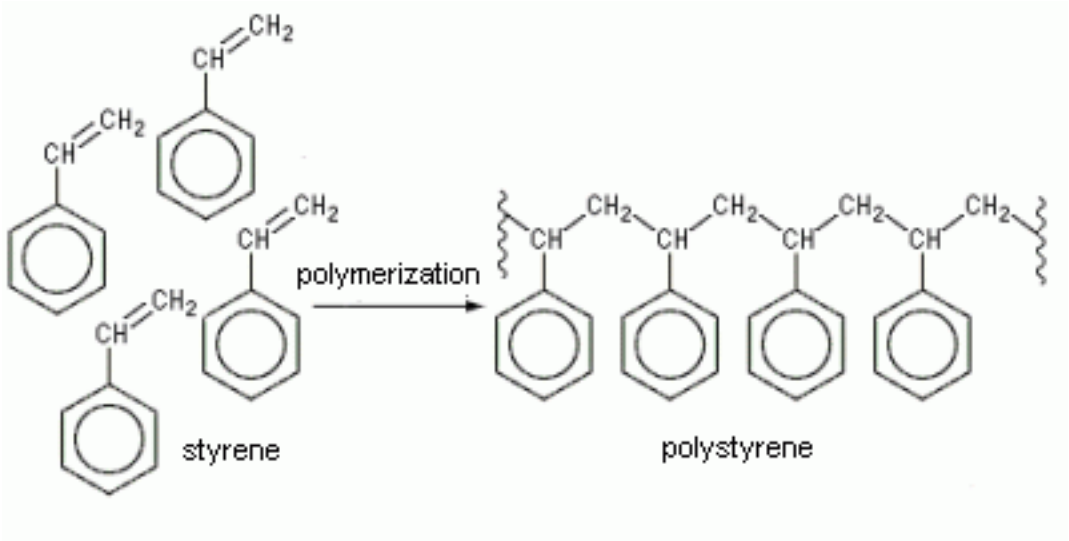

Figure 2.6 Polystyrene chemical structure (Styrotrade, 2004)

The product of PS can be either expandable polystyrene (EPS) or high impact polystyrene (HIPS), depending on the purpose for which it is going to be used. EPS is produced via an expansion process using blowing agents such as pentane. Therefore, EPS contains a high percent of air, resulting in thermal insulation capability (EUMEPS, 2002). Examples of EPS or Styrofoam in our daily life are to-go boxes from restaurants, coffee cups, egg cartons, and packing peanuts, as shown in Figure 2.7(a). PS is processed with rubber in order to produce HIPS, which provides more impact resistance. Yogurt cups, salad bowls, CD cases, and disposable knives, forks, and spoons are typical examples of HIPS products which are commonly used (PSPC Polystyrene Packaging Council (PSPC), accessed 12/09/2011), as shown in Figure 2.7(b).

a)

b)

Figure 2.7 Examples of polystyrene products (a) EPS, (b) HIPS

2.5 Co-Pyrolysis

At present, plastic pyrolysis has become more attractive since researchers have conducted plastic and biomass "co-pyrolysis" in order to enhance oil quantity, rather than using biomass alone. Sharypov et al. (2002) examined co-pyrolysis of wood biomass/synthetic polymers using a 1:1 weight ratio at 400^{o}C and found 2 times higher light liquid yield than expected based on each individual component. This is possibly due to interaction between product from biomass and polymers in the vapor phase, or the so-called "synergistic effect" as mentioned by the authors. Characterization of liquid product then was further studied to confirm the existence of the synergistic effect. Marin et al. (2002) and Sharypov (2003) found a remarkably high content of 2-alkenes, carbonyl, and hydroxyl groups, which could only be resulting from the interaction between biomass and polymers.

Caglar and Aydinli (2009) also studied co-pyrolysis of hazelnut shell and ultra-high molecular weight polyethylene (UHMWPE) at temperatures ranging from 425-650^{o}C. They noticed unusual higher liquid yield as well as gas products at 515^{o}C; they hypothesized that fixed carbon in the biomass was converted into liquid and gas by UHMWPE, resulting in higher liquid yield. In addition, they compared theoretical amounts of products based on pure feedstock with the experimental yield to confirm the interaction effect. Aydini and Caglar (2010) again conducted experiments on co-pyrolysis of hazelnut shell and polyethylene oxide (PEO) to compare with their previous work on UHMWPE using the same condition. Like previous work, the hazelnut shell and PEO blends showed an interaction effect that favored the oil yield; however, it influenced gas yield insignificantly. Moreover, Brebu et al. (2010) investigated the interaction between pine cone and various polymers including PE, PP, and PS in a glass reactor under atmospheric pressure at 500^{o}C; the polymers led to higher oil yield with lower char product. Oil product was further characterized by gas chromatography–mass spectrometry (GC-MS) and elemental analysis to specify oil composition. The authors noted that oil composition varied depending on the type of polymer, which agreed with Rutkowski's

work (2009). Rutkowski analyzed the chemical structure of pyrolysis oil from mixtures of pinewood sawdust with PS and PP at 450^{o}C; he noticed that oil compositions were more comparable to oil produced from each individual polymer with a lower amount of oxygenated compounds due to the influence of polymer addition.

Additional studies confirming the synergistic effect between biomass and polymers were also conducted in order to investigate thermal behavior of the mixtures. In 2006, Zhou et al. (2006) examined co-pyrolysis between pine wood sawdust and HDPE, LDPE, and PP. The experiment was conducted under N_2 atmosphere with temperature increasing from room temperature to 650^{o}C with heating rate of 20^{o}C/min. then, they compared the difference between experimental and theoretical weight loss based on a linear relationship. Approximately 6-12% weight loss was observed at 530-650^{o}C, which demonstrated a synergistic effect at high temperatures. Later, Aboulkas et al. (2008) also found a significant interaction between olive residue and HDPE using thermal gravimetric analysis (TGA). The experiment was carried out from room temperature to 1000^{o}C with different heating rates of 2, 10, 20, and 50^{o}C/min under N_2. They noticed overlapping decomposition curves between two materials, indicating that an interaction between solid-solid or solid-gas probably occurred. Besides, a 7-11% of difference in experimental and theoretical weight loss was observed at around 450-630^{o}C, indicating an obvious synergistic effect was detected at 10^{o}C/min heating rate. Further experiments between olive residue and other plastics including LDPE, PP, and PS were conducted using the same condition in the next year by Aboulkas et al. (2009). The authors confirmed that a significant interaction effect took place in high temperature region around 400-500^{o}C.

2.6 Research Objective

According to the previous discussion, two main feedstocks, *Sargassum* and polystyrene, are chosen for pyrolysis in this study in order to investigate product distribution and whether interaction during co-pyrolysis will influence product quantity and quality, as was found in previous studies for terrestrial biomass.

CHAPTER 3

METHODOLOGY

3.1 Feedstock Preparation

Particle size and moisture can affect pyrolysis efficiency; therefore, these two factors should be controlled to ensure they are consistent in all experiments. The feedstock should be ground and then screened using a proper sieve size which is not too large or small. A particle size that is too large or small affects bio-oil yield. Large particles can reduce the ability of heat to transfer into the particle core, so inside components are unable to be broken down into small fragments. On the other hand, particles that are too small will be overheated and oil vapor might be broken down into non-condensable gases which are unable to condense back into oil (Park et al., 2009 and Heo et al., 2010). Moreover, National Renewable Energy Laboratory (NREL) (2006) noted that additional cost is required to achieve smaller particle sizes. Bridgwater et al. (1999) suggested that the particle size used in pyrolysis can range from < 2 mm up to 6 mm. However, Shen et al. (2009) studied the effect of feed sizes (0.3 – 5.6 mm) on mallee woody biomass and concluded that particle size > 1.5 mm had no influence on oil yield. This also agreed with results from Park et al. (2008), which showed that particle size > 0.7 mm had insignificant effect on product yields. In this study, a larger particle size (3-4 mm) therefore will be used since it will not interfere with the experiments.

Moisture is another factor that should be carefully controlled because excess water in feedstock will consume some heat during pyrolysis for vaporization (NREL, 2006). Additionally, excess water will be present in the final oil product, causing unstable oil and a phase separation problem (Oasmaa and Czernik, 1999). NREL (2006) suggested an acceptable range of moisture content in feedstock of 5-10% weight. Consequently, a drying process was applied to

reduce moisture content from raw feedstock. Feedstock was placed in an oven at about 100 ^{o}C for 24 hours to ensure that the initial water content in feedstock is acceptable.

3.1.1 Plastic

Recycled Styrofoam pellets were provided by Dart Container Corporation which already ranged from 3-4 mm in size, as shown in Figure 3.1 (a). Additionally, some preliminary studies of real Styrofoam wastes such as to-go boxes and coffee cups (Figure 3.1 (b)) were conducted by elemental and thermogravimetric analysis (TGA) to compare the recycled pellets and the actual wastes.

(a)

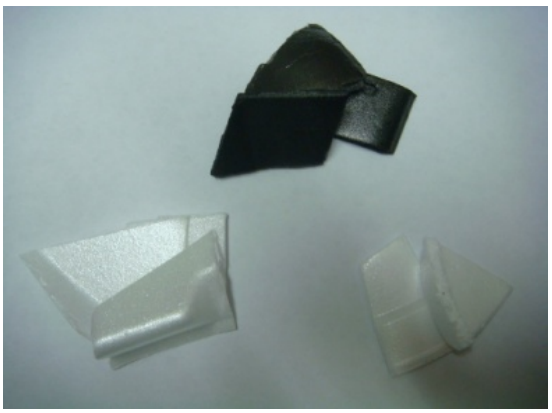

(b)

Figure 3.1 Plastic Feedstock (a) Recycled Styrofoam pellet, (b) Actual Styrofoam wastes

3.1.2 Sargassum

Sargassum was originally collected from Whitecap Beach, Corpus Christi, Texas. First, the sample was pre-washed using tap water to remove sand particles. Then, it was sun-dried for a day; after that, it was placed in an oven at around 100^{o}C overnight to ensure that the moisture dropped below 5%. After that, the sample was ground into small particles, and then sieved using no.4 and no.8 mesh size, with the particle size ranging between 3-4 mm. Then, the seaweed was kept in a vacuum bag to prevent decomposition caused by air and moisture as presented in the following figures.

a)

b)

b)

d)

e)

Figure 3.2 *Sargassum* Preparation Process: (a) *Sargassum* on the beach, (b) Pre-washed to remove sand particles, (c) Sun-dried, (d) After oven-dried, (e) Kept in vacuum bag.

3.1.3. Mixtures

The ratios chosen in this study based on TGA and elemental analysis, which will be discussed in the next chapter, were 5%, 15%, 25%, and 33% plastic by weight mixed with seaweed. Due to a concern about the homogeneity of the mixture, mechanical mixing in the solid phase seemed inappropriate. When the mixture is loaded into a reactor, plastic pellets could settle to the bottom of the reactor due to higher density; then separation of the mixture would likely occur, resulting in a heterogeneous mixture. Consequently, in this study plastic was first soaked in the solvent dichloromethane (DCM) to weaken the polymer chain. A magnetic stirrer was used to provide stirring until the desired weight of plastic completely dissolved in the DCM. A proportional seaweed amount was then soaked in the solution and stirred until well mixed (all the seaweed was coated by plastic solution). Then, the mixture was transferred to the aluminum tray and let dry under the hood overnight, since the boiling point of dichloromethane is quite low (about 40^{o}C). After the mixture completely dried, it was again ground and sieved using the same mesh size as the pure seaweed. The higher percent of plastic in mixture produces a whiter coating on the outside surface of the seaweed, as shown in Figure 3.3 below.

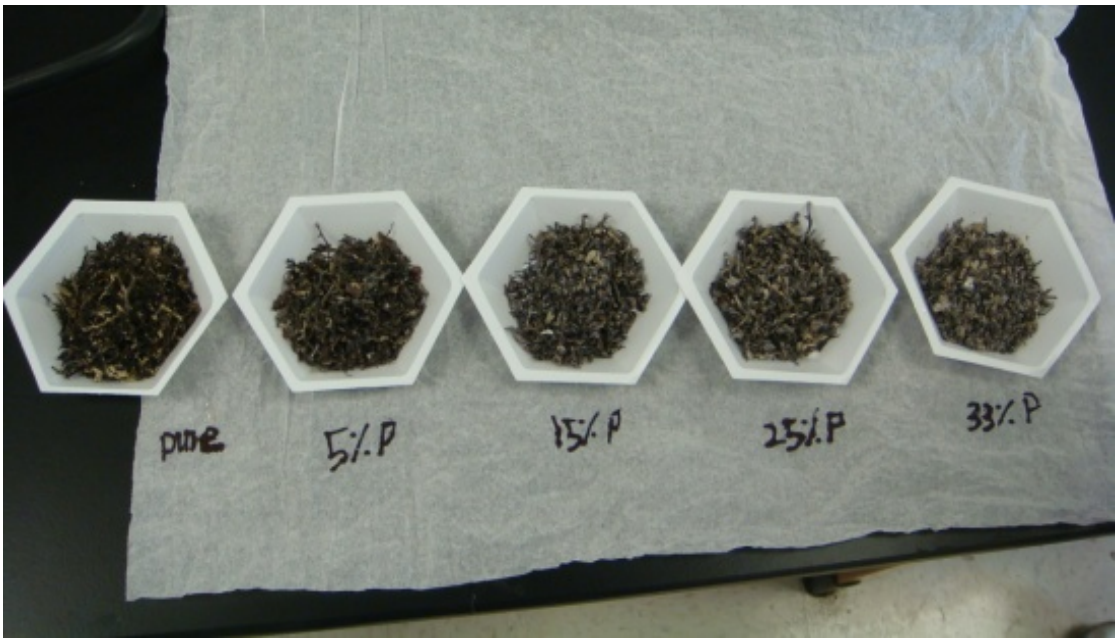

Figure 3.3 Mixtures in different ratios: from left to right pure seaweed, 5% plastic, 15% plastic, 25% plastic, and 33% plastic

3.1.4 Cedar Wood

To have a comparison with another kind of biomass biomass, cedar wood was used in this study to compare the product yield and quality to the seaweed. The wood was obtained from Oklahoma and then ground and sieved into same size, 3-4 mm. Then, it was dried in the oven overnight for moisture control. Figure 3.4 below shows the wood after it was dried.

Figure 3.4 Cedar wood

3.2 Pyrolysis Experiments

Pyrolysis experiments were conducted using the experimental set-up depicted schematically in Figure 3.5. The experimental reactor, with 1-inch inside diameter and 2 foot length, is illustrated in Figure 3.6 (b). The top of the reactor was connected to a steel tube and an elbow fitting for vapor exit (Figure 3.6 (c)). The other end of the reactor was connected to an inside thermocouple, which was used to measure inside temperature.

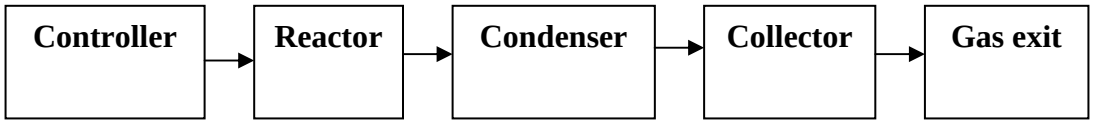

Figure 3.5 Pyrolysis diagram

Once the sample was loaded into the reactor (which was about 70 gram sample for each run), it was purged with N_2 gas for 15 minutes to ensure there was no air inside the reactor. Both ends of the reactor were tightly closed. At the top fitting, some stainless steel wool (Figure 3.6 (a)) was placed to prevent some char or particles from penetrating with the vapor. Then, an outside heater was wrapped around the reactor (Figure 3.6 (b)), and an outside

thermocouple was placed between the heater and the reactor. The reactor again was wrapped with an insulator to prevent heat loss during the process. The reactor was then connected to a control system and heat supply. In this study, the system was controlled by a set of controllers which consisted of an auto proportional–integral–derivative (PID) controller (CN7523, Omega) and a solid state relay, (SSR330DC25, Omega) shown in Figure 3.6 (d) and (e), respectively.

After the set up was done and the experiment started, the heat was provided externally to the reactor through the outside heater. Then the controller automatically controlled power input into the reactor, depending on the desired heating rate and temperature profiles. Based on TGA results of the seaweed, 400-700^{o}C temperatures were applied for pyrolysis. Then, the optimum temperature was later used to study pyrolysis of the mixture under different ratios. Pyrolysis test setup can be seen in Figure 3.7. For each run, the controller was set at a 10^{o}C/min heating rate. At a certain temperature, the sample decomposed and started generating water and oil vapors. The vapor exit of the reactor was connected to a condenser which used water as a cooling liquid; the water temperature was set at 1^{o}C, controlled by recirculating water chiller, as shown in Figure 3.7(c). The vapors traveled through the tubing system and then condensed inside the condenser. The liquid product was collected in the collector flask, while the non-condensable gases exited from the condenser through the bubbling system.

a)

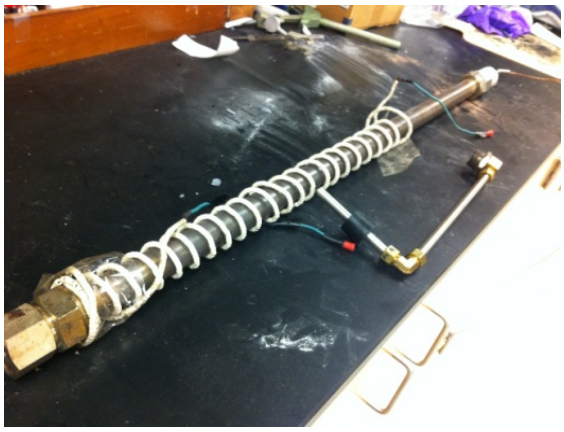

b)

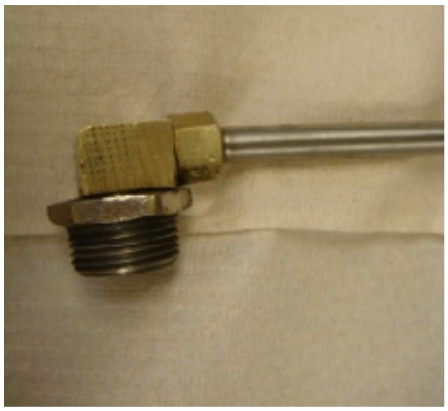

c)

d)

e)

Figure 3.6 Apparatus for pyrolysis experiment (a) Stainless steel wool (b) Reactor with an outside heating wire (c) An elbow fitting connected to the reactor (d) A PID controller (CN7523, Omega) (e) A solid-state relay (SSR330DC25, Omega)

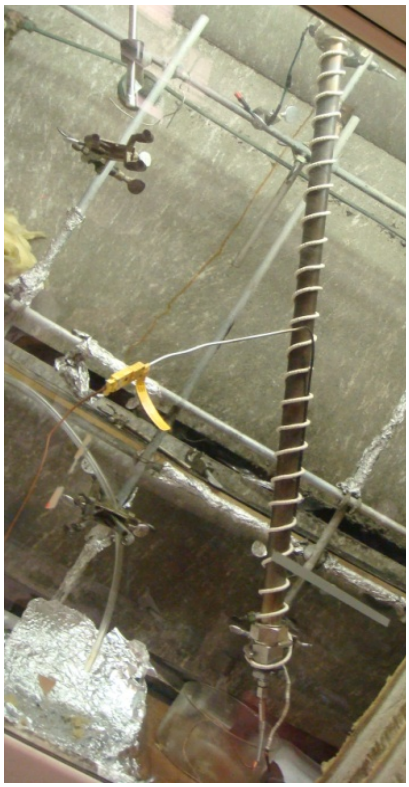

a)

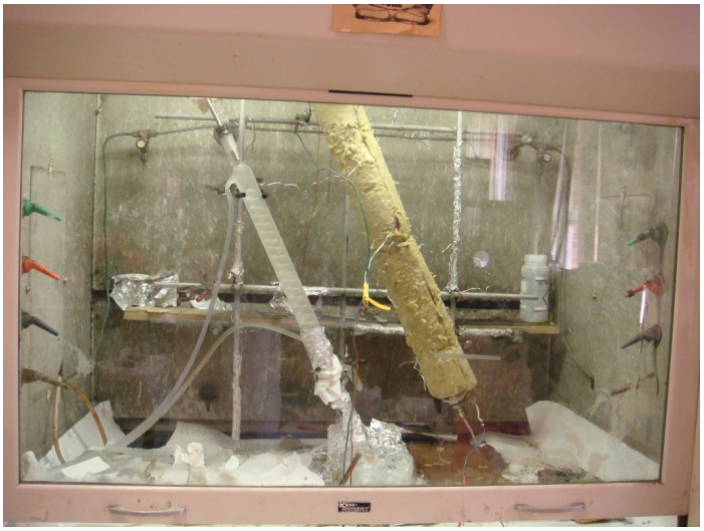

b)

c)

d)

Figure 3.7 Pyrolysis Test Setup (a) Reactor before being wrapped by insulator, (b) Full pyrolysis set-up, (c) Recirculating chiller, (d) Controller and thermocouple reader.

During the experiment, gas product was collected using 1-Liter Zefon Tedlar bags (Figure 3.8). The gas was collected at different three specific times: before the reaction, during the reaction, and after the reaction. Therefore, gas generation over time can be discussed.

a) b)

Figure 3.8 Gas collection set up (a) Gas collection and a bubble flask (b) 1-L tedlar bag and needle

Table 3.1 summarizes the ratios and temperatures use in this study. As mentioned earlier, temperatures and ratios were selected based on the TGA and elemental analysis. The ratios include both pure and mixed feedstocks. The experiment for each condition was performed in triplicate.

Table 3.1 Experimental plan of the research

(1)	(2)	(3)
Feedstock	Ratio by wt.	Temperature, ^{o}C
Algae:Plastic	100:0	400, 500, 600, 700
	95:5	600
	85:15	
	75:25	
	67:33	
	0:100	
Cedar wood		600

3.3 Feedstock Analysis

3.3.1 Elemental Analysis

Elemental analysis is normally applied in order to specify biomass composition including carbon (C), nitrogen (N), and hydrogen (H). In this study, a PerkinElmer 2400 Series II CHNS/O Elemental Analyzer was used to characterize feedstocks (both plastic and algae), oil product, and residue. According to PerkinElmer, Inc. (2005-2010), the machine operates under 4 different zones: combustion, gas control, separation, and detection zone as shown in Figure 3.9. O_2, He, and N_2 gas are required for combustion, carrier gas, and pressurizing the machine, respectively.

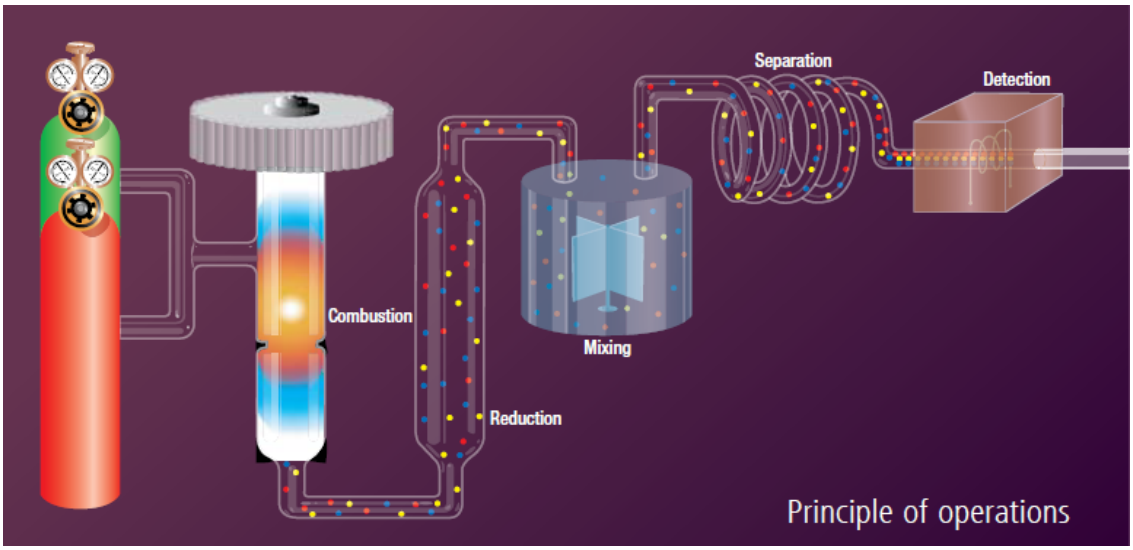

Figure 3.9 Operation diagram for elemental analyzer (PerkinElmer, Inc., 2005-2010)

When the sample is loaded into a sample injector, the sample is completely combusted under an excess of oxygen, resulting in elemental gases such as CO_2, H_2O, and N_2. Then, the gas products travel into the next zone, which is the gas control zone. In this zone, the gases are maintained and mixed at controlled pressure, temperature, and volume, resulting in homogenization of the gases before they are passed to the separation zone, which uses chromatograph technique to separate the compounds. The gases then move to the detection zone, where their concentration is determined using a thermal conductivity detector. The thermal conductivity detector shows the result in terms of stepwise signals, as presented in Figure 3.10, which is more accurate than peak signals (PerkinElmer, Inc., 2005-2010).

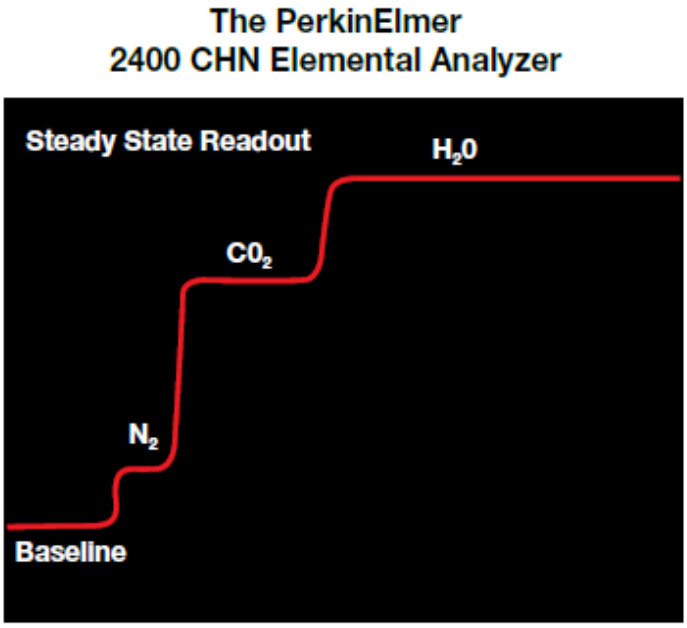

Figure 3.10 Illustration of stepwise changes from elemental analysis (PerkinElmer, Inc., 2005-2010)

In this study, only 2-5 mg of a sample was loaded into a sample container, which can be either a tin cup or tin pan, as shown in Figure 3.11. A tin cup is used for solid samples, including feedstock and residue, while a tin pan is used for liquid samples, which included oil in this study.

a)

b)

Figure 3.11 Sample container for elemental analysis (a) Tin cup, (b) Tin pan

Since elemental analysis is a small scale analysis, a solid sample should be ground into powder to make it homogenous before analysis. Before loading the sample, the tin cup was zeroed using a microbalance (Figure 3.12 (a)); then the sample was loaded in the cup and weighed. After the weight was recorded, the cup was removed and folded using forceps, following directions shown below (Figure 3.12 (c)).

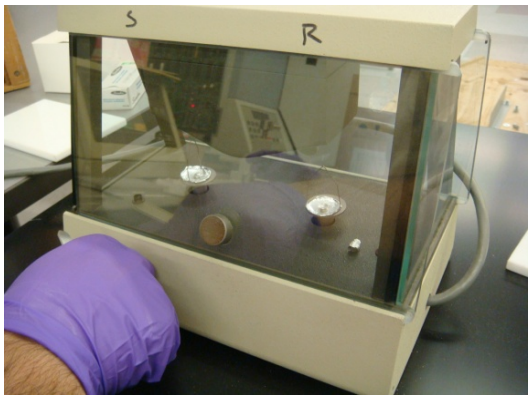

a)

b)

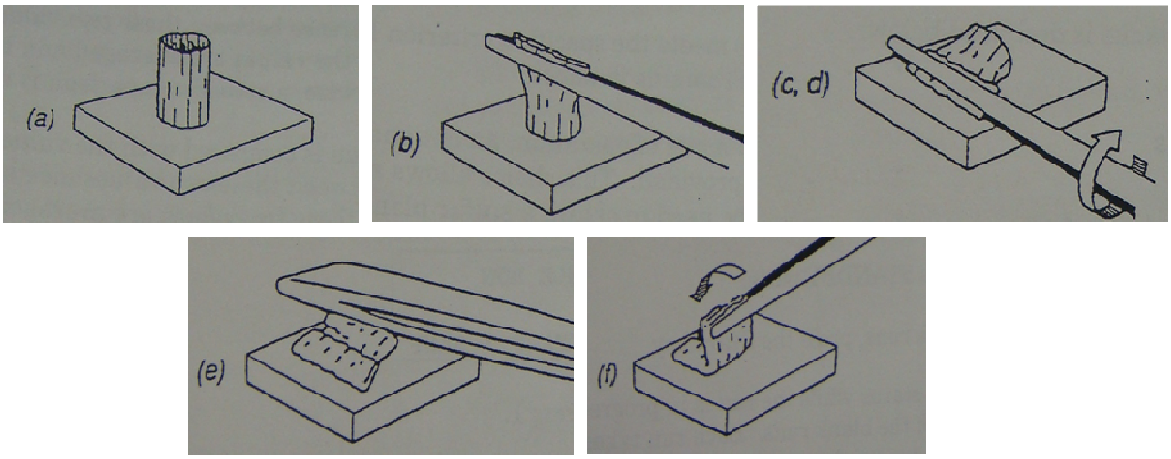

c)

Figure 3.12 Elemental analysis procedures (a) microbalance (b) before and after tin cup was folded (c) direction to fold the tin cup (PerkinElmer 2400 Series II CHNS/O Elemental Analyzer operation manual)

For liquid sample, the same procedures were followed as for the solid samples, but a tin pan was used instead of a tin cup. After the sample was loaded, the pan was pressed to a flat shape by a pressing tool, as shown in Figure 3.13.

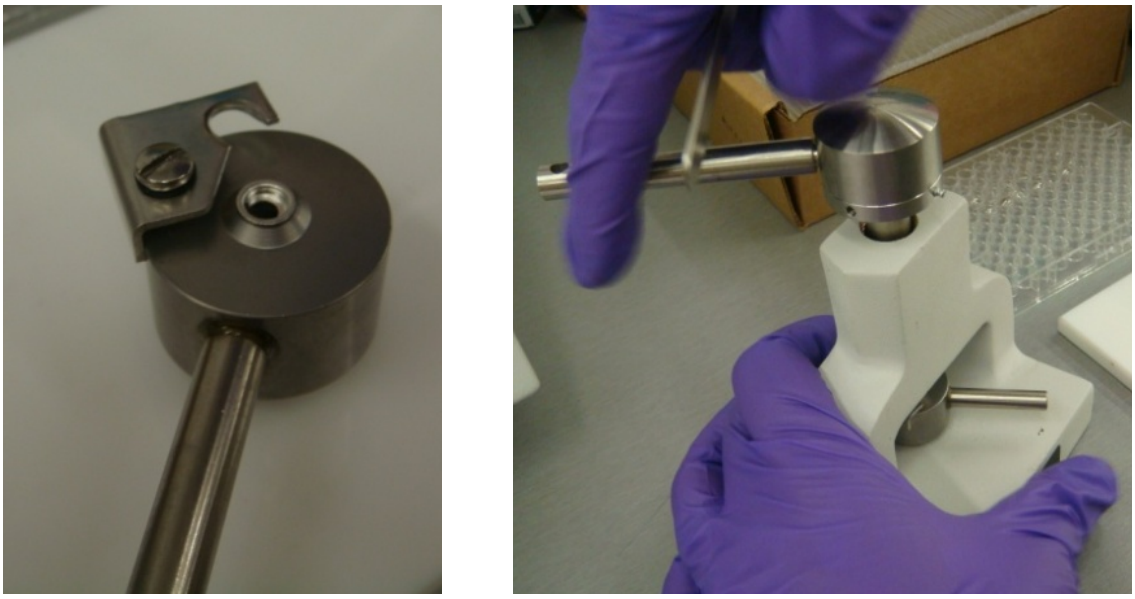

a) b)

Figure 3.13 Additional tools for liquid samples (a) Pressing tool for tin pan, (b) Pressing the tin pan

Once the sample was prepared, it was loaded into the machine slot as shown in Figure 3.14. Before running the samples, the machine was initially warmed up and then calibrated using a standard sample. The calibration was repeated until the results fell in acceptable ranges for the standard. In this study, the CHN mode was used and oxygen content was estimated by percent difference, assuming sulfur and other mineral contents are negligible. Temperature settings for the machine followed ASTM D5291-10: combustion temperature 925^{o}C, reduction temperature 640^{o}C, and detector oven temperature 84^{o}C. Each run takes about 6-8 minutes.

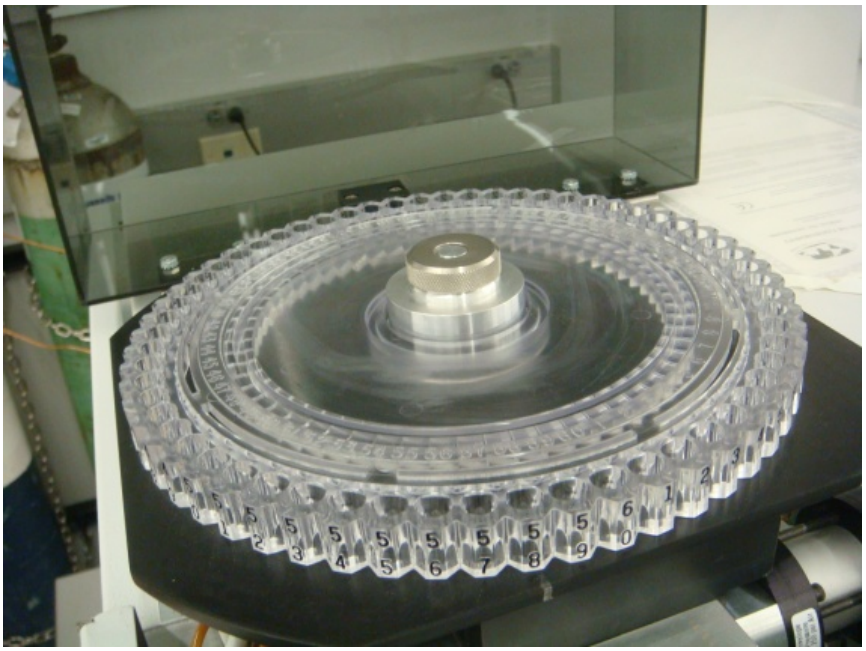

a)

b)

Figure 3.14 CHN analysis instrument (a) Sample slot (b) PerkinElmer 2400 Series II CHNS/O Elemental Analyzer

3.3.2 Thermogravimetric Analysis (TGA)

Thermogravimetric analysis, or TGA, is a thermal analysis that measures mass changes as a function of temperature and time when a material is decomposed under a controlled atmosphere (Scott, 2009). This technique is widely used to determine material compositions such as moisture content, volatile organic carbon, and fixed carbon based on mass loss. Besides, Mansfield et al. (2010) mentioned the use of TGA to predict kinetics of materials associated with structural decomposition, oxidation, corrosion, adsorption, desorption, and gas evolution. Normally, the temperature range applied to observe material decomposition can range from room temperature up to 1000^{o}C with adjustable heating rate (TA instruments, 2011). Different purge gases can be introduced into the system depending on experimental plans. For example, hydrogen (H_2) or oxygen (O_2) can be applied if hydrogenation or oxidation is preferred, respectively, while inert gases like nitrogen (N_2) , argon (Ar), or helium (He) will be used for common decomposition (Scott, 2009). However, under H_2 atmosphere, the concentration of H_2 gas should be controlled due to safety issues.

TGA has been frequently applied in pyrolysis research to initially investigate biomass thermal characteristics and its kinetics. Park et al. (2008) used TGA analysis to examine the pyrolysis temperature range and decomposition characteristics of Japanese larch under N_2 atmosphere at a heating rate of 5-20^{o}C/min. The results showed major decomposition occurred at about 300-380^{o}C, with maxima at 358, 370, 377, and 382^{o}C at 5, 10, 15, and 20^{o}C/min heating rates, respectively. Seo et al. (2010) studied pyrolysis of sawdust using TGA together with real-time gas analysis (GA). The experiments were conducted also under N_2 atmosphere at 5-30^{o}C/min heating rate up to 900^{o}C. Then, combined TGA and GA data with kinetic model percent liquid, gas, and char products were found as 58-64%, 20-25%, and 10-12%, respectively. Piskorz et al. (2003) also supported the use of TGA analysis to predict the product yields of pyrolysis for individual feedstocks.

TGA therefore is applied to this study using SDT Q600 from TA instrument (Figure 3.15 (a)) in order to investigate material compositions, thermal characteristics, and pyrolysis temperature ranges of various feedstock ratios. About 5-10 mg of prepared samples was loaded into an aluminum pan which was previously tared with a reference pan, which is an empty pan as shown in Figures 3.15 (b) and (c). A N_2 atmosphere was used to correspond to an actual pyrolysis condition (absence of air). Then, the samples were heated at a rate of 10^oC/min from room temperature to 1000^oC, to the point when no further change in mass loss occurs. Air condition was also applied in order to identify ash content of the samples. TGA results include a graph of sample weight loss as a function of temperature. Based on TGA, temperatures were selected for actual pyrolysis experiments.

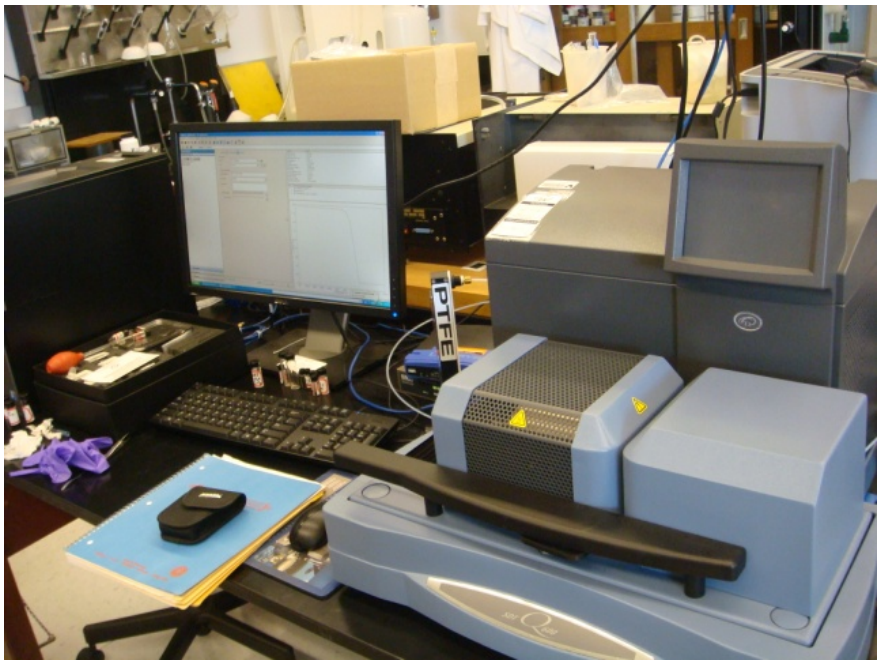

a)

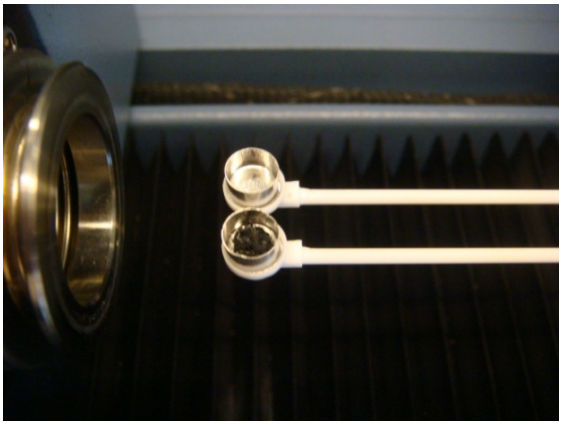

b) c)

Figure 3.15 TGA Instrument (a) SDT Q600 for TGA (TA Instruments, 2011), (b) Sample in a pan, (c) Reference and sample pan for a run

3.4 Oil Characterization

3.4.1 Elemental Analysis

Elemental analysis was also applied for the oil analysis with the same temperature program as discussed for the feedstocks.

3.4.2 Gas Chromatography (GC)

GC is normally used to separate the components of mixtures, either liquid or gas, and determine their concentration. Basically, operation of a GC is based on two phases, mobile and stationary. The mobile phase is normally a carrier gas which carries the sample along the column, while the stationary phase is typically a packed or capillary column, depending on the purpose and compounds. When the sample is injected into the GC, different compounds travel along the column at different rates and thus exit the column at different rates and retention times. The GC responds to the concentration of each compound by giving signals by either thermal conductivity detector (TCD) or flame ionization detector (FID) in term of chromatograph peaks.

In this study, the model of GC used for oil analysis and the set up are as follows:

GC: SRI 8610C, FID (Flame ionization detector), illustrated in Figure 3.16

Carrier gas 1: He with 5 psi, 10 mL/min

Carrier gas 2: H_2 with 22 psi, 25 mL/min

The column is from Restek Corporation which is:

Column type: Capillary column

Column: 6m, 0.53mm ID, 0.15µm MXT®-500 Simulated Distillation (cat.# 70104) cold on-column injection of Polywax® 655 in CS_2

The temperature program was set up following the ASTM D2887 (Standard test method for boiling range distribution of petroleum fractions by gas chromatography), as shown in Table 3.2.

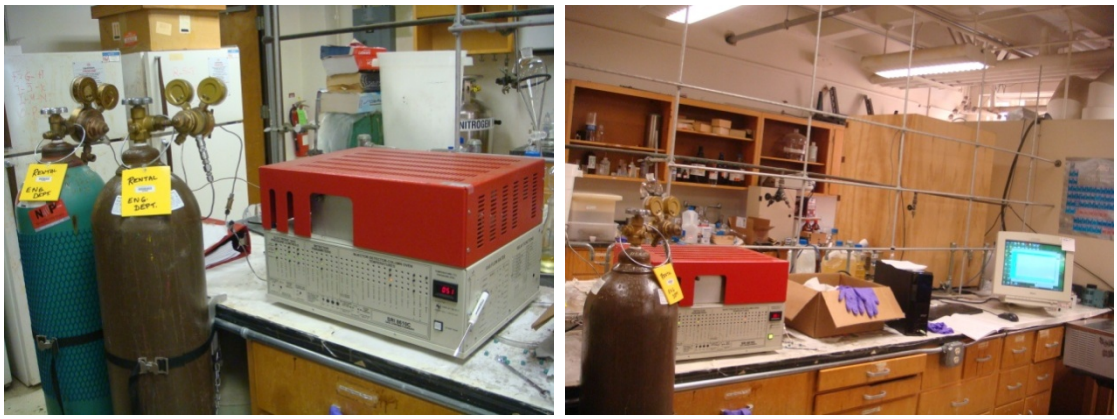

Figure 3.16 SRI 8610C GC for oil analysis

Table 3.2 Temperature program for oil analysis

Initial temperature, ^{o}C	Hold, min	Ramp, ^{o}C/min	Final temperature, ^{o}C
37	1	35	380
380	5	-50	39

Before injecting the oil sample to the GC, samples were prepared in an appropriate way. Around 200 μL of oil was transferred by auto pipette into a disposable centrifuge tube, and then put in the vacuum oven at low temperature for an hour to eliminate some moisture. After that, the sample was centrifuged for 20 minutes to precipitate small particles that might have deposited in oil phase. Then, 100 μL oil sample was drawn and transferred to a 2 dram glass vial, and the sample was diluted using 4 mL of toluene. Only 1 μL of dilution sample was injected into the GC using a 5 μL micro syringe. Figure 3.17 and 3.18 show the preparation steps and all apparatus used during the sample preparation.

a)

b)

c)

d)

Figure 3.17 Apparatus for liquid preparation (a) Disposable centrifuge tube, (b) 200 μL and 1000 μL auto pipettes, (c) Vacuum oven, (d) Centrifuge machine

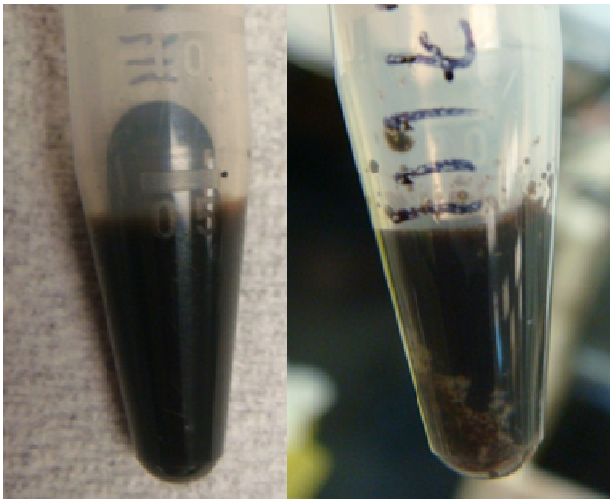

a)

b)

c)

Figure 3.18 Apparatus for liquid characterization (a) Sample before and after being centrifuged, (b) Sample after dilution, (c) Hamilton 5 μL syringe

3.5 Gas Characterization

The same technique for oil analysis using GC was also applied for gas analysis. However, a different detector was used for gas. In this study a TCD detector was used to detect the four main gases from the process, which are CO, CO_2, CH_4 and H_2.

In this study, the model of GC used for gas analysis and the set up are as follows:

GC: SRI 310C, TCD (thermal conductivity detector) shown in Figure 3.19 (a)

Carrier gas : He with 7 psi, 10 mL/min

The column is from Restek Corporation which is:

Column type: Packed column

Column: ShinCarbon ST 100/120 mesh (cat. # 19809) 1 meter x 1mm ID Silcosteel® micropacked column

The temperature program was set up using isothermal temperature, which is 70^{o}C and hold for 50 minutes. Only 0.1 mL of gas sample was injected into GC by gas tight syringe.

a)

b)

Figure 3.19 Apparatus for gas characterization (a) SRI 310C GC (b) SGE 0.5 mL gas tight syringe

3.6 Residue Characterization

3.6.1 Elemental Analysis

Elemental Analysis was again applied for residues using the same temperature profile.

3.6.2 Thermogravimetric Analysis (TGA)

TGA was also applied for residues but it was run only under N_2 to identify any remaining volatiles possibly left in the residues.

3.6.3 Surface Area Analysis and N_2 Adsorption (Quantachrome Corporation, 2011)

Surface area is a major characteristic to characterize porential adsorbents. Surface area analysis was performed by an outside laboratory, Quantachrome, using Autosorb iQ gas sorption analyzer (Figure 3.20). Initially, a sample was cleaned by a degassing process at 200^{o}C for 120 minutes to remove moisture and some volatiles. Once the degassing was completed, surface area was determined by passing N_2 gas into the sample cell, which was placed inside the liquid nitrogen container. Then, the gas molecules were adsorbed onto the sample surface and into its pores until it was saturated. Surface area was then estimated based on Brunarer, Emmett, and Teller (B.E.T) theory. Additionally, an isotherm between the gas volume adsorbed and relative pressure was also developed. In this study, the N_2 isotherm of the residue will be compared with commercial carbons, FluePac B and Filtrasorb 200.

Figure 3.20 Autosorb iQ gas sorption analyzer (Quantachrome Corporation, 2011)

3.6.4 Liquid Adsorption

In this study, liquid adsorption was conducted using methylene blue (MeB) dye as an adsorbate and the residue of pure seaweed at 600^{o}C as an adsorbent. The liquid adsorption isotherm for seaweed residue was then compared with that of a commercial carbon, Filtrasorb 200. An equilibrium time for both adsorbents with MeB was identified before the adsorption tests were carried out. For the residue, 250 mL of 50 mg/L MeB solution was prepared in Erlenmeyer flask; then about 0.1 g of the sample was put into the solution. The solution was stirred at around 1000 rpm by magnetic stirrer. Then, a sample was collected using a 5 mL syringe with 0.45 μm syringe filter to filter the adsorbent particles which were possibly suspended in the solution (Figure 3.21). Samples were taken at 15 minutes intervals for the first hour, and then once every hour until equilibrium was reached. Agilent Ultraviolet-visible spectroscopy (UV-vis) was used to quantify solution concentration, which is proportional to the peak signal of the solution at particular wavelength (Figure 3.22). The same procedure was followed for the

commercial carbon, except for the initial concentration of MeB was changed to 200 mg/L instead of 50 mg/L.

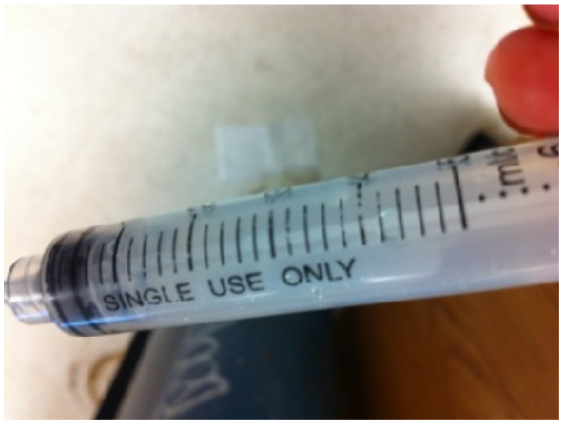

a)

b)

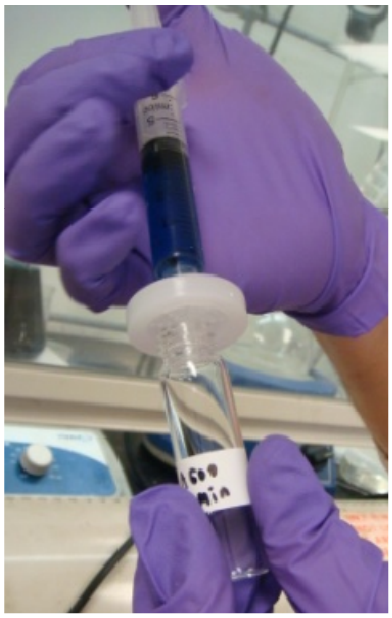

c)

Figure 3.21 Apparatus for liquid adsorption (a) 5 mL syringe, (b) 0.45 μm syringe filter, (c) filtration process

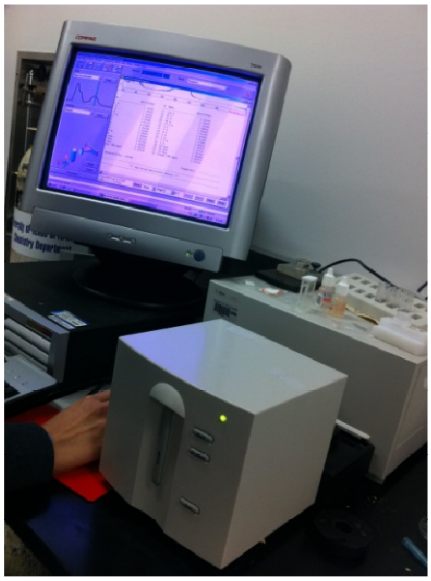

a)

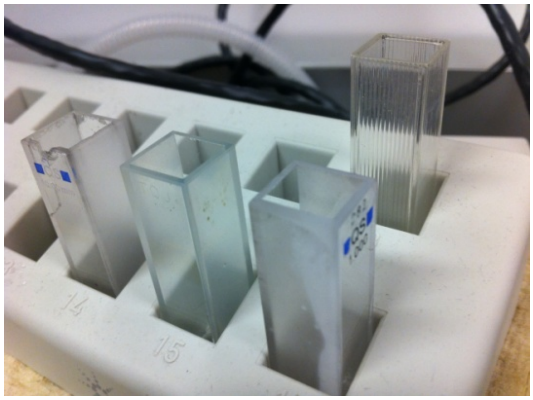

b)

Figure 3.22 Determination of MeB concentration (a) UV-vis, (b) quartz sample cell

Once the equilibrium time for both adsorbents was determined, the adsorption experiments were performed following ASTM D3860 - 98. Adsorbents of weights varying from 0.05 - 1.0 g were prepared and then placed in 100 mL of MB solution with 50 mg/L and 200 mg/L concentration for the seaweed residue and the commercial adsorbent, respectively. Then the flasks were kept shaking using a mechanical shaker until steady state was achieved: 5 hours for the residue and 5 days for the commercial carbon. Then, the sample was collected and filtered into 6 dram glass vial to measure the concentration of MB remaining in the liquid.

3.6.5 Scanning Electron Microscope (SEM)

A Scanning Electron Microscope (SEM) forms an image using an electron beam which is released from an electron gun through different electromagnetic fields and lenses. Once the beam hits a specimen, the beam will reflect back to a detector which will convert a signal from the beam into an image (Purdue University, 2012). The schematic of an SEM is illustrated in Figure 3.23.

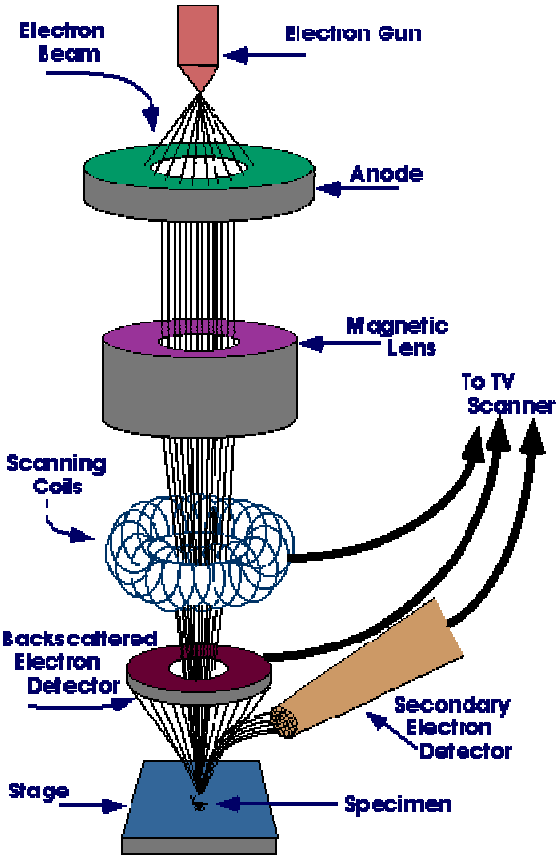

Figure 3.23 Schematic of SEM (Diagram courtesy of Iowa State University)

Since the SEM uses electrons to transmit the signal, a specimen should be conductive in order to obtain a good image resolution. Thus, the specimen was coated by silver using the coating machine (CrC-100) shown in Figure 3.24. Then, it was loaded into the Hitachi S-3000N SEM machine (Figure 3.25) and high vacuum conditions were applied.

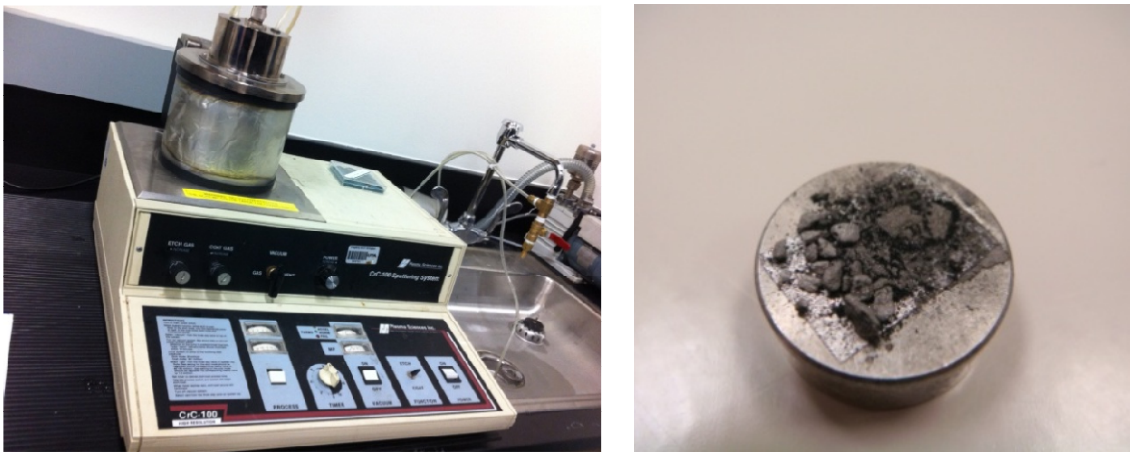

a) b)

Figure 3.24 Sample preparation for SEM (a) CrC-100 coating machine, (b) sample after coating with silver

a) b)

Figure 3.25 SEM machine (a) Hitachi S-3000N Scanning Electron Microscope (SEM), (b) sample loading

3.7 Analysis Method Summary

All analysis methods are summarized in the table below.

Table 3.3 Summary table for feedstock and product analysis

Characteristic	Method
Feedstock	
Element: C,H,O,N	elemental analysis
moisture, volatile, and fixed carbon	TGA analysis
Gas	
gas composition	GC
Oil	
Boiling point range	GC
Element: C,H,O,N	elemental analysis
Residue	
Element: C,H,O,N	elemental analysis
moisture, volatile, and char	TGA analysis
surface area	surface area analysis
adsorption isotherm	Gas and liquid adsorption
morphology	SEM

CHAPTER 4

RESULTS AND DISCUSSION

4.1 Feedstock Analysis

4.1.1 Elemental Analysis

The results of elemental analysis of each feedstock are shown in Table 4.1. It is noticeable that *Sargassum* seaweed has quite low carbon, but high oxygen content, resulting in a high O/C ratio. Besides, high nitrogen is observed since the seaweed is well known as a nutrient-rich source, especially in terms of protein. It should be noted that the oxygen content is obtained by difference after a subtraction of ash content, which is mainly inorganic. However, the oxygen can still be overestimated in this study since the algae possibly contains significant sulfur from sulfate polysaccharide. Similar results for a number of macroalgae species including red, green, and brown have been reported by different authors, as summarized in Table 4.2. Most of the species have 30-40% carbon, 35-60% oxygen, 4-6% hydrogen, and 1-3% nitrogen. The variation of elements in seaweed probably comes from seasonal and environmental variations.

Cedar wood contains higher carbon than the seaweed and vice versa for oxygen. Consequently, the O/C ratio of the wood is lower than that for seaweed. However, the oxygen content for both of them is still high, resulting in low heating value, which is not good for a fuel source. Noticeably, the nitrogen content in the wood is only 0.49%, which is about 2.5 times lower than the seaweed. This agrees with the literature shown in Table 3: most terrestrial biomass has relatively low nitrogen (only 0.1-1%), whereas most macroalgae contain at least 1% nitrogen. Higher plants contain about 40-50% carbon, 30-40% oxygen, and 5-6% hydrogen. There is not much difference in hydrogen content between the seaweed and the wood.

Table 4.1 Elemental analysis of different feedstocks in this study

Feedstock	% C	% H	% N	% O[a]	H/C	O/C
Sargassum	34.1(±1.60)	3.90(±0.57)	1.30(±0.26)	45.2(±1.85)	1.37	1.34
Cedar wood	42.2(±0.84)	4.65(±0.28	0.49(±0.22)	48.4(±0.89)	1.32	0.94
Recycled pellet	90.0(±0.23)	3.81(±0.21)	0.00(±0.00)	6.19(±0.44)	0.51	0.05
EPS white to-go box	91.7(±0.03)	8.30(±0.08)	0.00(±0.00)	0.00(±0.00)	1.10	0.00
EPS black to-go box	90.9(±0.87)	8.02(±0.07)	0.00(±0.00)	1.08(±0.94)	1.06	0.01
EPS coffee cup	91.8(±0.10)	8.10(±0.08)	0.05(±0.01)	0.05(±0.01)	1.06	0.00

Note: [a] percent oxygen obtained by difference, after the ash content is subtracted.

Table 4.2 Elemental analysis of different macroalgae species from literature

Species	Type	% C	% H	% N	% O	Reference
Enteromorpha clathrata	Green	22.74	6.27	3.14	16.19	Wang et al. (2007)
Fucus vesticulosus	Brown	52	7.3	3.7	N/A	Ross et al. (2009)
Laminaria hyperborea	Brown	50	7.6	1.6	N/A	
Macrocystis pyrifera	Brown	41	6.1	3.1	N/A	
Gracilaria cacalia	Red	31.11	5.60	0.83	33.93	Yu et al. (2008)
Laminaria japonica	Brown	20.47	4.64	2.49	25.40	
Fucus vesiculosus	Brown	32.88	4.77	2.53	35.63	Ross et al. (2008)
Chorda filum	Brown	39.14	4.69	1.42	37.23	
Laminaria digitata	Brown	31.59	4.85	0.90	34.16	
Fucus serratus	Brown	33.5	4.78	2.39	34.44	
Laminaria hyperborea	Brown	34.97	5.31	1.12	35.09	
Macrocyctis pyrifera	Brown	27.3	4.08	2.03	34.8	
Sagassum natans	Brown	25.9	5.57	3.58	24.18	Wang et al. (2009)
Undaria pinnatifida	Brown	34.01	4.99	3.34	56.95	Bae et al. (2011)
Laminaria japonica	Brown	30.60	4.89	1.51	62.44	
Porphyra tenera	Red	40.60	4.65	6.13	47.4	

Table 4.3 Elemental analysis of different terrestrial biomass from literature

Terrestrial Biomass	% C	% H	% N	% O	Reference
Oat straw	42.75	5.22	1.06	38.71	Ross et al. (2008)
Miscanthus	46.32	5.58	0.56	41.79	
Willow coppice	52.69	5.92	0.48	41.90	
Radiata pine	44.8	5.9	0.1	46.2	Kang et al. (2006)
Sawdust	44.64	5.38	Negligible	39.98	Seo et al. (2010)
Rice straw	43.25	5.62	2.11	48.8	Jung et al. (2008)
Bamboo	46.9	5.85	0.21	47.02	
Pine bark	50.18	5.41	0.45	43.96	Sensoz (2003)
Oriental white oak	50.3	6.4	0.3	43.0	Park et al. (2009)
Japanese larch	50.8	6.8	0.1	42.4	Park et al. (2008)
Corn stover	47.4	5.01	0.77	39.7	Kumar et al. (2008)

For polystyrene, three samples of Styrofoam wastes were analyzed to compare with polystyrene recycled pellets. Since plastic is a petroleum product, the pellet is obviously rich in carbon content about 90%, which is the same as the carbon content found in actual Styrofoam wastes. There is no nitrogen content found in either the pellet or the wastes. Hydrogen content in the pellet is lower, while oxygen content is higher, than the actual wastes, which is possibly due to contamination of the pellets during the collection and recycling process; these differences in hydrogen and oxygen content are statistically significant at a 95% level of confidence. The results agreed with Kim and Kim (2004), Rutkowski and Kubacki (2006), Rutkowski (2009), Park et al. (2003), and Li et al. (2003), which also found 90-91% carbon, 7-8% hydrogen, but only 0-1% oxygen in styrene polymer. Compared to the biomass, the pellet has 2-3 times higher carbon content than the wood and seaweed, while much lower oxygen,

resulting in a lower O/C ratio. However, the hydrogen content for the pellet and the biomass is similar; thus the lower H/C ratio of the pellet is only caused by higher carbon.

4.1.2 Thermogravimetric Analysis (TGA)

Table 4.4 demonstrates proximate analysis results obtained from TGA. Since *Sargassum* and cedar wood were oven dried, they contain relatively low moisture content. For polystyrere, both the pellet and the wastes have no moisture and low fixed carbon. There was no difference in volatile matter and fixed carbon between the pellet and the actual waste, to a 95% level of confidence. In contrast, plastics have the highest volatile content, followed by the wood, while the seaweed ranks the last. The same conclusion can be observed from Table 4.5 and 4.6. According to various authors, macroalgae contains roughly 30-50% volatile matter, whereas volatile content in terrestrial biomass can be as high as 60-80%. However, both fixed carbon and ash content in seaweed are higher than for terrestrial biomass. Fixed carbon is the residue after devolatilization under an inert atmosphere, mainly composed of carbon which still can serve as a solid fuel source under oxidizing conditions, while the ash is residue that remains unburned following oxidizing conditions, which primarily consists of inorganic material. Ross et al. (2008) suggested that this is due to the marine environment: the greater amount of minerals and trace elements found in seaweed compared to terrestrial biomass leads to higher ash content.

Table 4.4 Proximate analysis of different feedstocks in this study

Feedstock	% Moisture	% Volatile matter	% Fixed Carbon	% Ash
Sargassum	4.00(±0.37)	61.3(±1.52)	19.2(±0.28)	15.5(±1.57)
Cedar wood	6.40(±0.86)	76.0(±1.75)	13.3(±0.02)	4.34(±0.16)
Recycled pellet	0.00(±0.00)	98.5(±0.95)	1.50(±0.11)	0.00(±0.00)
EPS white to go box	0.00(±0.00)	94.7(±1.21)	5.30(±0.51)	0.00(±0.00)
EPS black to go box	0.00(±0.00)	95.6(±0.91)	4.40(±0.21)	0.00(±0.00)
EPS coffee cup	0.00(±0.00)	95.6(±1.81)	4.40(±0.42)	0.00(±0.00)

Table 4.5 Proximate analysis of different macroalgae species from literature

Species	Type	% Moisture	% Volatile matter	% Fixed Carbon	% Ash	Reference
Enteromorpha clathrata	Green	13.30	41.82	7.79	37.09	Wang et al. (2007)
Ulva lactuca	Green	4.93	58.38	11.97	24.72	Wang et al. (2006)
Dictyopteris divaricata	Brown	5.00	57.62	12.71	24.67	
Grateloupia filicina	Red	4.69	55.93	17.01	22.37	
Fucus vesticulosus	Brown	11	46	N/A	24	Ross et al. (2009)
Laminaria hyperborea	Brown	12	54	N/A	17	
Macrocystis pyrifera	Brown	8	42	N/A	26	
Gracilaria cacalia	Red	11.65	54.50	19.01	14.84	Yu et al. (2008)
Laminaria japonica	Brown	13.44	38.53	14.99	33.04	
Fucus vesiculosus	Brown	N/A	51.4	23.8	11.8	Ross et al. (2008)
Chorda filum	Brown	N/A	52.2	24.9	9.9	
Laminaria digitata	Brown	N/A	53.4	25.3	10.0	
Fucus serratus	Brown	N/A	45.5	24.2	18.6	
Laminaria hyperborea	Brown	N/A	53.5	21.5	11.2	
Macrocyctis pyrifera	Brown	N/A	42.4	33.4	18.5	

Table 4.5 - continued

Species	Type	% Moisture	% Volatile matter	% Fixed Carbon	% Ash	Reference
Pophyra yezoensis	Red	9.2	36.8	22.1	31.3	Li et al. (2011)
Plocamium telfairiae	Red	11.7	30.6	24.3	33.2	
Corallina pilulifera	Red	10.5	32.2	18.4	38.6	
Sagassum natans	Brown	10.46	48.85	11.60	29.09	Wang et al. (2009)
Undaria pinnatifida	Brown	9.50	53.62	11.04	25.84	Bae et al. (2011)
Laminaria japonica	Brown	7.65	53.10	10.97	28.28	
Porphyra tenera	Red	6.41	69.66	13.49	10.44	

Table 4.6 Proximate analysis of different terrestrial biomass from literature

Terrestrial Biomass	% Moisture	% Volatile matter	% Fixed Carbon	% Ash	Reference
Fir wood sawdust	7.54	80.86	17.16	1.98	Wang et al. (2006)
Oat straw	N/A	64.9	16.9	6.7	Ross et al. (2008)
Miscanthus	N/A	74.2	14.1	2.1	
Willow coppice	N/A	67.5	19.1	5.3	
Sawdust	9.55	67.32	22.68	0.45	Seo et al. (2010)
Rice straw	6.8	82.8	1.5	8.9	Jung et al. (2008)
Bamboo	7.3	90.9	0.1	1.7	
Pine bark	3.00	72.0	26.67	1.3	Sensoz (2003)
Corn stover	N/A	74.85	N/A	8.18	Kumar et al. (2008)

The amount of alkali and alkali earth metals, including Na, K, Ca, and, Mg, in higher plants and seaweeds are compared in Table 4.7. The metal content in seaweed ranges from a few to twenty thousand ppm; the metal content for higher plants ranges from a few hundred to a few thousand. Furthermore, Ross et al. (2009) compared the thermal characteristics of seaweeds before and after pre-treatment by acid wash remove metals, in order to investigate the influence of mineral-to-ash content in the seaweed. The seaweed originally contains about 2.5-4.5% halogens, mainly related to Na, K, Ca, and Mg from the marine environment. Other trace metals were also reported, including Sr, Zn, Co, Al, Fe, As. Noticeably, the loss of volatile matter in acid-washed seaweed is higher than the original, while the residue is lower, and the loss of minerals in the high temperature region is obviously reduced, because 90% alkali and alkali earth metals in the seaweed were removed during the acid wash process. Therefore, they concluded that the minerals influence thermal behavior of seaweed.

Table 4.7 Alkali and alkali earth metal concentrations in different kinds of biomass

Feedstock	Na, ppm	K, ppm	Ca, ppm	Mg, ppm	Reference
Terrestrial biomass					
Radiata pine	46.8	891.7	491.4	165.3	Kang et al. (2006)
Rice straw	10702	9237	1599	1430	Jung et al. (2008)
Bamboo	41.6	344.7	3819	405.6	
Oriental white oak	66.4	1498	6537	215	Park et al. (2009)
Japanese larch	92.1	348.1	529.5	103.3	Park et al. (2008)
Macroalgae					
Fucus vesiculosus	23040	28020	42750	9710	Ross et al. (2009)
Laminaria hyperborea	26980	24170	13450	8080	
Macrocystis pyrifera	25270	21640	12340	7750	
Undaria pinnatifida	68510	5694	11190	10970	Bae et al. (2011)
Laminaria japonica	26790	102470	7726	5942	
Porphyra tenera	12350	38710	3013	3369	

Another interesting result obtained from TGA is stepwise decomposition of the feedstocks. The weight loss steps for *Sargassum* and cedar wood are illustrated in Figure 4.1(a). It is noticeable that both wood and seaweed show three main decomposition steps in general. An initial small mass loss in both feedstocks occurs at temperature < 150^{o}C, due to dehydration of moisture content. Then, the seaweed starts decomposing earlier than the wood at around 150^{o}C, while the wood is decomposed at higher temperature around 200^{o}C. The main decomposition step due to loss of volatile compounds in the seaweed and wood occurs between 180-550 ^{o}C and 200-530^{o}C, respectively. Then, both feedstocks continue with gradual loss at high temperature >500^{o}C; however, the seaweed exhibits a more significant loss at high temperature region than the wood.

The rate of mass loss is more visibly defined in Figure 4.1(b). The differences in mass loss between the two kinds of biomass can be observed during the main decomposition step. There are two individual peak losses for the seaweed, while there is an only major peak loss for the wood. Moreover, the seaweed shows continuous slow mass loss, with another noticeable peak in the high temperature region around 600-700^{o}C. A number of studies have been conducted on pyrolysis characteristics of macroalgae which confirm three stepwise mass loss with two main peak losses during the main devolatilization step (Wang et al., 2007; Ross et al., 2009; Yu et al., 2008; Li et al., 2011; and Bae et al., 2011).

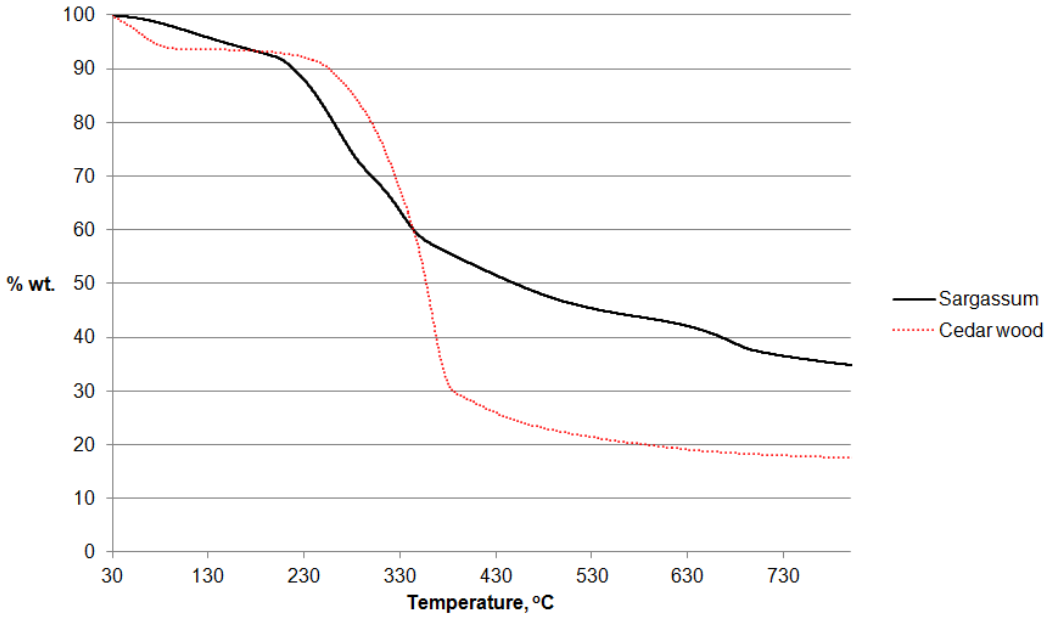

(a)

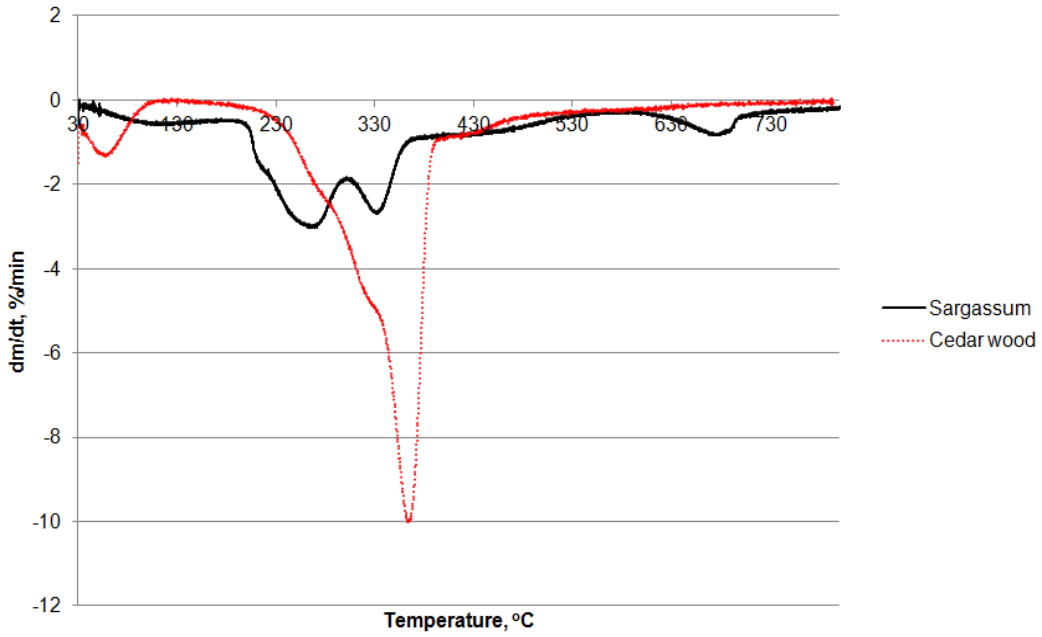

(b)

Figure 4.1 Plots of (a) weight loss versus temperature, and (b) rate of weight loss versus temperature of oven-dried *Sargassum* and Cedar wood under N_2 atmosphere with 10^{o}C/min heating rate

Wang et al. (2006) suggested two possible causes of the dissimilarities between terrestrial and macroalgae biomass decomposition: structure and salt content Wang et al. investigated the thermal behavior of three seaweeds compared to fir wood sawdust under 100 ml/min N_2 atmosphere from room temperature to 700^{o}C with 10^{o}C/min heating rate. They noticed that the decomposition of the seaweeds occurred at lower temperature than the wood. In addition, different steps of mass loss were found in seaweeds; however, only one step of mass loss peak was observed in wood biomass. Similarly, Ross et al. (2008) observed the thermal behavior of six brown seaweed species compared to three terrestrial biomass under 50 ml/min N_2 atmosphere from 40-950^{o}C with 25^{o}C/min heating rate. They demonstrated that mass loss for both groups occurs in three temperature ranges, excluding moisture. For terrestrial biomass, decomposition at 200-270^{o}C mainly comes from hemicellulose, next is cellulose between 270-370^{o}C, and the last is lignin. In contrast, seaweed starts decomposing at lower temperature with a three step loss: 180-270^{o}C due to carbohydrate, 320-450^{o}C due to protein, and >500^{o}C due to volatile metal and carbonates. In addition, some inorganic material decomposes at 750-800^{o}C.

Both Wang et al. (2006) and Ross et al. (2008) concluded that wood is typically composed of more complex components, including cellulose, hemicelluloses, and lignin, which provide stronger structural support, compared to seaweed, which is composed of basic polysaccharides, protein, and lipid; consequently, the seaweed is easier to decompose. Moreover, Wang et al. (2009) studied combustion characteristics of seaweed and compared ash composition between land plants and seaweed; they found much higher K and Na content in ash of the seaweed than in the land plants, due to the seaweed marine environment. As a result, high alkali content serves as a catalyst reducing fusion and ignition temperature of the seaweed. However, they suggested that high ash content probably leads to slagging problems during thermal treatment.

To clearly understand thermal decomposition steps of brown macroalgae, Anastasakis et al. (2011) specifically studied pyrolysis behavior of four main carbohydrates in brown macroalgae which are alginate, mannitol, laminarin, and fucoidan under 50 ml/min N_2 from 40-900^{o}C with 25^{o}C/min heating rate. In common, all carbohydrates acquire three stepwise mass loss starting with dehydration at 25-110^{o}C. Next step is the main decomposition of volatile between 150-555, 220-400, 175-685, and 175-740^{o}C for alginate, mannitol, laminarin, and fucoidan, respectively. During the second step, alginate and mannitol show only one main loss peak, while two loss peaks are observed in laminarin and fucoidan. The last step occurs >700^{o}C, and represents slow mass loss of the residues.

Table 4.8 Proximate analysis of four carbohydrates in brown macro-algae (Anastasakis et al., 2011)

Carbohydrate	% Moisture	% Volatile matter	% Fixed Carbon	% Ash
Alginate	8.5	66	20	5
Mannitol	1.3	95.3	1.7	1.7
Laminarin	9.4	88.3	0.6	1.7
Fucoidan	12.5	61.7	N/A	31

Table 4.9 Elemental analysis of four carbohydrates in brown macro-algae (Anastasakis et al., 2011)

Carbohydrate	% C	% H	% N	% O	% S	Metal, ppm
Alginate	36.31	4.81	<0.2	N/A	<0.2	675
Mannitol	39.65	7.76	<0.2	N/A	<0.2	17500
Laminarin	39.17	6.40	<0.2	N/A	0.29	7050
Fucoidan	24.25	4.19	<0.2	N/A	8.15	109500

As shown in Tables 4.8–4.9 reported by Anastasakis et al. (2011), laminarin and mannitol have the highest volatile matter, carbon and hydrogen contents since these carbohydrates are the storage products of seaweed. Fucoidan has the highest metal content (mostly alkali and alkali earth metals, including Na, Mg, K, and, Ca) which corresponded to the highest ash content. Additionally, the researchers found that, excluding moisture loss, the actual seaweed decomposition could be illustrated by the loss of four carbohydrates: first at around 200-300^{o}C, representing alginate and fucoidan, and next at 300-400^{o}C, due to the loss of mannitol and laminarin, and the high temperature loss of fucoidan.

On the other hand, Biagini et al. (2006) compared devolatilization of land biomass, including pine wood, wood pellets, olive residue, and hazelnut shells, to hemicellulose, cellulose, and lignin by TGA under 60 ml/min N_2 atmosphere from 100 to 1000^{o}C with 20^{o}C/min heating rate. They indicated that the thermal decomposition of the selected kinds of biomass is obviously associated with hemicellulose, cellulose, and lignin decomposition. Hemicellulose and lignin start decomposing at around the same temperature of 250^{o}C, but hemicellulose is decomposed by 300^{o}C, while lignin is not fully decomposed until 500^{o}C. Cellulose starts decomposing later than the hemicellulose or lignin, at around 300^{o}C to 400^{o}C. Besides, it is noticeable that the percent weight loss of cellulose is the highest, followed by hemicelluloses, and lignin ranks the last. Moreover, Hajaligol et al. (2001) observed cellulose decomposition

under 150 ml/min under He atmosphere heated up to 800^{o}C with 20^{o}C/min heating rate, the main peak shows between 300-360^{o}C then followed by the small loss about 5% up until 700^{o}C.

Their results agree with other studies on actual biomass samples. For example, Jung et al. (2008) performed TGA of rice straw and bamboo sawdust under N_2 at 5 and 10^{o}C/min heating rate up to 900^{o}C; they reported that both kinds of biomass exhibit similar decomposition steps, beginning with the initial weight loss due to moisture content, followed by the loss of hemicelluloses until 250^{o}C, and the fast rate of loss during 250-400^{o}C due to cellulose decomposition, and the final gradual loss over a wide temperature range above 400^{o}C due to lignin content in the biomass. Kumar et al. (2009) obtained similar results for pyrolysis of corn stover under 40 ml/min N_2 atmosphere from 25^{o}C to 850^{o}C using 10 30, and 50^{o}C/min heating rate. Three decomposition stages were demonstrated, including the first stage at 25-125^{o}C of moisture loss and light volatiles, the second stage at 250-450^{o}C of one peak loss due to hemicellulose and cellulose, and the third stage of slow final loss occurring at 450-850^{o}C, representing loss of lignin and complex compounds.

Another difference between macroalgae and terrestrial biomass during thermal decomposition is the type of reaction involved. Li et al. (2011) noticed that for seaweed, the main devolatilization stage is exothermic, while the moisture loss is endothermic. This agrees with Yu et al. (2008), who reported that seaweed decomposition at temperatures greater than 300^{o}C is exothermic. Besides, Wang et al. (2006) compared differences of thermal behavior between wood biomass and seaweed; they found that the main mass loss peak for seaweed was exothermic, but endothermic for wood biomass. They proposed that the mineral and salt content in the seaweed helps promote exothermic reaction due to charring process. Thus, they recommended a combination of seaweed with other materials as a fuel since seaweed by releasing heat would reduce the need for heat input.

Table 4.10 Decomposition temperatures of different feedstocks in this study

Feedstock	Decomposition stages	Decomposition temperature range, ^{o}C	Main decomposition temperature, ^{o}C
Sargassum	3	150-550	260,330
Cedar wood	3	200-530	365
Recycled pellet	1	330-480	411
EPS white to go box	1	350-475	411
EPS black to go box	1	350-475	405
EPS coffee cup	1	340-480	413

Unlike biomass feedstocks, polystyrene pellets and waste samples exhibit a simple decomposition step due to volatile compounds, which starts at around 300^{o}C and lasts until 480^{o}C. There is only maximum peak loss at around 410^{o}C, as shown in Figures 4.2 (a) and (b). This result is comparable to those obtained in other studies. Brebu et al. (2010) and Park et al. (2003) conducted TGA of PS under N_2 atmosphere using 10 ^{o}C/min heating rate. They reported that PS starts decomposing at 350-380^{o}C, and then exhibits one main peak loss at 420-430^{o}C. Besides, they observed no residue remained from the run, which means PS yielded almost 100% conversion. Similarly, Kim and Kim (2004) observed pyrolysis characteristics of polystyrene; they noticed that the polymers were not decomposed before 300^{o}C, but started decomposing at around 360-380^{o}C, reaching a maximum at around 400^{o}C. The decomposition stages and temperature for each feedstock are summarized in Table 4.10.

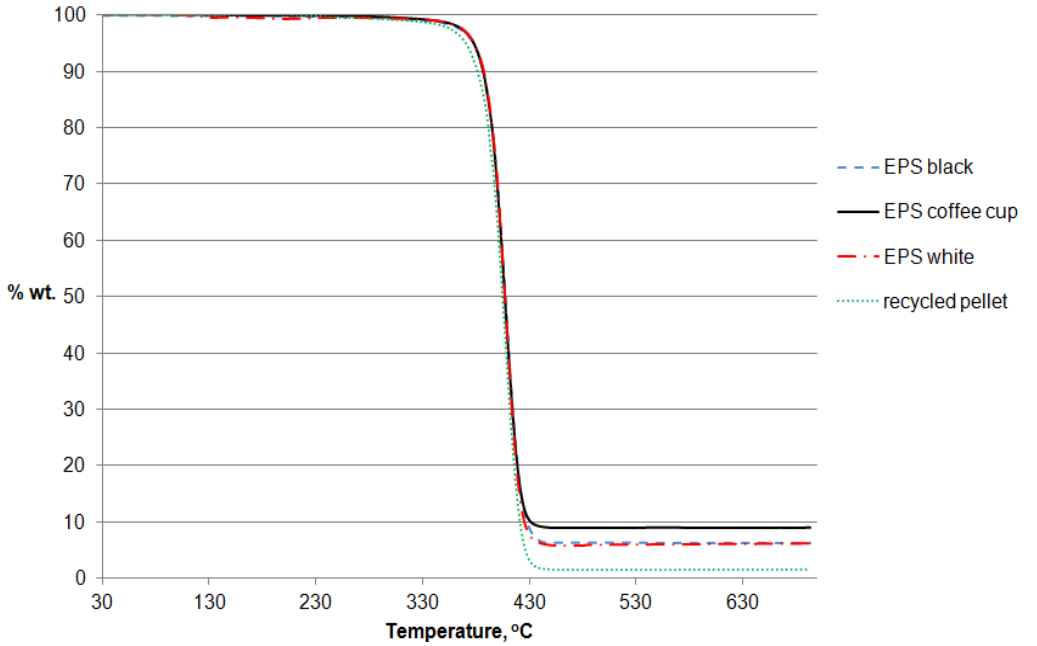

(a)

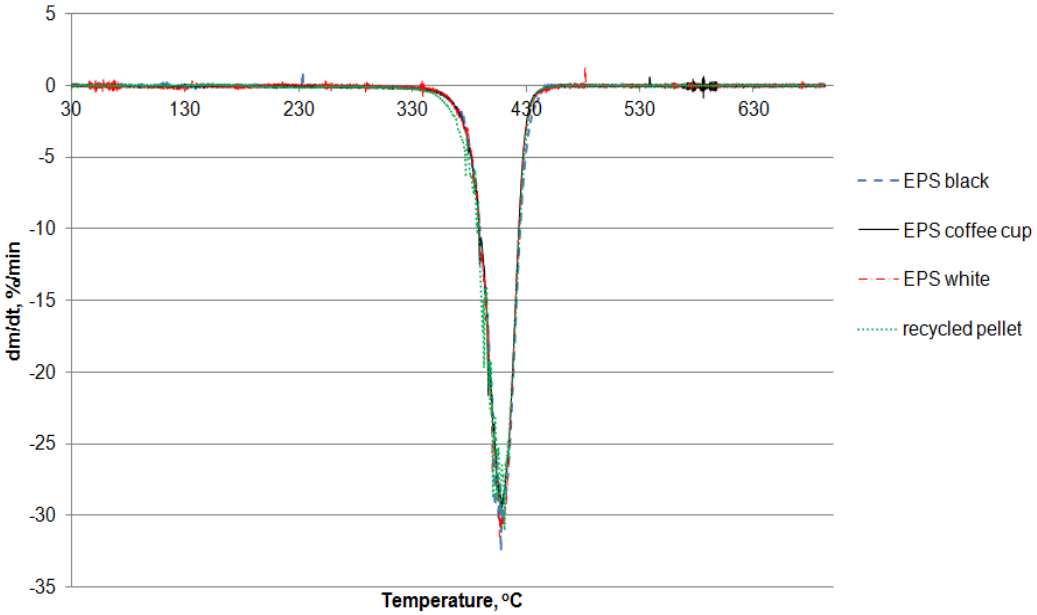

(b)

Figure 4.2 Plot of (a) weight loss versus temperature, and (b) rate of weight loss versus temperature of different Styrofoam plastics under N_2 atmosphere with 10^{o}C/min heating rate

According to elemental analysis and TGA results, the PS pellets have almost twice as much volatile content and three times higher in carbon content than seaweed. In addition, it is noticeable that at around 350^{o}C when the pellet just starts to decompose, the remaining weight of the seaweed is approximately 50%. Hence, the ratio of mixture should be at least 2:1 seaweed, or 33% plastic. The plastic percent is then decreased to 25%, 15%, and 5%, respectively.

Since a number of TGA studies have revealed an interaction between biomass and polymers, the TGA of the mixture is also applied in this study. The proximate analysis of the various mixture ratios is demonstrated in Table 4.11. It is noticeable that the volatile matter increases as the ratio of plastic in the mixture increases, and vice versa for the fixed carbon and the ash content. This is due to the fact that plastic is a major source of volatiles, while the seaweed is a source of fixed carbon.

Table 4.11 Proximate analysis of different mixture ratios in this study

% Plastic	% Moisture	% Volatile matter	% Fixed Carbon	% Ash
5	7.00(±0.20)	63.0(±0.64)	16.9(±1.97)	13.1(±0.56)
15	6.90(±0.23)	66.2(±0.92)	14.4(±0.39)	12.5(±1.69)
25	6.40(±0.06)	70.1(±0.69)	12.3(±0.54)	11.2(±1.09)
33	5.60(±0.62)	72.4(±0.13)	11.1(±1.50)	10.9(±0.58)

Additionally, the comparison between theoretical and experimental proximate analysis is illustrated in Figure 4.3. The experimental volatile matter values are 1.5-2% higher predicted, which corresponds to 1.5-2% lower fixed carbon. However, the observed and predicted ash contents are comparable for all mixture ratios. An interaction between the algae and the polymer could possibly account for the difference between the measured and predicted values.

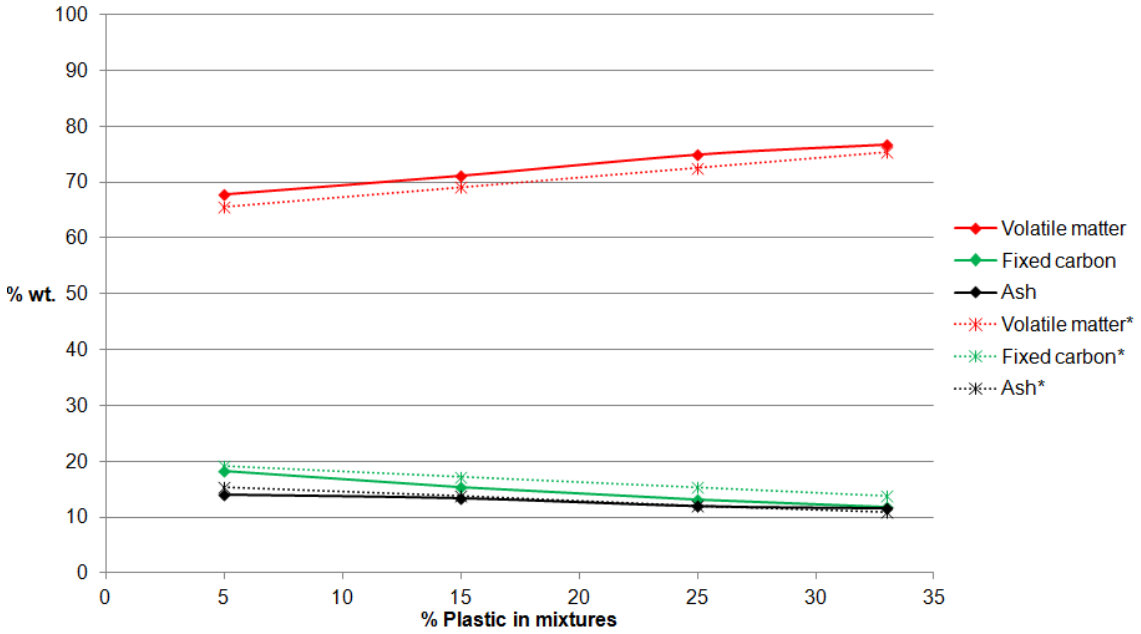

Figure 4.3 Comparison of predicted (dashed lines) and observed (solid lines) volatile matter, fixed carbon, and ash content at different mixture ratios

Considering TGA plot of weight loss versus temperature in Figure 4.4(a), the mixture exhibits a weight loss trend similar to that of the seaweed, except for the sharp loss at around 400^{o}C, which corresponds to the loss of the plastic. It is clearly seen that as the plastic ratio increases, the decomposition region of the plastic becomes more obvious. A remarkable point is observed in Figure 4.4(b) when the rate of mass loss is plotted versus temperature. Noticeably, the temperature at which the maximum mass loss rate occurs shifts 6-10^{o}C higher, as the seaweed content increases (and plastic percent decreases). Based on other studies, discussed below, this upward shift of the temperature associated with the maximum loss rate indicates an interaction between the seaweed and PS. On the other hand, there is an insignificant effect of the polymer on decomposition temperature of the algae biomass since the main decomposition of the seaweed is almost completed before the decomposition of the pellet.

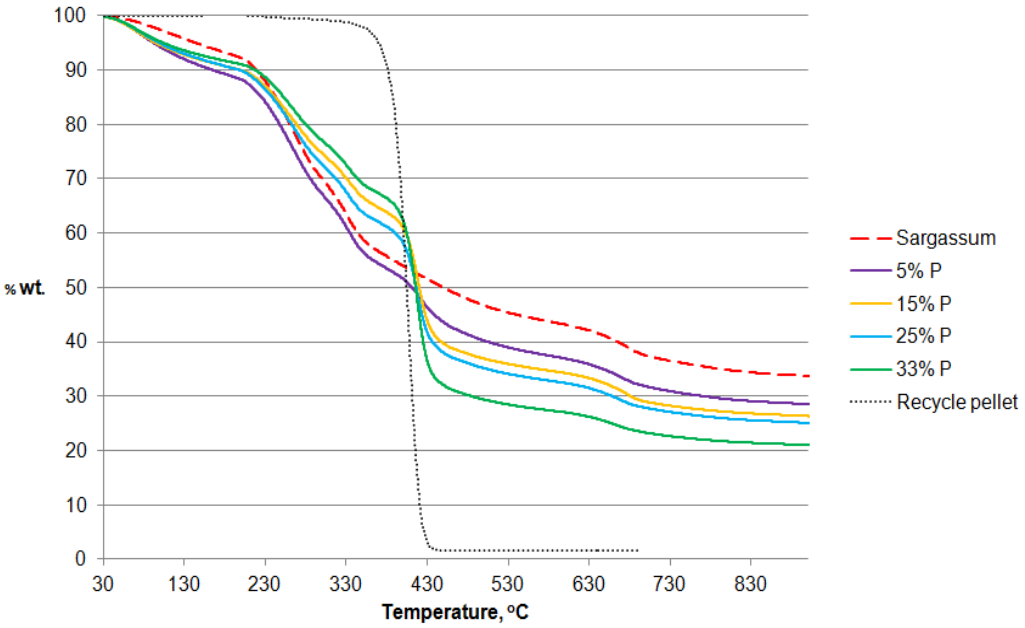

(a)

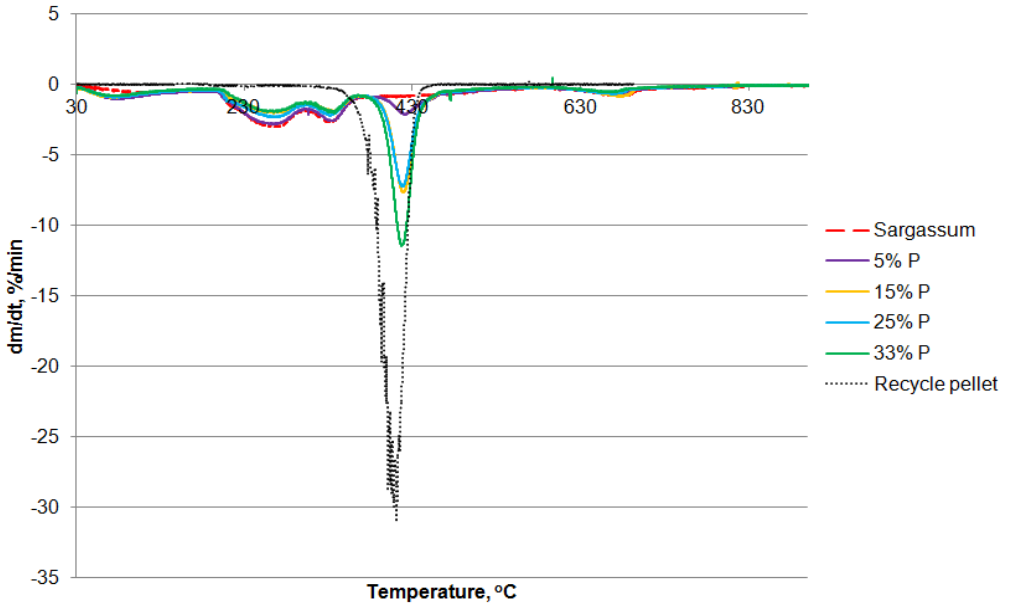

(b)

Figure 4.4 Plots of (a) weight loss versus temperature, and (b) rate of weight loss versus temperature of pure and different mixture ratios under N_2 atmosphere with 10^{o}C/min heating rate

Similarly, Aboulkas et al. (2008) examined co-pyrolysis between olive residue and HDPE using a 1:1 ratio under 60 ml/min N_2 atmosphere from 30 to1000^oC with 2, 10, 20, and 50^oC/min heating rates. They observed about 6-15^oC and 1-5^oC higher shift in temperature associated with peak weight loss of the polymer and the olive residue, respectively, compared to pure feedstocks; this indicates a higher thermal stability of the mixture. Besides, they found a 7-11% difference between observed and predicted weight loss at 450-650^oC, which could be evidence of the interaction. They suggested that two kinds of interactions may occur: either between the biomass char product and the polymer, or the biomass gaseous product and the polymer, since the polymer starts decomposing when the biomass is almost completely degraded. Later in 2009, Aboulkas et al. further studied the pyrolysis behavior of olive residue with more polymer types including HDPE, LDPE, PP, and PS, using a 1:1 ratio for all blends. Results similar to the previous study were obtained, raising the decomposition temperature about 6-21^oC for polymers, but with no change for the biomass. Moreover, they detected a synergistic effect at the decomposition stage around 400-510^oC, which exhibits a partial overlap of the decomposition peaks.

Zhou et al. (2006) reported similar results in an investigation of thermal characteristics of HDPE, LDPE, and PP blended with pine wood sawdust in ratios of 70:30, 45:55, and 70:30, respectively, under 30 ml/min N_2 atmosphere from room temperature to 650^oC with 20^oC/min heating rate. They confirmed the interaction of the mixtures by comparing theoretical to experimental weight loss. A significant interaction was found in the high temperature region of 530-650^oC, which yielded the differences in weight loss of approximately 6-12%. Specifically, a more obvious interaction was found in the mixtures of HDPE and PP rather than LDPE. Moreover, they noticed overlapping of two peaks during the devolatilization stage of the mixtures, while only one peak was reported for individual material.

Cao et al. (2009) also discussed thermal analysis of sawdust and waste tire (60:40) under 90 ml/min N_2 atmosphere with 30^oC/min heating rate. Only a 1.8^oC difference in

maximum decomposition temperature between pure and mixed samples was reported; they still stated that an interaction between the mixtures perhaps exists and possibly influences oil quantity.

Jakab et al. (2001) clarified the influence of biomass on polymer decomposition after they investigated the thermal behavior of the 1:1 ratio mixture of PS with wood-derived materials including beech wood, beech lignin, charcoal, and cellulose under argon atmosphere with 10^{o}C/min heating rate using Thermogravimetry direct mass spectrometry (TG-MS) to detect evolution of product species. For the mixture, a 10-20^{o}C higher decomposition temperature at maximum mass loss was reported, associated with an increase in primary chain scission product. They implied that the mechanism behind this result was the biomass material initially enhancing chain scission of the polymer, resulting in elevated decomposition temperature. Following the chain scission, the biomass inhibits the depolymerization and an intramolecular hydrogen transfer reaction. As a result, styrene yield is decreased; styrene monomer and its oligomers are normally the major products from PS thermal degradation. On the other hand, the mixture promotes an intermolecular hydrogen transfer reaction, resulting in higher toluene and phenyl compounds such as 1,3-diphenyl propane and 1,3-diphenyl propene, formed from unsaturated molecules. The previous reaction is illustrated in Figure 4.5.

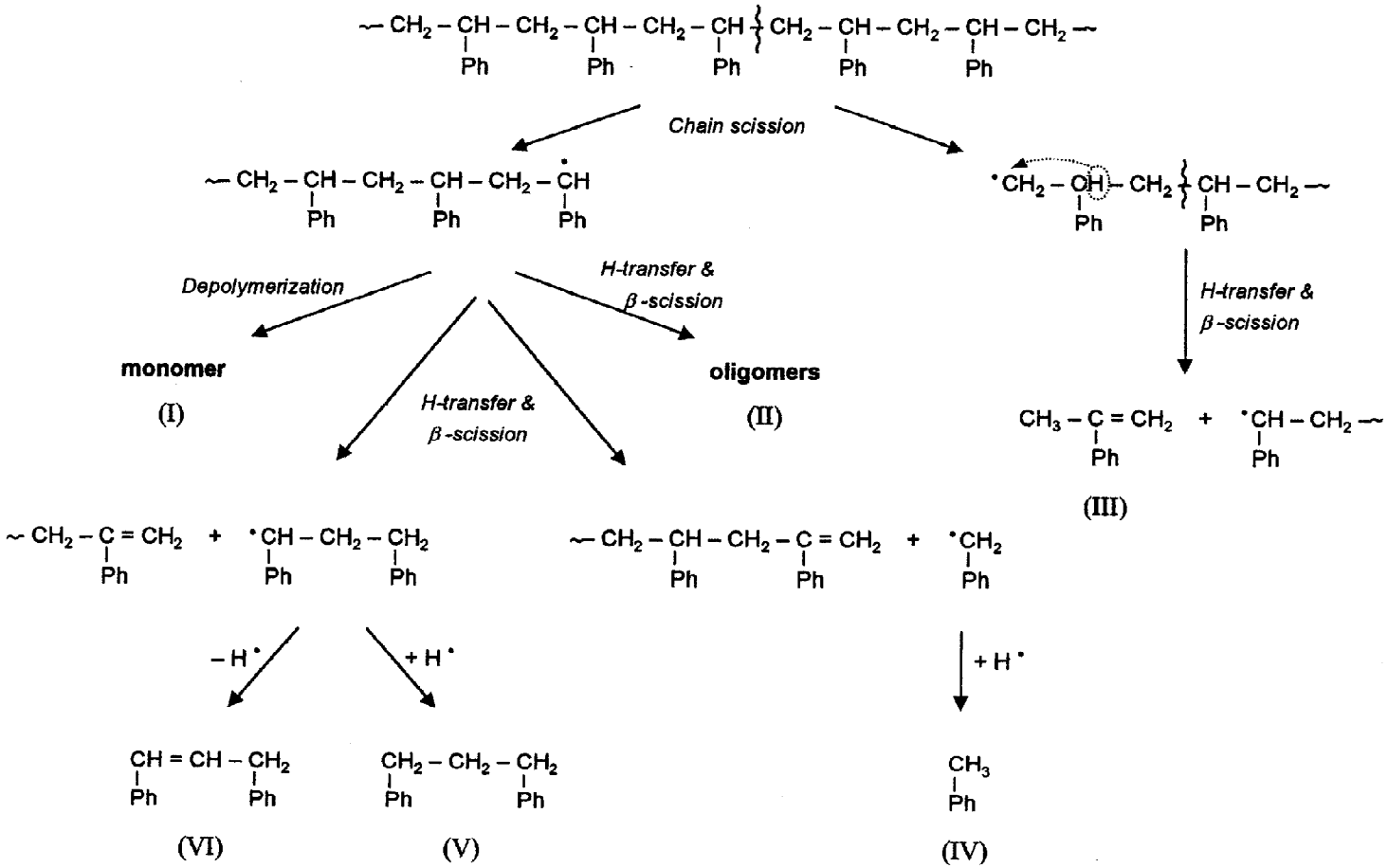

Figure 4.5 PS degradation mechanism in the presence of wood biomass (Jakab et al., 2001)

4.2 Pyrolysis

4.2.1 Pyrolysis of pure feedstock

Initially, pyrolysis of *Sargassum* was conducted at different temperatures to determine the optimum temperature to be applied for co-pyrolysis. The result of product distribution is expressed in Table 4.12 and Figure 4.6. For the different pyrolysis temperatures, significant differences (at α = 0.05 level) are observed among the percents of all products except for water phase product. As the temperature increases, the gas and liquid product, including water and oil phases, increases until it reaches a maximum at 600^{o}C; after 600^{o}C, the yield decreases slightly. However, the opposite trend is observed for the residue. Similar results were obtained by Bae et al. (2011), Jung et al. (2008), Park et al. (2009), Apaydin-Varol et al. (2007), Aguiar et al. (2008), Sensoz and Kaynar (2006), Demirbas (2006), Ucar and Karagoz (2009), Sensoz (2003), Wang et al. (2010), and Park et al. (2008), who conducted pyrolysis of three marine macroalgae, rice straw and bamboo sawdust, oriental white oak, pistachio shell, orange peel residue, soybean cake, four nut shells including hazelnut, walnut, almond, and sunflower, pomegranate seeds, pine bark, herb residue, and Japanese larch, respectively. They explained that incomplete pyrolysis at low temperature leads to high residue, but low gas and liquid product. On the other hand, excessively high temperature results in thermal cracking or secondary decomposition of vapor compounds generating more gases, but lower liquid. Therefore, 600^{o}C was chosen as the optimum temperature for the mixture and other feedstocks.

Table 4.12 Pyrolysis product distribution of different pure feedstocks at different temperatures.

Feedstock	Temperature, °C	Products			
		% Water phase	% Oil phase	% Residue	% Gas[a]
Sargassum	400	21.8(±1.24)	1.67(±0.21)	52.4(±0.31)	24.1(±1.24)
Sargassum	500	23.0(±0.56)	2.38(±0.10)	47.5(±0.75)	27.1(±1.13)
Sargassum	600	23.2(±0.79)	2.90(±0.15)	43.6(±0.09)	30.3(±1.13)
Sargassum	700	22.2(±0.71)	2.50(±0.09)	44.0(±0.30)	31.3(±1.11)
Cedar wood	600	35.2(±1.13)	7.70(±0.12)	32.4(±0.55)	24.7(±1.35)
Recycled pellet	600	0.00(±0.00)	90.2(±0.41)	4.15(±0.59)	5.63(±0.18)

Note: [a] percent gas production obtained by difference.

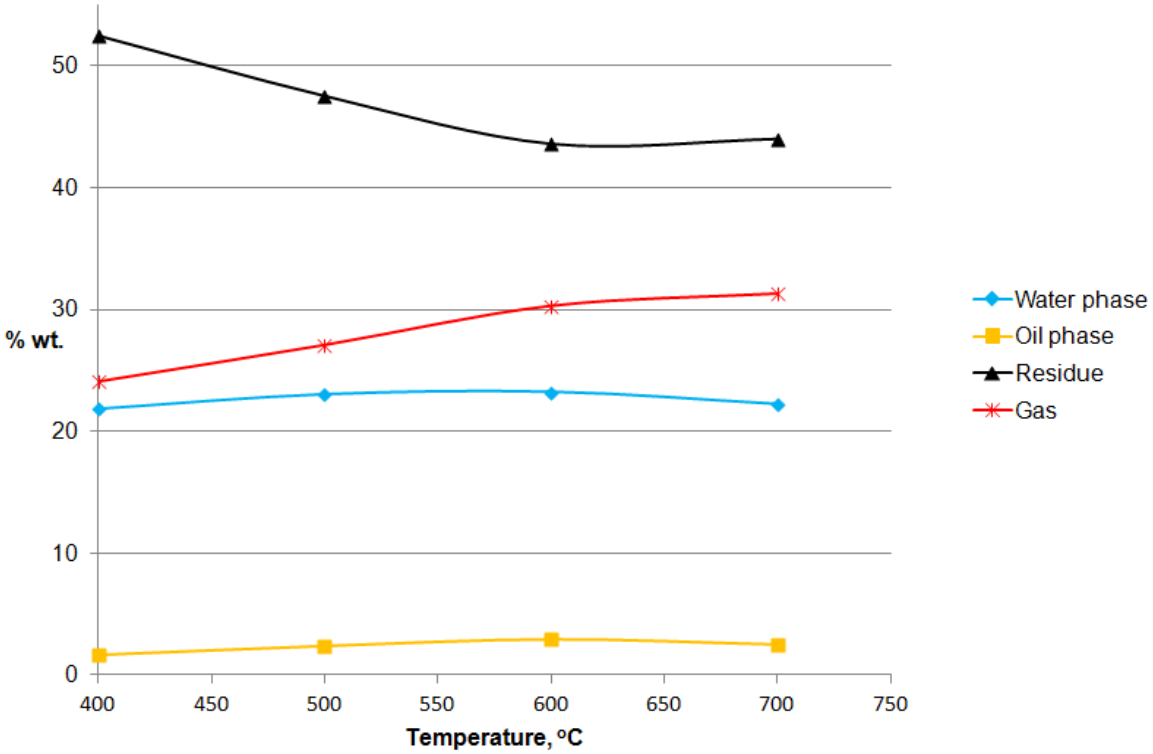

Figure 4.6 Percent pyrolysis product distribution of pure *Sargassum* versus temperature

The oil yield from the algae is much lower, whereas the residue is higher than the cedar wood, which represents terrestrial biomass in this study. This agreed with the results from

TGA; the wood contains more volatile matter but less char than the seaweed. However, both kinds of biomass produce a large amount of water phase since they are rich in oxygen content. Based on TGA results in Section 4.1.2, the seaweed contains about 60% volatile material, but it is mostly converted to either aqueous phase or gas product. The residue of the seaweed is quite high, about 40%, which is comparable to the residue obtained from the TGA at 600^{o}C. As discussed earlier, high metal content in the seaweed is perhaps a reason for this. The illustration of liquid product and char from the algae pyrolysis is shown in Figure 4.7 and 4.8. The water phase has a light yellow color, but the oil phase color is dark brown. The residue after pyrolysis is completely burnt and becomes black.

Bae et al. (2011) investigated pyrolysis of two brown and one red macroalgae at 500^{o}C; they also obtained two phases of liquid product, together comprising 35-45% of the products. The aqueous phase alone represented about half of the total liquid; this is comparable to the 23% water phase product obtained in this study. Nevertheless, their oil phase is much higher than this study, which possibly comes from operating conditions, since the seaweeds from both studies exhibit similar elemental and proximate analysis.

(a) (b)

Figure 4.7 Liquid products from *Sargassum* pyrolysis (a) Water phase (b) Oil phase

(a) (b)

Figure 4.8 (a) *Sargassum* before pyrolysis (b) the residue after pyrolysis

For the pellet, 90% of the material is converted to oil, while no water production is observed. There is a small amount of gas and residue from the pellet, approximately 5% for each product. This result concurs with the TGA result, in which the plastic was almost completely degraded and low residue remained. Similarly, Liu et al. (2000) reported 98% liquid yield from PS pyrolysis at 600^{o}C, with a negligible amount of gas and char (0.70% and 0.20%, respectively). Additionally, Onwudili et al. (2009) investigated pyrolysis of PS at 300-500^{o}C. They noted PS is almost completely decomposed to oil at 350^{o}C, with 1% residue and an insignificant amount of gas. Gas production was highest at 500^{o}C, but was still only about 2.5%. They further studied co-pyrolysis between LDPE and PS blend; they observed that an increase in PS in the plastic mixture results in less gas production. Williams and Williams (1997), Siddiqui and Redhwi (2009), Williams and Slaney (2007), and Pinto et al. (1999)'s work also follow the previous trend.

4.2.2 Co-pyrolysis

The product distribution from co-pyrolysis between the algae and the plastic is demonstrated in Table 4.13. It is clear that the oil phase increases as the ratio of the plastic in the mixture increases and vice versa for other products. The result is reasonable since the product from the pure pellet contains no water phase, and a small amount of residue and gas. In addition, to identify a synergistic effect, a comparison between theoretical and experimental yields is illustrated in Figure 4.9. It should be noted that the moisture content in original feedstock is excluded from the water phase yield. Surprisingly, the oil yield is less than expected, while the water yield is greater, except for the case of 33% plastic. This is corresponded to a lesser amount of gas than predicted. There is some variation in the residue yield, which shows a lower yield at 5 and 15% plastic, then shifts to higher yield at larger plastic ratios.

Table 4.13 Co-pyrolysis product distribution of different mixture ratios at 600^{o}C.

Mixtures	Products			
	% Water phase	% Oil phase	% Residue	% Gas[a]
5% Plastic	25.9(±0.16)	5.90(±0.41)	40.2(±0.98)	28.0(±1.07)
15% Plastic	24.8(±0.22)	12.0(±0.43)	37.2(±0.64)	26.0(±0.14)
25% Plastic	21.0(±0.64)	19.4(±0.40)	35.6(±0.24)	24.0(±0.75)
33% Plastic	16.5(±1.00)	28.9(±0.21)	30.8(±0.30)	23.8(±1.02)

Note: [a] percent gas production obtained by difference.

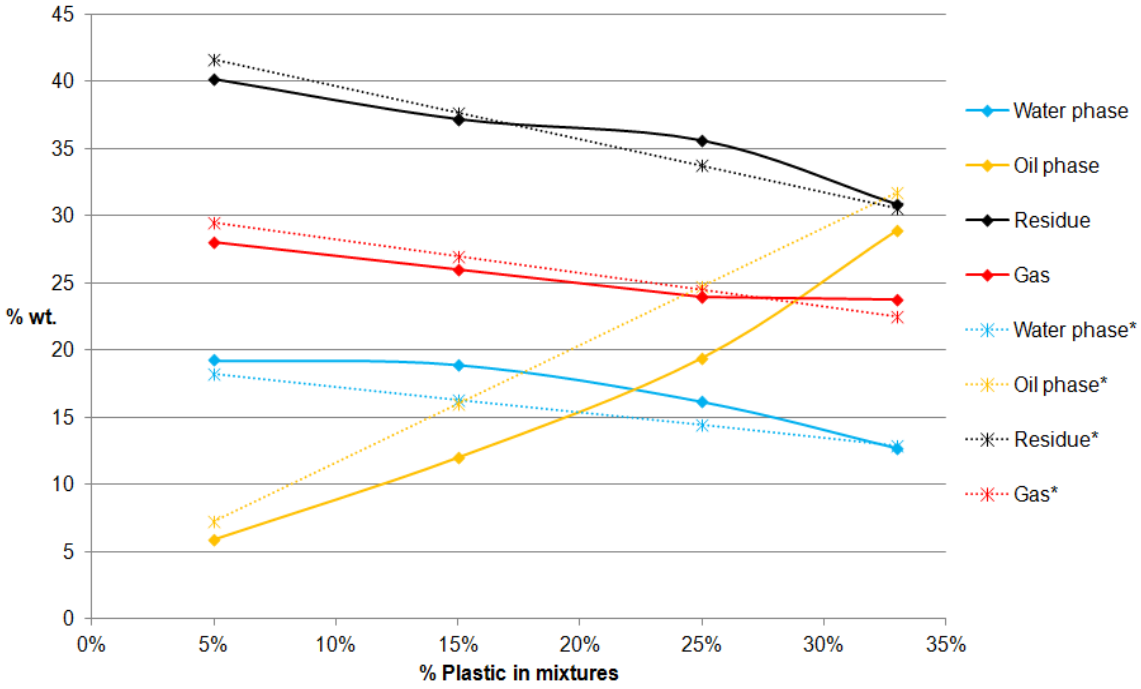

Figure 4.9 Comparison of predicted (dashed lines) and observed (solid lines) product distribution at different mixture ratios

The results illustrated above are unlike those from Cao et al. (2009). Cao et al. investigated an interaction between sawdust and waste tire using 40% and 60% tire ratios at 500^{o}C. They compared the theoretical yield of liquid products based on calculation to experimental values. They observed higher experimental oil yield than predicted, while the aqueous phase varied in proportion to the sawdust ratio in the mixture. Consequently, they noted that the difference in oil comes from the interaction between the two feedstocks. Brebu et al. (2010) also found higher experimental oil yield but lower char compared to theoretical values, in co-pyrolysis of pine cone with different polymers including PP, PE, and PS. They explained that the hydrogen transferred from the polymers possibly diminishes the char formation process. However, there is no influence of co-pyrolysis on gas and water phase yield.

On the contrary, no improvement on the oil yield is reported in Paradela et al. (2009)'s study on co-pyrolysis of pine and plastic wastes at 350-450^{o}C. According to Berrueco et al.

(2004), the synergistic effect yielded higher water phase but lower oil than predicted for co-pyrolysis of 1:1 ratio sawdust and HDPE under temperatures varying from 640-850^{o}C. Moreover, they noticed a substantially higher amount of H_2 production. Thus, they claimed that the water elimination process is enhanced during co-pyrolysis. Berrueco et al.'s explanation of enhanced water elimination may also explain the interaction between the biomass and the polymer in this study. The product characterization in the following section provides additional information about the interaction.

4.3 Oil Characterization

4.3.1 Elemental Analysis

As shown in Table 4.14 below, there is an insignificant variation in carbon and hydrogen content for the seaweed oil at different temperatures, at an α = 0.05 level. In contrast, a significantly lower nitrogen but higher oxygen is shown at 400^{o}C, which possibly indicates more nitrogen bonds are ruptured at high temperature. Compared to the original seaweed, the carbon and hydrogen in the oil is twice as much; however, an increase in both contents does not influence the H/C ratio. On the other hand, a great reduction in oxygen is observed, resulting in much lower O/C ratio than the raw material. Bae et al. (2011) obtained a similar result from pyrolysis of three macroalgae species. In their study, oil from the algae also showed a reduction in oxygen, but an increase in carbon and hydrogen, like that shown in Table 4.15. However, they noted that high nitrogen from the seaweed oil could lead to high nitrogen oxide (NO_x) emissions if it served as fuel. Compared to land biomass, the seaweed in their study exhibited much higher in nitrogen content but comparable in carbon and hydrogen content; these results agree with this study. In our study, the oil from cedar wood has only 1.70% nitrogen, while the *Sargassum* has approximately 8% nitrogen. For the pellet, as expected the oil is rich in carbon, while relatively low in oxygen, similar to the original feedstock. Therefore, it should be noted that the type of feedstock has a great impact on the bio-oil production.

Table 4.14 Elemental analysis of oil production of different pure feedstocks and different temperatures

Feedstock	Temperature, ^{o}C	% C	% H	% N	% O[a]	H/C	O/C
Sargassum	400	74.7(±0.41)	8.80(±0.00)	4.70(±0.01)	11.8(±0.42)	1.41	1.61E-03
Sargassum	500	74.1(±1.11)	8.00(±0.17)	8.10(±0.31)	9.80(±0.85)	1.30	1.32E-03
Sargassum	600	74.4(±0.95)	8.60(±0.71)	8.00(±0.12)	9.00(±0.47)	1.39	1.21E-03
Sargassum	700	73.9(±0.10)	8.80(±0.46)	8.10(±0.50)	9.20(±0.06)	1.43	1.22E-03
Cedar wood	600	71.2(±0.11)	7.20(±0.20)	1.70(±0.05)	19.9(±0.04)	1.21	2.95E-03
Recycled pellet	600	91.2(±0.60)	7.90(±0.27)	0.00(±0.00)	0.90(±0.02)	1.04	8.22E-05

Table 4.15 Bio-oil properties from different biomass feedstocks

Feedstock	% C	% H	% N	% O	References
Undaria pinnatifida (brown macroalgae)	56.5	5.7	7.2	29.8	Bae et al. (2011)
Laminaria japonica (brown macroalgae)	73.5	7.9	5.7	12.9	
Porphyra tenera (red macroalge)	65.7	7.4	9.6	17.3	
Rice straw	49.2	5.55	1.83	43.1	Jung et al. (2008)
Bamboo sawdust	41.4	7.03	2.01	49.6	
Pistachio shell	67.4	7.82	0.42	24.3	Apaydin-Varol et al. (2007)
Soybean cake	67.9	7.77	10.84	13.5	Sensoz and Kaynar (2006)
Pomegranate seed	66.6	8.03	2.23	23.1	Ucar and Karagoz (2009)
Pine bark	63.9	7.61	0.10	28.4	Sensoz (2003)
Herb residue	57.7	7.04	2.14	33.1	Wang et al. (2010)
Japanese larch	57.0	7.0	1.80	34.2	Park et al. (2008)

Note: properties obtained from product at optimum experimental conditions

Further enhancement in the oil quality is detected in the co-pyrolysis oil, as demonstrated in Table 4.16. A significant development is found in higher carbon and lower oxygen, resulting in a much lower O/C ratio, as well as lower nitrogen. Besides, the greater the percent of the plastic, the more improvement can be observed. The oil quality of the mixtures is similar to that of the pellet oil, which consists of low oxygen but is rich in carbon, resulting in a low O/C ratio. However, an obvious influence of the seaweed is a significant nitrogen content, which is not found in the pellet oil.

Table 4.16 Elemental analysis of oil production of different mixture ratios

Mixtures	% C	% H	% N	% O[a]	H/C	O/C
5% Plastic	80.8(±0.31)	7.10(±0.54)	6.60(±0.29)	5.50(±0.10)	1.05	0.65E-03
15% Plastic	83.2(±0.03)	7.40(±0.30)	5.50(±0.91)	3.90(±0.74)	1.07	0.45E-03
25% Plastic	87.9(±0.41)	8.30(±0.16)	2.20(±0.05)	1.60(±0.12)	1.13	0.17E-03
33% Plastic	89.3(±0.72)	8.40(±0.08)	2.00(±0.21)	0.30(±0.03)	1.13	0.00

Even though the co-pyrolysis oil has much better quality than the original seaweed oil, the H/C ratio is low compared to other traditional fossil fuels (Figure 4.10) due to low hydrogen content in the oil. Distilled fuels such as diesel and gasoline normally have high H/C ratios ranging from 1.8- 2.0, but the oil in this study is only 1.05-1.13. The higher H/C ratio gives better oil quality since there is more hydrogen attached to the carbon chain. A probable reason is related to low hydrogen content in both raw materials. From previous elemental analysis, the algae and the pellet contain similar hydrogen content of 3.80%. Therefore, hydrogenation of the oil should be considered for an upgrading and refining process. Otherwise, other rich hydrogen feedstock should be considered in co-pyrolysis.

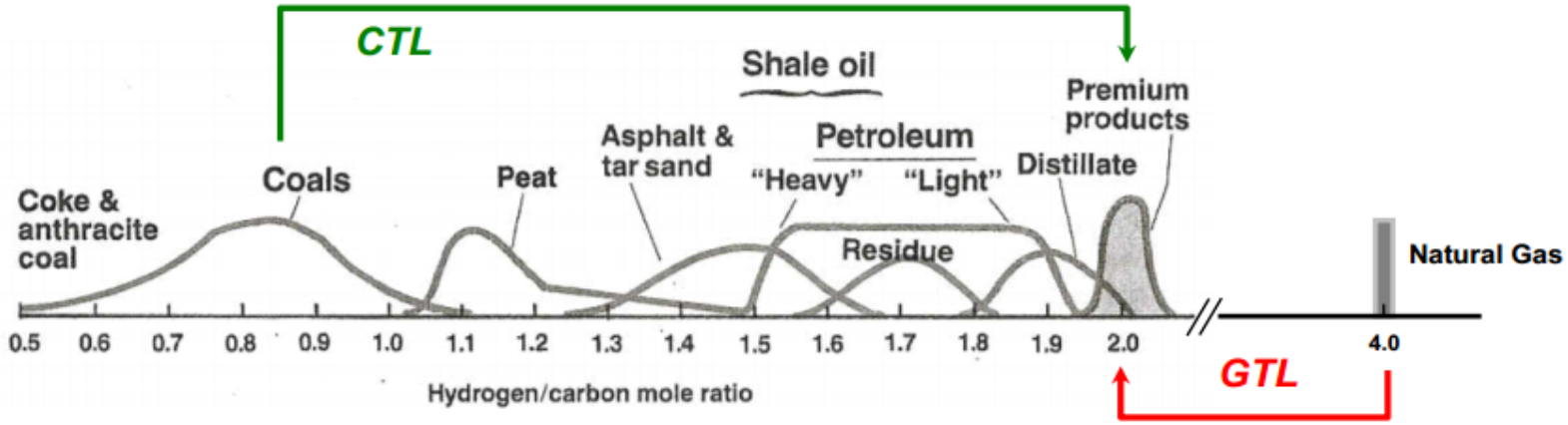

Figure 4.10 H/C ratio in fossil fuels (Winslow and Schmetz, 2009)

4.3.2 Gas Chromatography (GC)

Figure 4.11 below illustrates oil from both pure feedstocks. The red solid line represents *Sargassum* oil, which shows the main peak in the 5-6 minute retention time range, with some significant peaks again at 7-9 minute retention time. In addition, the algae oil responds in small fractions at almost all ranges less than 10 minutes. According to the standard curve in Figure 4.12, and boiling point data in Table 4.17, major compounds in the seaweed oil should be between C_{16}-C_{20}, which have boiling points ranging from 320-390^{o}C. Some C_{28}-C_{36} compounds with boiling points 400-500^{o}C are also present in the oil. Thus, it should be noted that the seaweed oil contains various types of components resulting from carbohydrate decomposition. Based on Ross et al. (2008), and Ross et al. (2009), compounds in the seaweed oil are mainly composed of oxygenated compounds such as ketones, furans, alcohols and pentosans. Besides, nitrogen containing fractions are also reported. Bae et al. (2011) also observed one and two nitrogen compounds in their seaweed oil from three macroalgae species.

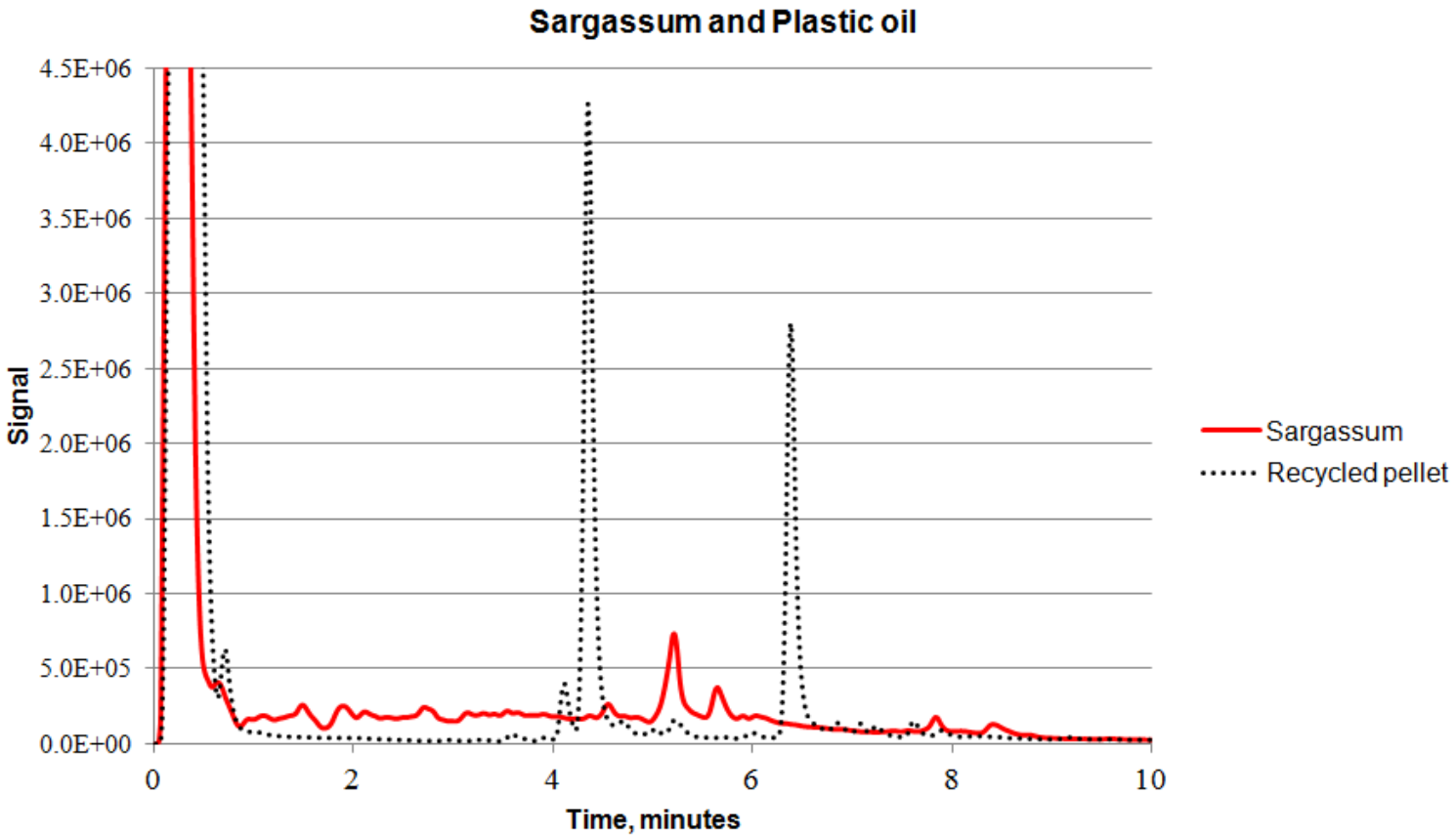

Figure 4.11 Gas chromatography of oil product from pure *Sargassum* and the recycled pellet at 600^{o}C

For the pellet oil, the peak largely concentrates at 4-5 minutes, with another lower peak at 6-7 minute retention time. Compared to the standard curve, the major components in the oil correspond to C_{16}-C_{18}, and C_{24}-C_{28} with boiling points of 280-320^{o}C, and 390-400^{o}C, respectively. According to Liu et al. (2000), liquid product from PS pyrolysis primarily contains styrene monomer, dimer, and trimer with some monoaromatics including toluene, benzene, ethylbenzene, and α-methlystyrene. Furthermore, they differentiated compounds based oil boiling point ranges:

– Low boiling point fraction $\leq$ 200^{o}C consists of styrene and monoaromatics such as benzene, toluene, ethylbenzene, xylene, styrene, α-methylstyrene, and others

– Medium boiling point fraction 200^{o}C < BP $\leq$ 350^{o}C consists of dimer and others such as 1,2-Diphenylethane, 1,3-Diphenylpropane, 2,4-Diphenyl-1-butene (dimer), 2,4-Diphenyl-1-pentene and others.

– High boiling point fraction > 350^{o}C: trimer and others such as 2,4,6-Triphenyl-1-hexane (trimer) and others.

Similarly, Williams and Bagri (2004) and Karaduman (2002) reported high concentrations of styrene and its oligomers as well as other aromatic compounds including benzene, toluene, ethylbenzene, and cumene (Onwudili et al. (2009), Park et al. (2003), Lee et al. (2003), Williams & Williams (1997)). Pinto et al. (1999) suggested that benzene is formed due to bond cracking between aromatic rings and alkane chains, while toluene is formed due to bond cracking of alkane chains. Additionally, Siddiqui and Redhwi (2009) reported PS pyrolysis oil also consists of polycyclic aromatics such as naphthalene, fluorine, diphynylmethane, and phenanthrene, and alkylated derivatives. In light of these previous studies, the two main peaks in this study possibly stand for styrene oligomers and phenyl compounds. However, styrene monomer (C_8H_8) is not detected in this work since the GC is not able to response and separate compounds lower than C_9.

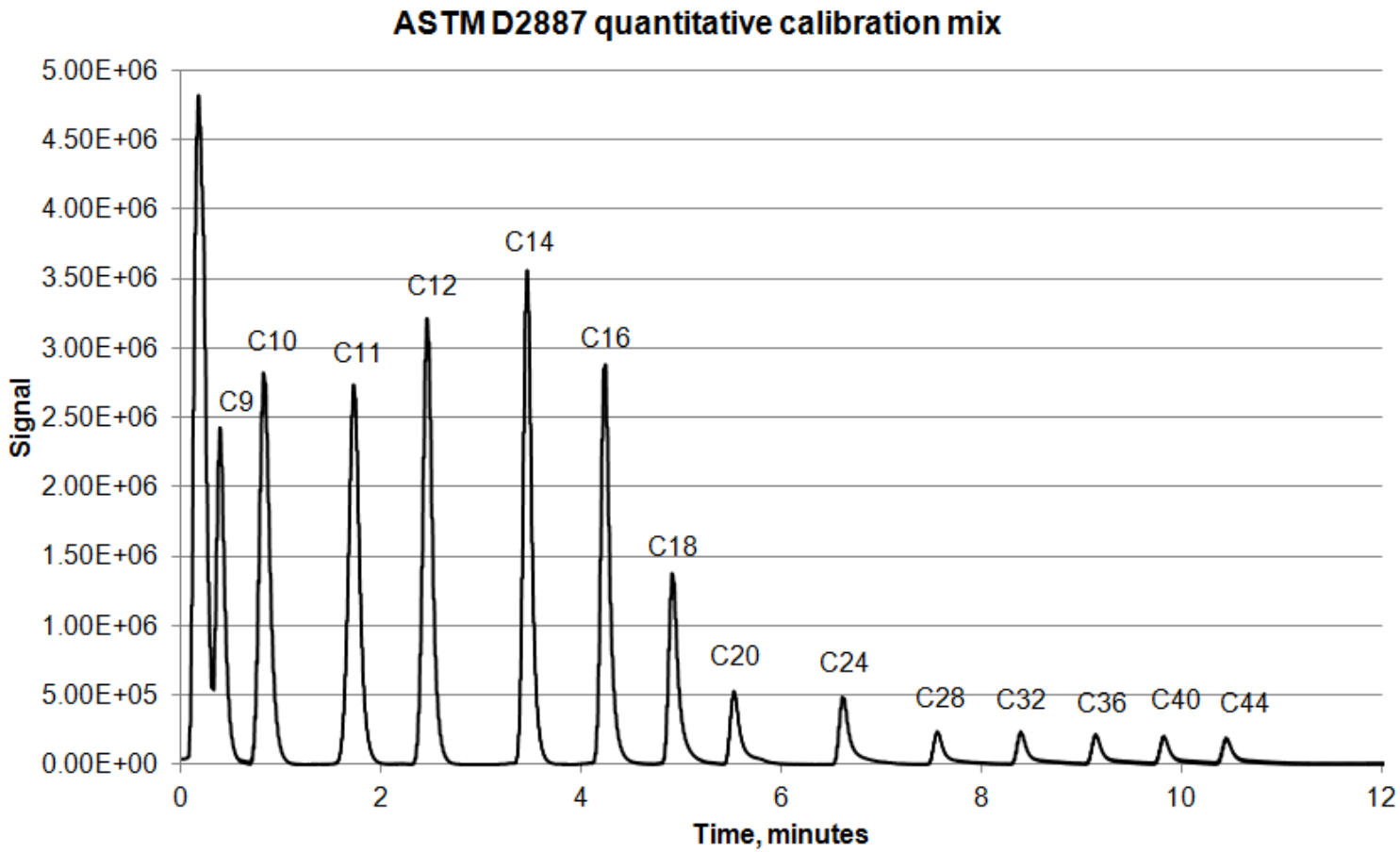

Figure 4.12 Gas chromatography of ASTM D2887 quantitative calibration mix

Table 4.17 Boiling point and retention time of standard components

Name	Formula	Temperature, ^{o}C	Time, minutes
Nonane	C_9H_{20}	151	0.400
Decane	$C_{10}H_{22}$	174	0.816
Undecane	$C_{11}H_{24}$	196	1.716
Dodecane	$C_{12}H_{26}$	216	2.450
Tetradecane	$C_{14}H_{30}$	253	3.450
Hexadecane	$C_{16}H_{34}$	287	4.233
Octadecane	$C_{18}H_{38}$	317	4.900
Eicosane	$C_{20}H_{38}$	359	5.516
Tetracosane	$C_{24}H_{50}$	391	5.600
Octacosane	$C_{28}H_{58}$	408	7.550
Dotriacontane	$C_{32}H_{66}$	450	8.383
Hexatriacontane	$C_{36}H_{74}$	507	9.133
Tetracontane	$C_{40}H_{82}$	525	9.816
Tetratetracontane	$C_{44}H_{90}$	547	10.433

Noticeably, co-pyrolysis oil of the mixture is influenced more by plastic rather than biomass. As the plastic weight increases, the two peaks corresponding to the plastic increase. The experimental peaks are much higher than predicted. Moreover, there is an apparent peak around 3.5-4 minutes which is not observed from either pure seaweed or plastic. This peak is related to compounds with boiling points in the range of 250-280^{o}C, and carbon number between C_{14}-C_{15}. On the other hand, the peak around 5-6 minutes, which is the major peak of the seaweed, is smaller than expected. This should be noted as a result from the interaction.

Rutkowski (2009) conducted co-pyrolysis of pinewood sawdust and PP or PS with 3:1 and 1:1 ratio at 450^{o}C. The characterization of the oil showed that less oxygenated compounds

including carbonyl, carboxylic acid, phenol, and alcohol were detected, which is associated with less oxygen content from their elemental analysis. Likewise, oxygenated compounds produced during co-pyrolysis of sawdust and HDPE at 1:1 ratio were also lower than expected from Berrueco et al. (2004)'s work. Rutkowski and Kubacki (2006) also supports that an interaction between products of cellulose and polystyrene take places during the decomposition of the two materials. As a result, lower amounts of carbonyl groups, and no carboxylic acid or alcohol, is observed in the oil. Additionally, improvements in density, acid number, and pour point of the mixture oil were also reported.

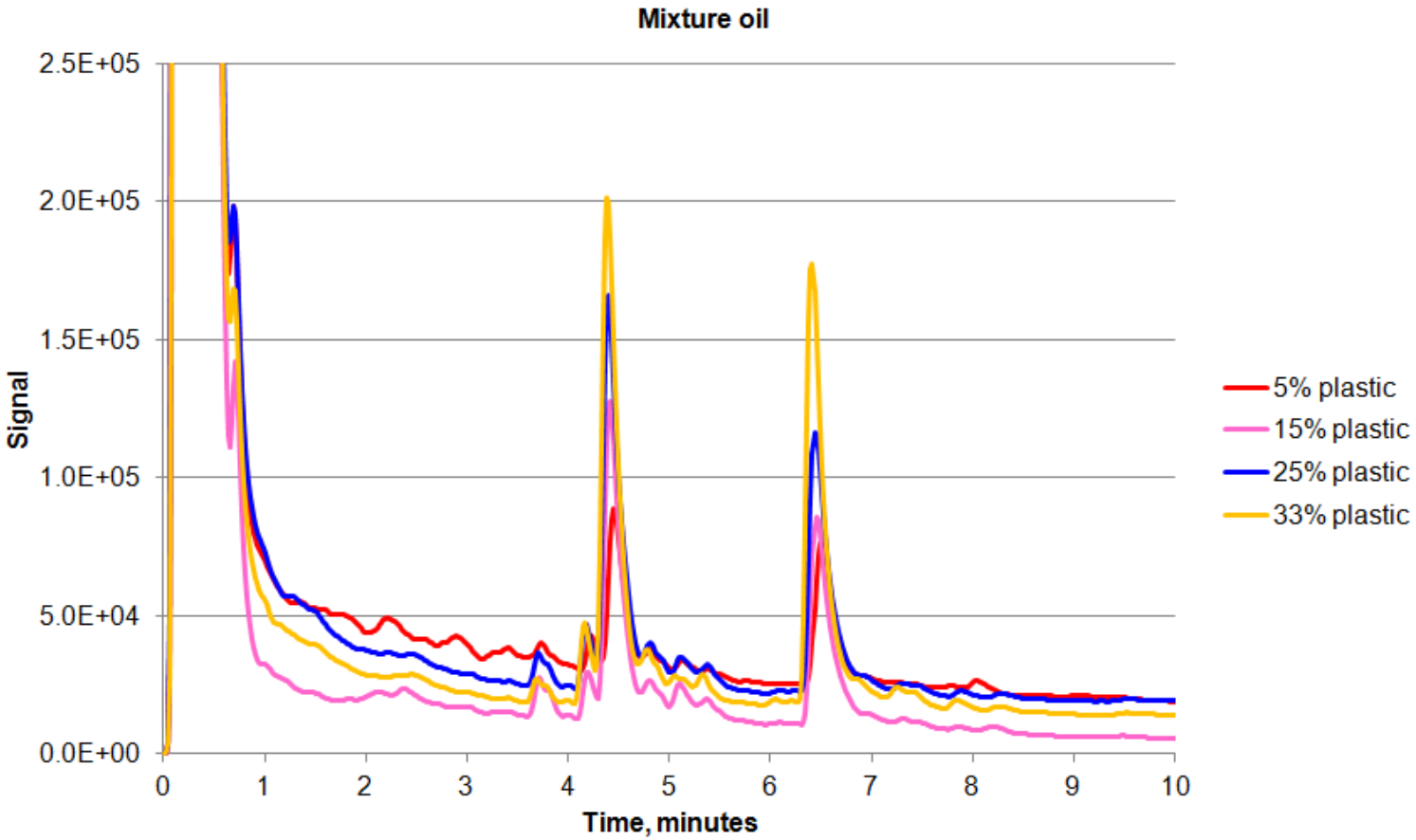

Figure 4.13 Gas chromatography of oil product from the mixtures at different ratios

Sharypov et al. (2002) investigated co-pyrolysis of pine wood, beech wood, and cellulose with PP at 400^{o}C using 20:80, 50:50, and 80:20 ratios. They detected twice as much light liquid product as expected, and less unsaturated hydrocarbon gases. They stated that this possibly stems from interaction between the products of individual components. Marin et al. (2002) and Sharypov et al. (2003) discussed the pathways of synergistic effects after they characterized both light and heavy liquid products. At 400^{o}C the biomass is completely decomposed and produces a solid residue which is relatively reactive and becomes a source of radicals. The biomass radicals soon assist the chain scission process of the polymer, resulting in light liquid product. Once the polymer chain breaks, a combination of biomass radicals and hydrogen transferred from the polymer can lead to different reactions such as depolymerization, dehydration, and dehydrogenation, resulting in various compounds. For example, they reported high amount of some oxygenated compounds and 2-alkenes in heavy and light fractions of liquid product from the mixture, respectively, which can only be ascribed to the interaction between biomass and the polymer. Moreover, they indicated a donation of hydrogen from the polymer helps stabilize products of biomass; as a result, less gas and char are formed, while liquid product increases.

Cao et al. (2009) conversely explored an effect of biomass over tire decomposition when they found much lower polycyclic aromatic hydrocarbons (PAHs) in the mixture oil between sawdust and tire than expected, which is claimed as an evidence of synergistic effect during co-pyrolysis. They discussed a possible reaction in which oxygenated radical species from biomass inhibit the polymerization process of PAH precursors from the tire; as a result, less PAHs are formed during co-pyrolysis.

Based on the previous discussion, it is reasonable to apply the idea of synergistic effect during co-pyrolysis in this study, resulting in lower oxygen-containing compounds from the seaweed, which agreed with the elemental analysis results. However, more plastic side components are generated, which correspond to the higher peak of the pellet oil. Furthermore,

unexpected lower boiling point compounds are examined. It can be concluded that the co-pyrolysis of the seaweed with polymers enhanced oil quality by lowering the oxygenated compounds in the oil. Conversely, there is no obvious difference between the mixture oil compared to the virgin pellet oil since the mixture oil exhibits similar peaks to the pellet oil.

A number of reactions can occur during co-pyrolysis influenced by both biomass and polymers. Chain scission of the polymers is driven by biomass radicals, resulting in hydrogen transferred reactions. Then, the hydrogen from biomass interacts with the macro-radicals from the polymers; consequently, the polymerization of the polymer radical molecules is decreased. In parallel, water elimination from the hydroxyl group of the biomass influenced by hydrogen from the polymer is also happening, resulting in more water phase product with less oxygenated compounds in the oil phase. The water elimination reaction possibly occurs at a higher rate than the oil producing reactions; hence, there is lower oil yield, as reported by others. Nevertheless, an improvement of the oil quality is demonstrated in this study. Less hydrogen component in the raw material is probably a reason: in other studies, polymers with hydrogen content at least 7-8% were used, whereas in this study, polymer with hydrogen content of 3.8% was used. Subsequently, deficient hydrogen helps promotes oil generating reactions since much of the oxygen content of the biomass is removed during the co-pyrolysis via water elimination process.

4.4 Gas Characterization

Four main gas components were analyzed: H_2, CO, CH_4, and CO_2. An example chromatograph is shown in Figure 4.14, and the mass distribution of each gas is demonstrated in Table 4.18. The gas product was collected during three stages at specific time intervals. The first stage, named G_1, represents “an initial stage” in which the gas was collected before the first liquid drops. The next stage is G_2, corresponding to “a reaction stage,” in which liquid product is continuously being produced. The last stage is “a final stage,” or G_3, when no observed liquid is found after the desired temperature is reached. Consequently, development of gas product can be discussed in this work.

Noticeably, a primary gas component from the seaweed decomposition is CO_2, which is emitted at the initial stage, then in lower amounts during the other two stages, as other gases start to develop. During the reaction stage, CO_2 is still the major gas, followed by CO, and CH_4, respectively. H_2 appears only in the final stage at high temperature. This result agrees with Bae et al. (2011), who measured main four gases, H_2, CO, CO_2, and C_1-C_4 hydrocarbons, from two brown and one red macroalgae. For all species they found a similar trend, in which CO_2 is initially the major gas produced from all samples; CO_2 then reduces as the temperature increases. In contrast, C_1-C_4 hydrocarbons and H_2 production increase as the temperature increases, while there is not much variation in CO production.

In addition, Wang et al. (2007) applied TG-MS in their study to investigate changes in gaseous products during pyrolysis of a green seaweed species. They reported CO_2 evolution in the low temperature region (180-500^oC) due to carboxy group in protein and polysaccharide decomposition, as well as at high temperature (720^oC), possibly due to organic residues and carbonate minerals decomposition. H_2 is observed at around 400-600^oC due to polycondensation of the free radicals released during pyrolysis. For CH_4, three peaks show between 180-600^oC, which might come from the secondary reaction of volatiles. The development of CO is hardly discussed because C_2H_4 also responds at the same signal, resulting in overestimated of CO. Moreover, they noted that H_2O shows two peaks at 90^oC and 240^oC due to moisture loss and polycondensation of hydroxyl group, respectively.

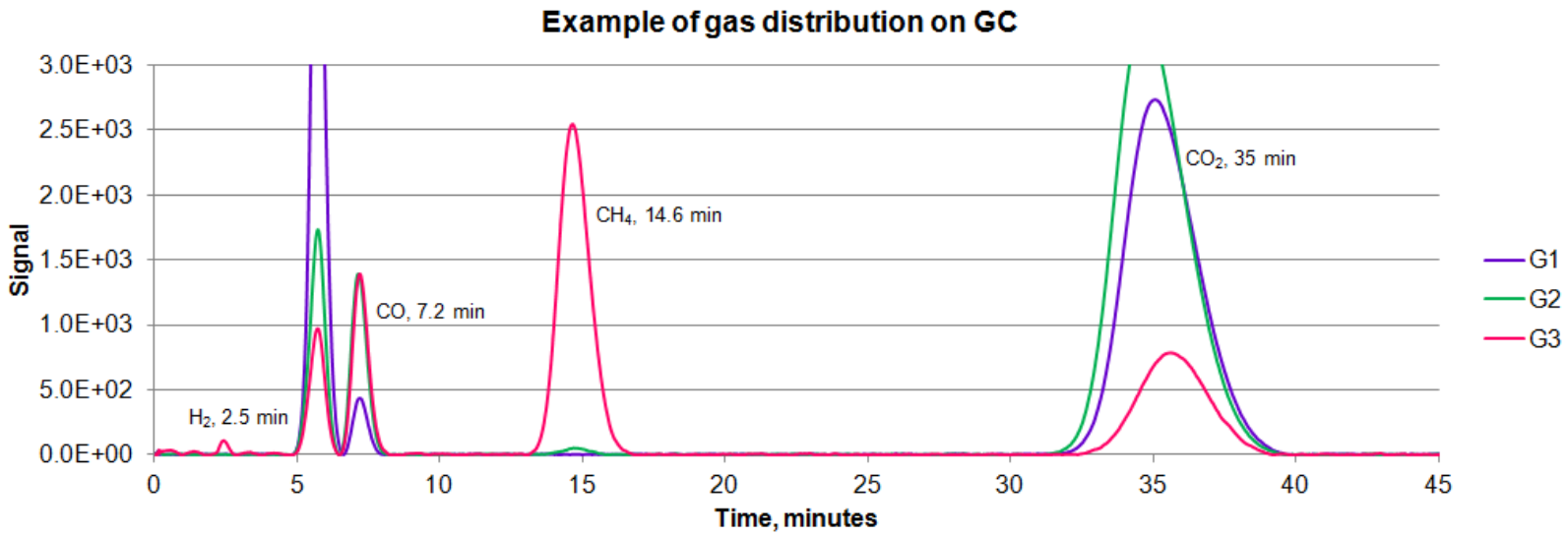

Figure 4.14 Example of gas chromatograph of gas product

Table 4.18 Gas product distribution of pure *Sargassum* and the mixtures

Feedstock	Gas production, % wt.			
	H_2	CO	CH_4	CO_2
Initial stage				
Sargassum	0.0	1-2.5	0.0	97-98
5% Plastic	0.0	0.0	0.0	100
15% Plastic	0.0	0.0	0.0	100
25% Plastic	0.0	0.0	0.0	100
33% Plastic	0.0	0.0	0.0	100
Reaction stage				
Sargassum	0.0	5-10	0.5-3	86-93
5% Plastic	0.0	5-10	2-10	80-93
15% Plastic	0.0	6-12	4-12	75-93
25% Plastic	0.0	5-12	3-7	80-90
33% Plastic	0.0	5-12	2-9	80-90
Final stage				
Sargassum	4.5-6.5	25-35	15-25	40-45
5% Plastic	5-7	30-40	15-25	40-45
15% Plastic	5.5-6.5	30-35	20-25	35-40
25% Plastic	4.5-7.5	25-30	25-30	40-45
33% Plastic	5-6.5	20-30	25-30	40-45

Since the gas produced during the pure pellet pyrolysis is relatively low, it was not analyzed. Therefore, the gas product is discussed according to numerous literatures. Pinto et al. (1999) noted that the main gas production from PS pyrolysis is CH_4 (about 20%), with other C_2-C_5 alkane gas fractions. Karaduman et al. (2001) reported 21-28% CH_4, and a large portion of

C_2-C_4 (60-70%) from pyrolysis of PS under vacuum between 700-875^oC. Onwudili et al. (2009) and Williams & Williams (1997) also observed a high concentration of CH_4 from their experiments. Not only are alkane hydrocarbon gases including methane and ethane, propane, and butane produced during PS pyrolysis, but Williams and Slaney (2007) also detected a low fraction of alkenes. Therefore, it can be concluded that PS gas products mainly consist of hydrocarbons, both alkanes and alkenes, and especially CH_4.

The higher the plastic ratio, the less gas product from co-pyrolysis is emitted throughout the experiment period. On the other hand, gas product distribution for co-pyrolysis shows a similar trend during the three stages to the pure seaweed since it is the main source of gaseous product. However, the mixtures seem to generate higher CH_4, but a little lower CO_2, than the pure seaweed during the second stage. Even though the major gas from the pellet pyrolysis is CH_4 as stated by others, the observed value is much higher than expected. This possibly comes from the interaction between the two feedstocks. The charring process of the seaweed at high temperature may induce the chain scission of the plastic, as discussed earlier; then H_2 is released and further reacted with oxygen gaseous molecules, resulting in another possible reaction, called “a water gas shift reaction” (Eq.1). This reaction is normally presents at high temperature and produces some amount water and CH_4, which agrees with the results in this study.

$$(n/2 + m)H_2 + mCO \rightarrow C_mH_n + mH_2O \qquad \text{(Eq. 1) (Marano and Ciferno, 2001)}$$

The production of CH_4 from co-pyrolysis would be advantageous in that the methane could be burned as an energy source; production of methane gas is preferred over production of CO_2, in which the carbon is already completely oxidized, and therefore has no fuel value. However, if the goal is maximizing production of liquid fuel, then the less transfer of carbon to the gas phase the better. For pyrolysis of pure PS, little gas was generated, with more carbon being retained in the liquid phase.

4.5 Residue Characterization

4.5.1 Elemental Analysis

According to Table 4.19, even though the oxygen content in *Sargassum* residues is lower than the raw feedstock and decreases at elevated temperatures, it is still almost 20% of the content. However, this is possibly overestimated due to sulfur content, as discussed earlier. A significant difference in elemental contents at an $\alpha = 0.05$ level is observed between low and high temperature runs. A similar trend is observed for hydrogen and nitrogen except for 700^{o}C. A decrease in nitrogen content of the residue corresponds to an increase of the nitrogen content in the oil, which confirms that at higher temperature, more nitrogen bonds are cracking, resulting in nitrogen containing compounds deposited in the oil phase. Since the residue contains high oxygen and a significant nitrogen level, it is not attractive as a solid fuel. High oxygen content leads to lower heating value of the fuel, while nitrogen in a fuel can lead to nitrogen oxide emissions when the fuel is burned. On the other hand, the residue could possibly be applied for soil amendment purposes, and would be a good source of nutrients for plants. The residue could also potentially be used as an adsorbent, as will be discussed in Sections 4.5.3 – 4.5.5.

Table 4.19 Elemental analysis of *Sargassum* at different temperatures

Feedstock	Temperature, ^{o}C	% C	% H	% N	% O[a]
Sargassum	400	48.2(±1.20)	2.60(±0.18)	1.80(±0.19)	19.8(±0.63)
Sargassum	500	49.2(±0.40)	2.00(±0.22)	1.60(±0.09)	20.0(±0.33)
Sargassum	600	54.1(±1.41)	1.40(±0.19)	1.20(±0.04)	16.7(±1.14)
Sargassum	700	54.6(±0.17)	1.70(±0.93)	1.40(±0.04)	15.3(±0.77)

Note: [a] percent oxygen obtained by difference, after ash content is subtracted.

The ultimate analysis of co-pyrolysis residue is shown in Table 4.20. There is not much variation in nitrogen, oxygen, and carbon content in the residues. Interestingly, only hydrogen exhibits an obvious trend, which generally decreases in the content as the mass of plastic increases. Moreover, the mixture residues contain less hydrogen than predicted, which again

confirms a synergistic effect between the two materials. As previously mentioned in Section 4.1.2, based on Jakab et al. (2001), a reduction of hydrogen in the residues possibly comes from an enhancement of intermolecular hydrogen transfer, in which the radical molecules from the polymer react with hydrogen from the biomass.

Table 4.20 Elemental analysis of mixture residues at different ratios

Mixtures	% C	% H	% N	% O[a]
5% Plastic	53.9(±0.42)	0.80(±0.07)	1.40(±0.11)	17.1(±0.34)
15% Plastic	54.7(±0.53)	0.70(±0.03)	1.50(±0.71)	16.2(±0.49)
25% Plastic	53.1(±0.62)	0.00(±0.00)	1.60(±0.04)	17.7(±0.33)
33% Plastic	55.2(±0.98)	0.20(±0.04)	1.40(±0.06)	16.1(±1.04)

Note: [a] percent oxygen obtained by difference, after ash content is subtracted.

Similar to the residue from pyrolysis of seaweed by itself, the residues obtained from the co-pyrolysis still contain relatively high oxygen, with a considerable amount of nitrogen, which make it not attractive as the solid fuel. However, nitrogen content of the residues is possibly a good source of natural fertilizers in soil.

4.5.2 Thermogravimetric Analysis (TGA)

TGA analysis is again conducted for the residues after pyrolysis to demonstrate the actual amount of volatile that is pyrolyzed. Therefore, the TGA is carried out only under nitrogen atmosphere to determine the left over volatile matter as shown in Table 4.21-4.22.

Table 4.21 Proximate analysis of *Sargassum* residues from different pyrolysis temperatures

Temperature, ^{o}C	% Moisture	% Volatile matter	% Char
400	2.90(±0.03)	36.9(±0.99)	60.2(±0.73)
500	2.30(±0.27)	30.8(±1.22)	66.9(±0.95)
600	2.22(±0.49)	24.9(±1.23)	72.9(±0.25)
700	1.80(±0.02)	18.8(±0.58)	79.4(±0.84)

There is an obvious loss in volatile matter after pyrolysis, as demonstrated by the proximate analysis of *Sargassum* residues in Table 4.21. Volatile loss ranges from 25-40% compared to the raw material, excluding moisture. A significant difference in volatile and char percents at different pyrolysis temperatures is observed, at an $\alpha = 0.05$ level. As expected, less volatile matter in the residues is observed when pyrolysis temperature is increased, which indicates an increase of the volatile loss as a function of temperature. This result supports a higher yield of liquid product at higher temperature except for 700^{o}C. At 700^{o}C, excessively high temperature possibly causes further thermal cracking of the volatiles, which are converted to gaseous product instead of liquid product.

Table 4.22 Proximate analysis of mixtures residues at different ratios

Mixtures	% Moisture	% Volatile matter	% Char
5% Plastic	1.50(±0.29)	25.2(±0.63)	73.3(±0.88)
15% Plastic	1.30(±0.03)	25.2(±0.81)	73.5(±0.36)
25% Plastic	1.10(±0.26)	25.3(±0.80)	73.6(±1.06)
33% Plastic	2.30(±0.03)	23.4(±0.52)	74.3(±0.01)

For co-pyrolysis, all mixtures contain approximately 25% volatiles, and 74% char in the residue, as illustrated in Table 4.22. The volatile loss after pyrolysis is 42-52% compared to the raw materials. Furthermore, higher loss is observed as the plastic mass in the mixture increases. This observation also corresponds to the product yield from co-pyrolysis, when the higher plastic ratio produces more liquid products.

4.5.3 *Scanning Electron Microscope* (SEM) Image

The residue of pure *Sargassum* at 600^{o}C was further studied by SEM, surface area analysis, and adsorption, since there is an insignificant variation in carbon content between pure and mixture residues. Besides, seaweed produces the main residue from pyrolysis, while more than 90% of the plastic is converted to either gas or liquid product. Two commercial activated

carbons were used as the references to compare their physical properties and adsorption capacity to the seaweed residue. Fitrasorb 200 was the activated carbon used for liquid phase, while the Fluepac-B was used for the gas phase. The pictures of three different materials are shown in Figure 4.15.

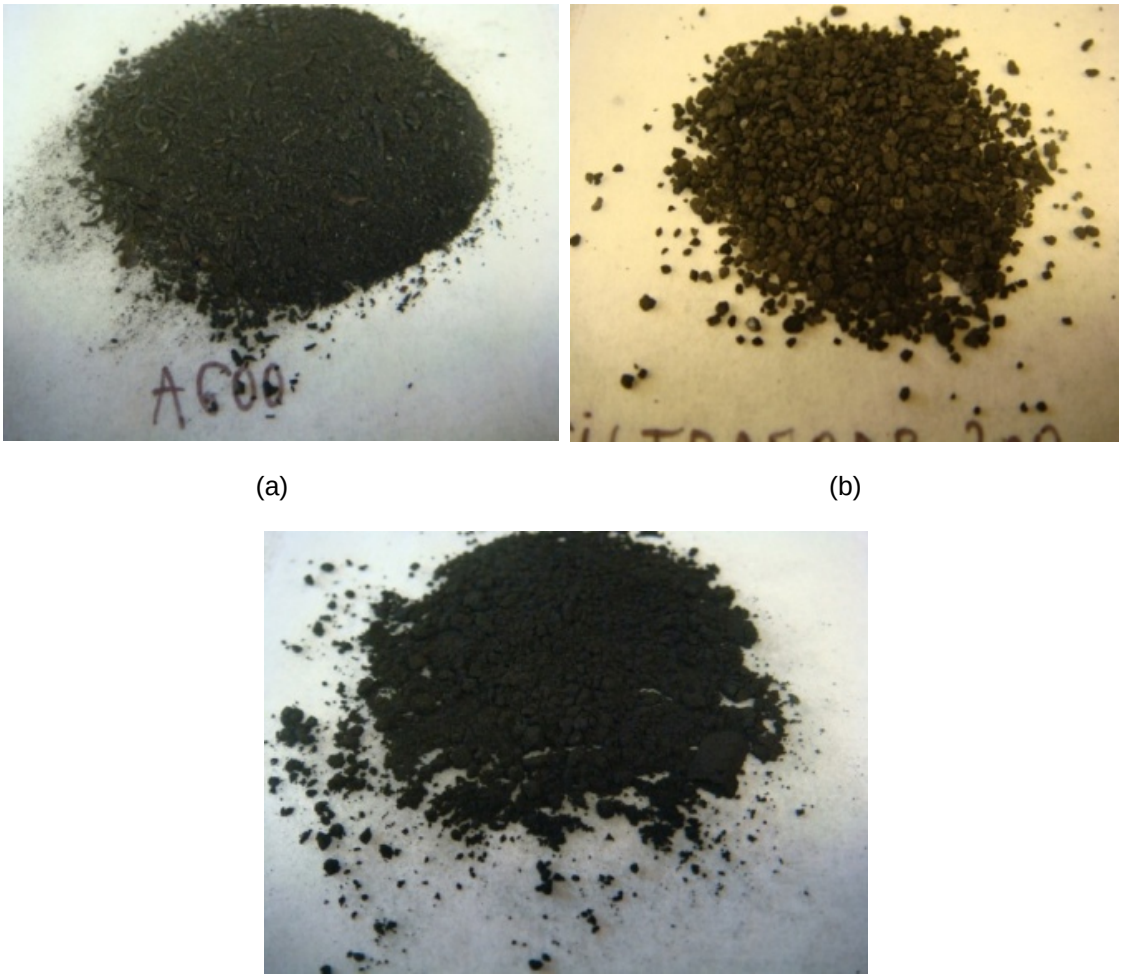

(a) (b)

(c)

Figure 4.15 Image of (a) *Sargassum* residue, (b) Filtrasorb 200, and (c) Fluepac-B

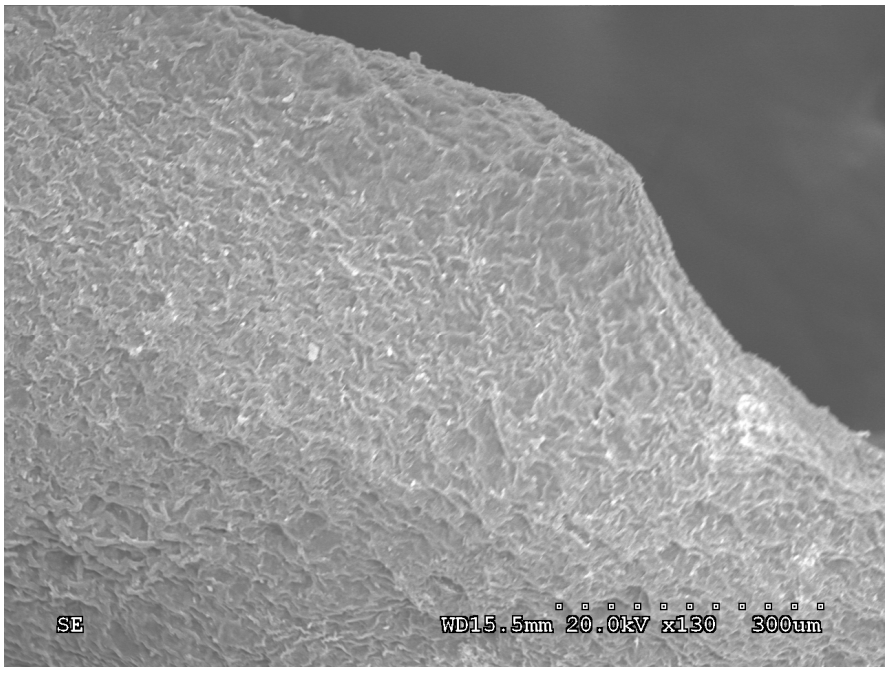

(a)

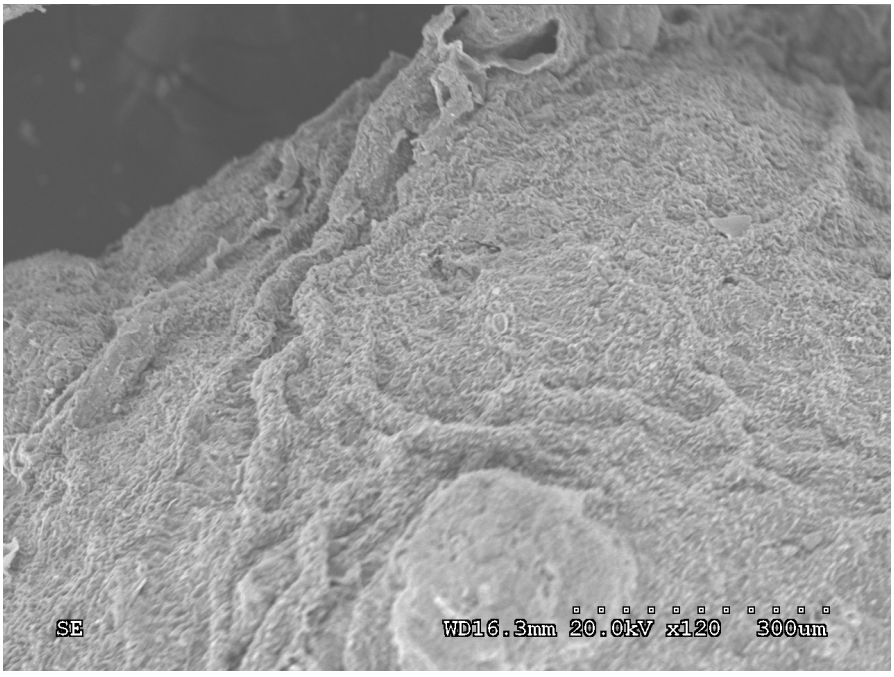

(b)

Figure 4.16 *Sargassum* surface (a) Before pyrolysis, and (b) After pyrolysis

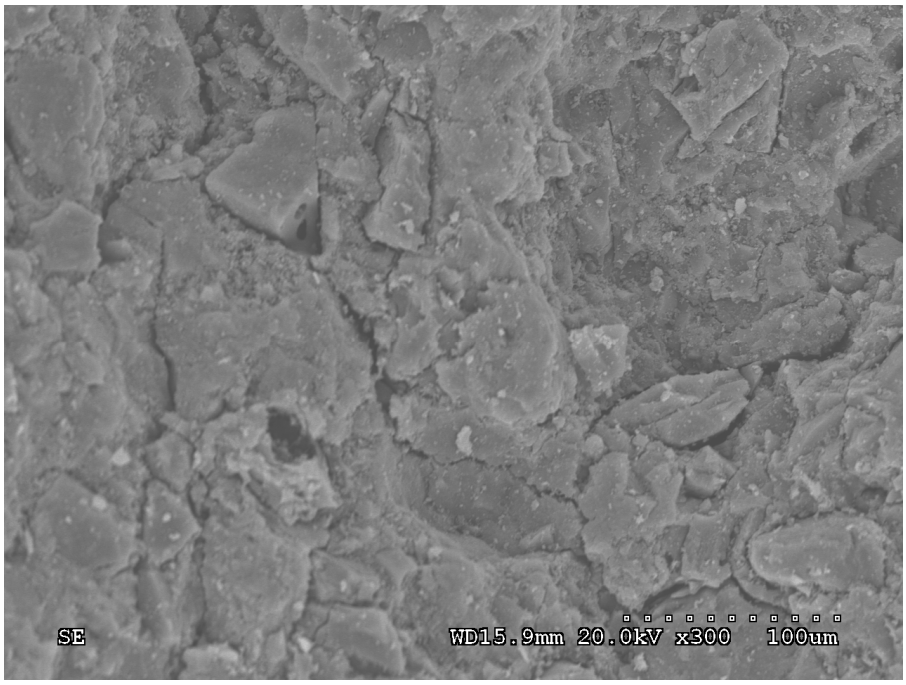

(a)

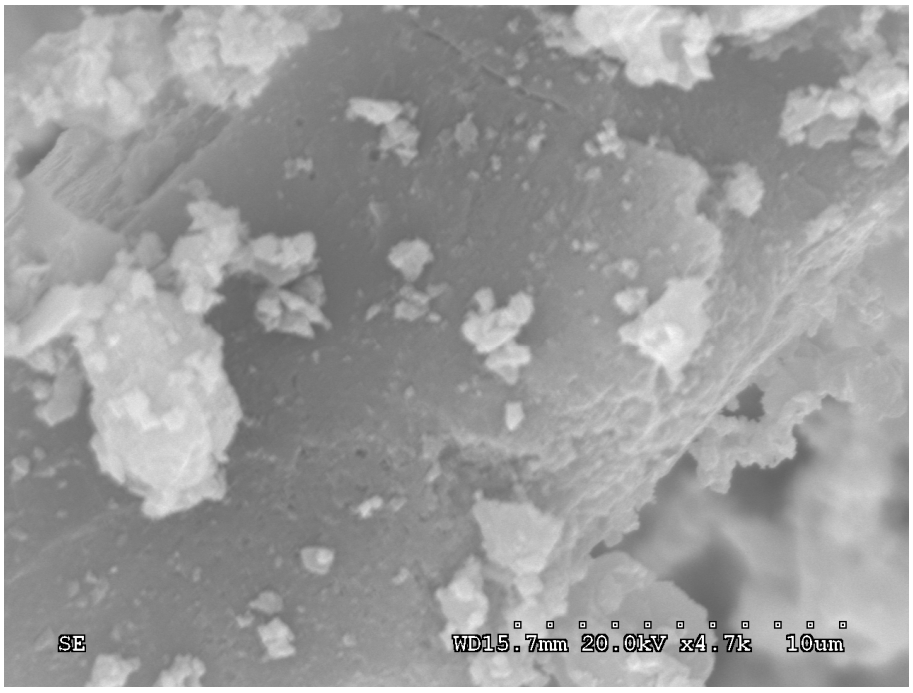

(b)

Figure 4.17 Surface of commercial activated carbon (a) Filtrasorb 200, and (b) Fluepac-B

SEM images of the seaweed before and after pyrolysis are shown in Figure 4.16. The magnification used is an optimum condition for this study since the material is non-conductive; thus, a larger magnification could not be applied. It is noticeable that the surface of the seaweed becomes rougher and drier due to dehydration and devolatilization of volatiles. However, the pores of the seaweed are not shown in the Figure 4.16(b). This may be due to two reasons: either the seaweed contains pores that are too small to observe, or no pores were created during the pyrolysis process. In Figure 4.17, Filtrasorb 200 shows uneven surface area and some cracks, while Fluepac-B surface is relatively smooth. Similar to the seaweed, the pores of both of the commercial adsorbents are not observed.

4.5.4 Surface Area Analysis and N_2 Gas Adsorption

To determine the potential of the residue as an absorbent, the carbon content, surface area, pore volume, and pore size are important physical properties to characterize. Elemental analysis results are presented in Table 4.23. Even though carbon content in the seaweed residue increases after pyrolysis, the seaweed residue still contains much lower carbon, but higher oxygen, than the commercial carbons. Moreover, the residue exhibits extremely small surface area and total pore volume compared to the commercial adsorbents, as shown in Table 4.24. Bird et al. (2011) observed similar results when they investigated biochars from eight different species of green macroalgae following pyrolyzed at 300-500^{o}C. They reported low biochar carbon content, which varied from 20-32%, depending on pyrolysis temperature and algae species. In addition, BET surface areas for biochars in their work ranged from 1.15 m^2/g to 4.26 m^2/g, which is similar to the surface area of 4.60 m^2/g in this study. Furthermore, they noticed that higher pyrolysis temperatures yielded larger surface areas. Additionally, they compared their results to those for other biochars, including char from poultry waste and terrestrial biomass; they concluded the biochars from seaweed exhibits similar properties to chars from poultry waste, but different from terrestrial biomass.

According to Chun et al. (2004), terrestrial biomass residue has much larger surface area than the algae. Char derived from pyrolysis of wheat between 300-700^{o}C results in high BET surface area, ranging from 116-438 m^2/g, with area increasing as temperature increases, except for 700^{o}C, which resulted in a reduced surface area. They claimed that excessively high temperature damages fine pore structures of the wheat char. Moreover, the wheat residue also provides higher carbon content, approximately 70-88% which is comparable to the commercial absorbents, although the surface area is lower. However, Mullen et al. (2010) examined the chars from pyrolysis of corn cob and stover at 500^{o}C. The corn cob and stover residues have BET surface areas of 0 and 3.1 m^2/g, respectively, even though both of them have relatively high carbon content, ranging from 57-78%. Bird et al. (2011) recommended that low surface area biomass residues, like those from seaweed, be beneficially reused as soil amendments and organic fertilizers, since the seaweed residues contain significant cations, phosphorus, and nitrogen.

Table 4.23 Comparison of elemental analysis for commercial activated carbons and the seaweed residues

Materials	% C	% H	% N	% O
Sargassum residue	54.1	1.40	1.20	16.7
Filtrasorb 200	84.3	1.00	0.50	14.2
Fluepac-B	73.7	1.50	0.40	24.4

Table 4.24 Comparison of surface area and pore volume for commercial activated carbons and the seaweed residue

Property →	BET Surface Area	Bulk Density	Total Pore Volume
Carbon ↓	(m^2/g)	(g/cc)	(cc/g)
Fluepac-B	522	0.36	0.239
Filtrasorb 200	845	0.61	0.387
Sargassum residue	4.60	0.60	0.013

The adsorption isotherms under N_2 atmosphere for *Sargassum* and commercial adsorbents are illustrated in s 4.18, and 4.19, respectively. The seaweed residue adsorbs less than 10 cc/g of the gas volume at STP, whereas the adsorption capacity of Filtrasorb 200 and Flupac-B are as much as 250 and 180 cc/g of gas at STP, respectively. This result corresponds to the higher surface area and pore volume of the commercial adsorbents.

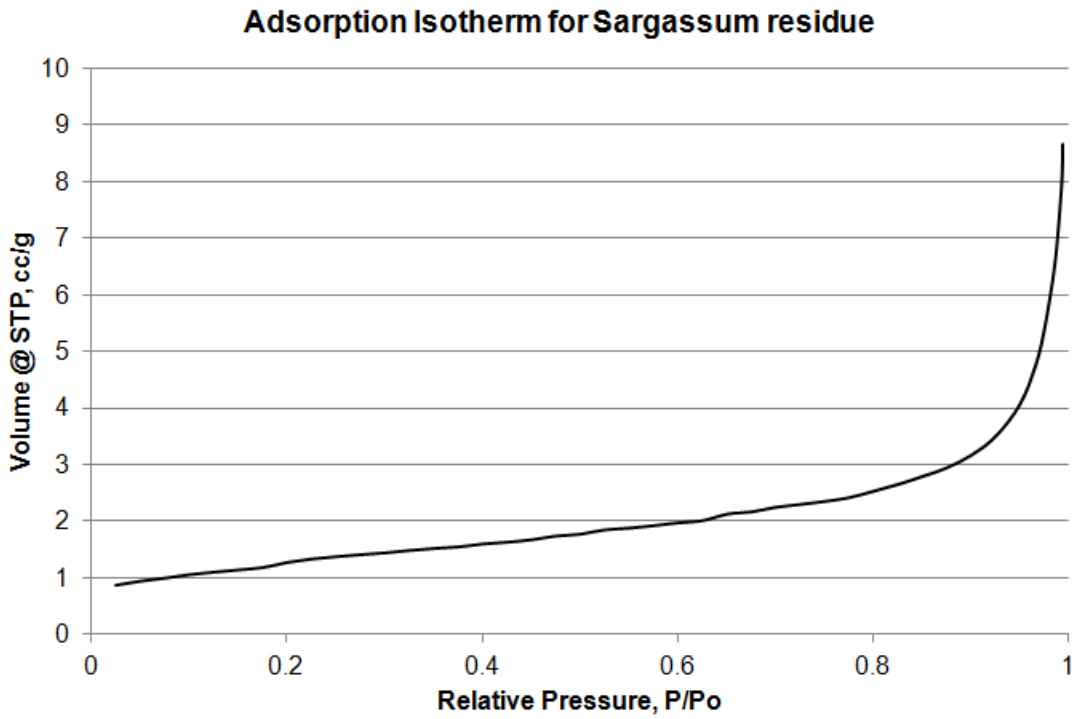

Figure 4.18 Adsorption isotherm of *Sargassum* under N_2

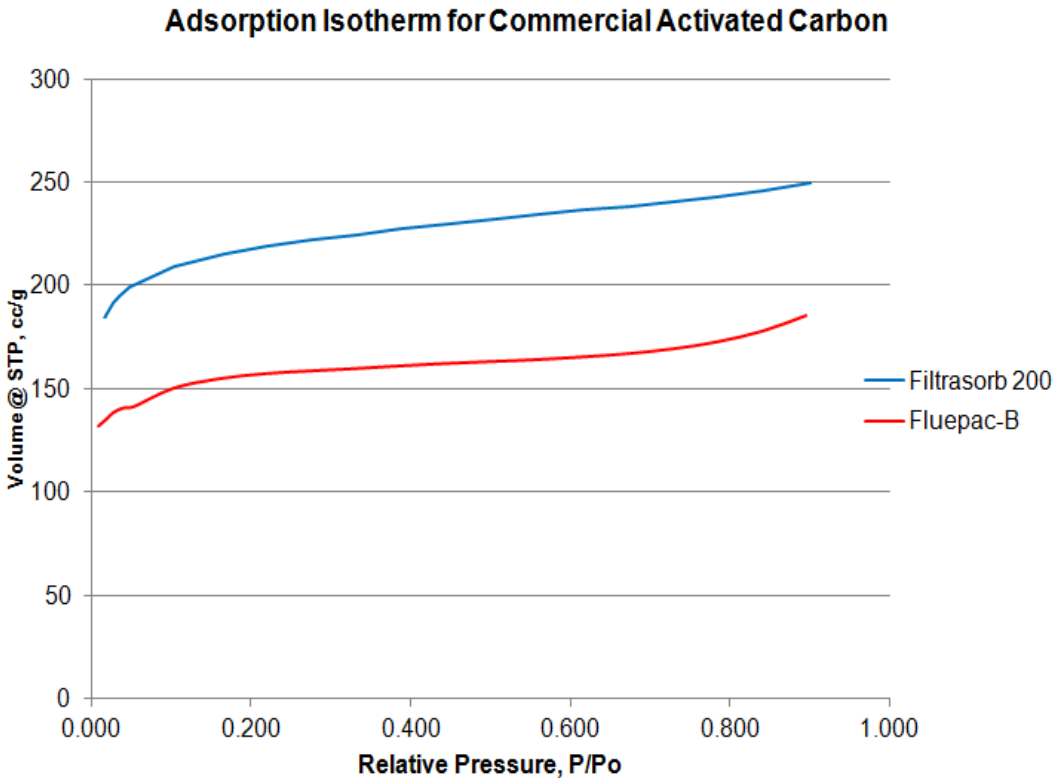

Figure 4.19 Adsorption isotherm of commercial activated carbon under N_2

4.5.5 Liquid Phase Adsorption

Liquid phase adsorption was conducted using methylene blue or MeB ($C_{16}H_{18}N_3SCl$) as an adsorbate. The concentration of MeB was evaluated using ultraviolet-visible spectroscopy (UV-vis) with 610 nm wavelength. Initially, the equilibrium time of the seaweed residue and Filtrasorb 200 was determined. *Sargassum* char reached equilibrium in about 4-5 hours (Figure 4.20), while the commercial activated carbon took 5 days to reach the equilibrium (Figure 4.21) since it has higher surface area and is capable of adsorbing more adsorbate.

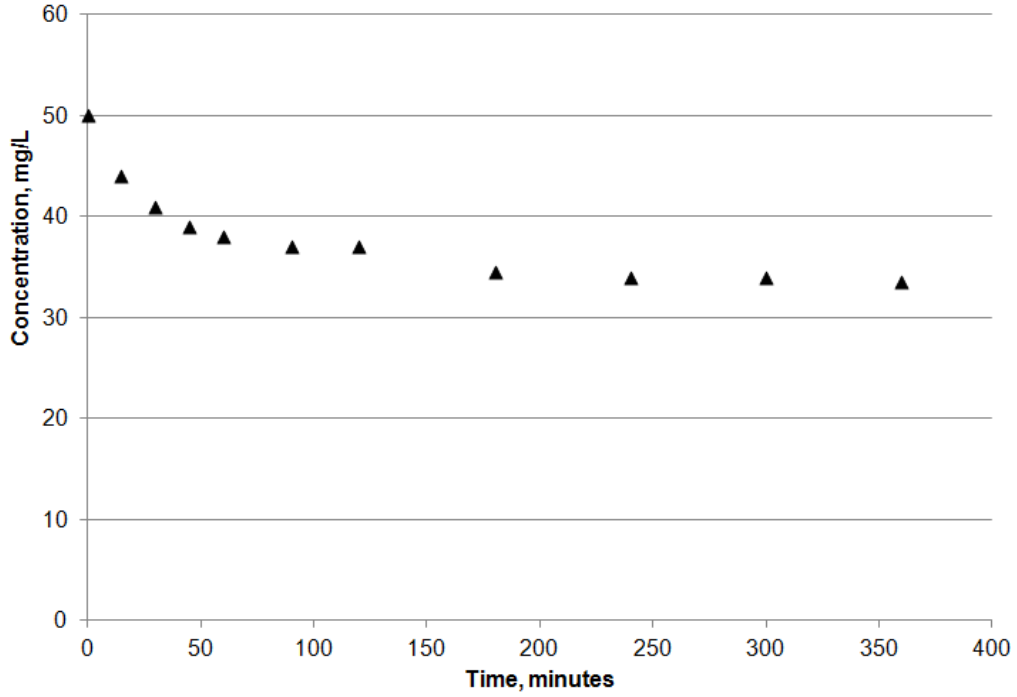

Figure 4.20 Equilibrium time for *Sargassum* residue after pyrolysis at 600^{o}C with MeB

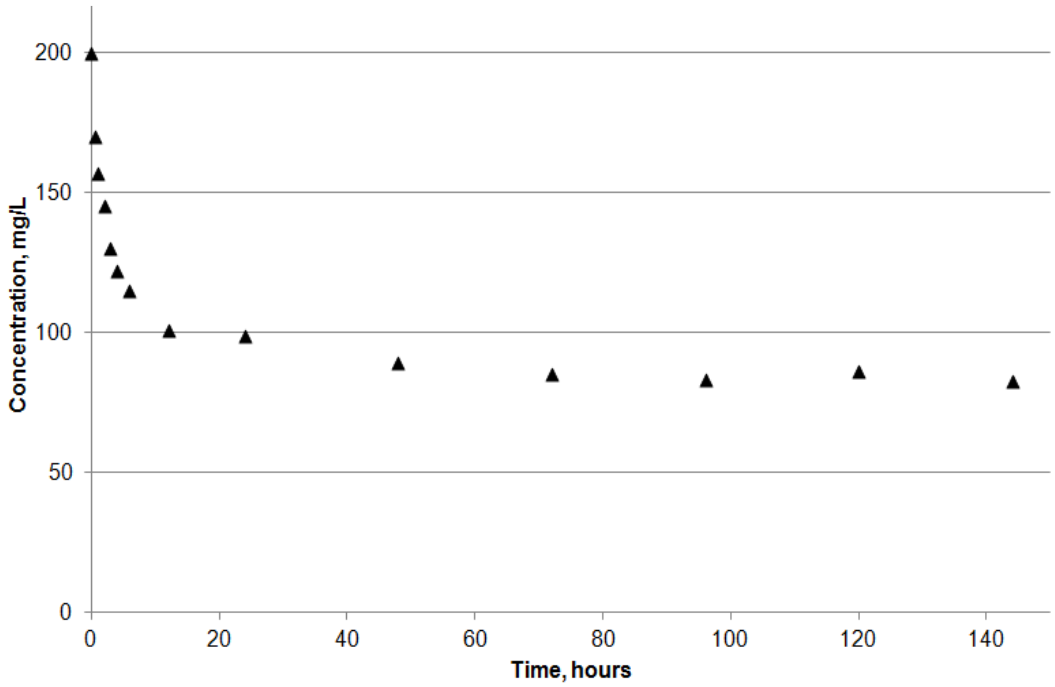

Figure 4.21 Equilibrium time for Filtrasorb 200 with MeB

Once the equilibrium time was verified, an adsorption isotherm experiment was carried out. Samples of MeB solution were collected as illustrated in Figure 4.22. The plots of MeB concentration at equilibrium versus the amount of MeB adsorbed per gram of the adsorbent are shown in Figures 4.23 and 4.25 for the seaweed and the commercial adsorbent, respectively. Besides, experimental data are compared with two common adsorption models, Langmuir and Freundlich (Arana and Mazzoco, 2010). The equation for each model is given below.

$$C_e/q_e = \frac{1}{b \bullet q_{max}} + \frac{C_e}{q_{max}} \quad \text{(Eq. 2)}$$

$$q_e = K_f \bullet C_e^{\,1/n} \quad \text{(Eq. 3)}$$

where q_{max} = maximum adsorption capacity, mg adsorbate/ g adsorbent

q_e = adsorption capacity at equilibrium, mg adsorbate/ g adsorbent

C_e = solution concentration at equilibrium, mg/L

b = Langmuir equilibrium constant, L/g

K_f = Freundlich adsorption constant, $(L/g)^{1/n}$

$1/n$ = a degree of adsorption

The Langmuir model assumes single monolayer assumption, and no interaction between adsorbate molecules. The Freundlich model represents a logarithm relationship between the equilibrium concentration and the adsorption capacity.

(a)

(b)

Figure 4.22 (a) Filtrasorb 200, and (b) *Sargassum* residue

The curve-fits to the data with the Langmuir and Freundlich models are shown in Figures 4.24 and 4.26 for *Sargassum* residue and Filtrasorb 200, respectively. Both models provide a relatively high correlation coefficient (R^2) for the curve-fit of the seaweed, while Freundlich gives a better R^2 for the commercial carbon. Based on the Langmiur equation, the maximum adsorption capacity of Filtrasorb 200 is approximately 300 mg adsorbate/g adsorbent, while it is ten times lower for the seaweed residue.

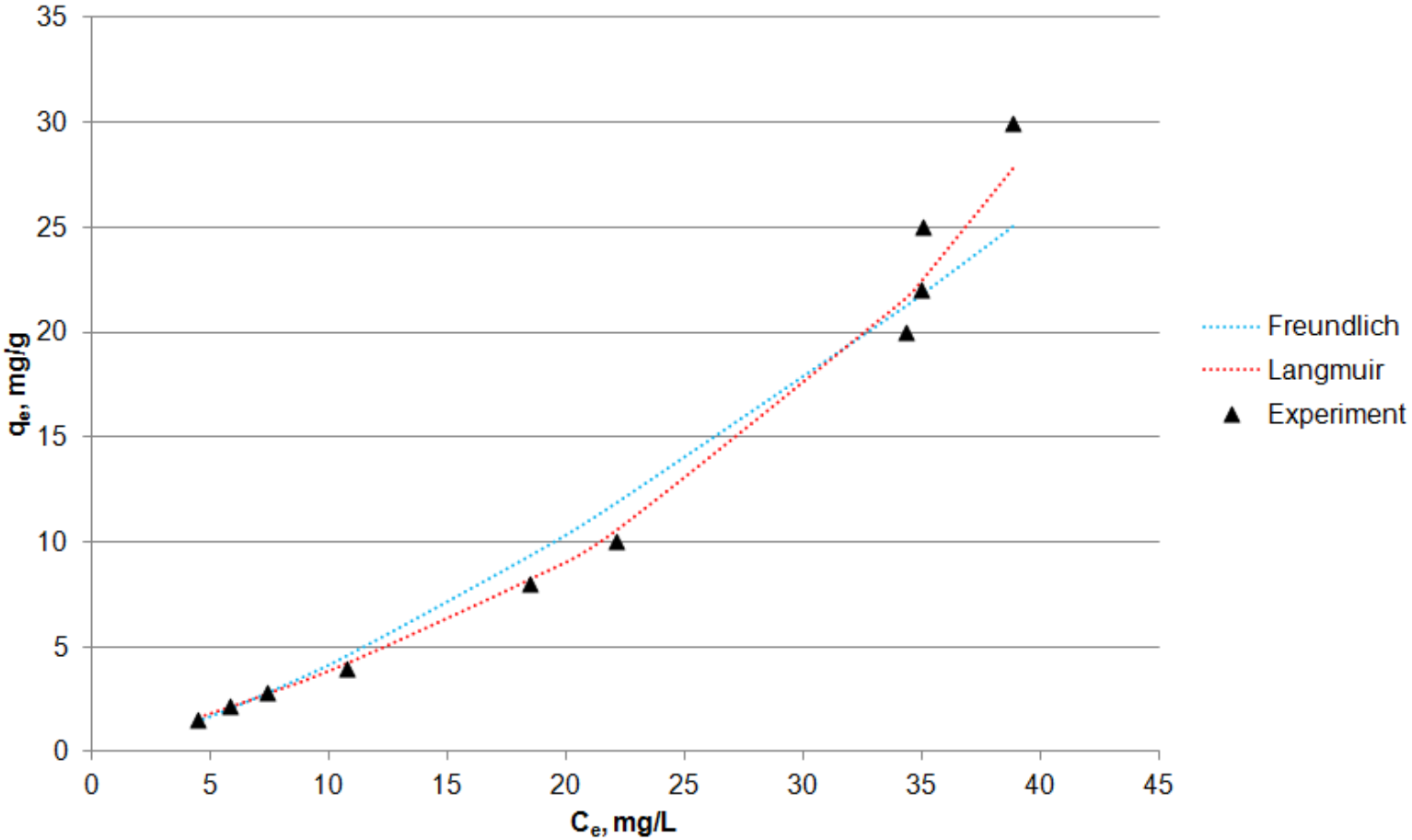

Figure 4.24 Adsorption isotherm of *Sargassum* residue

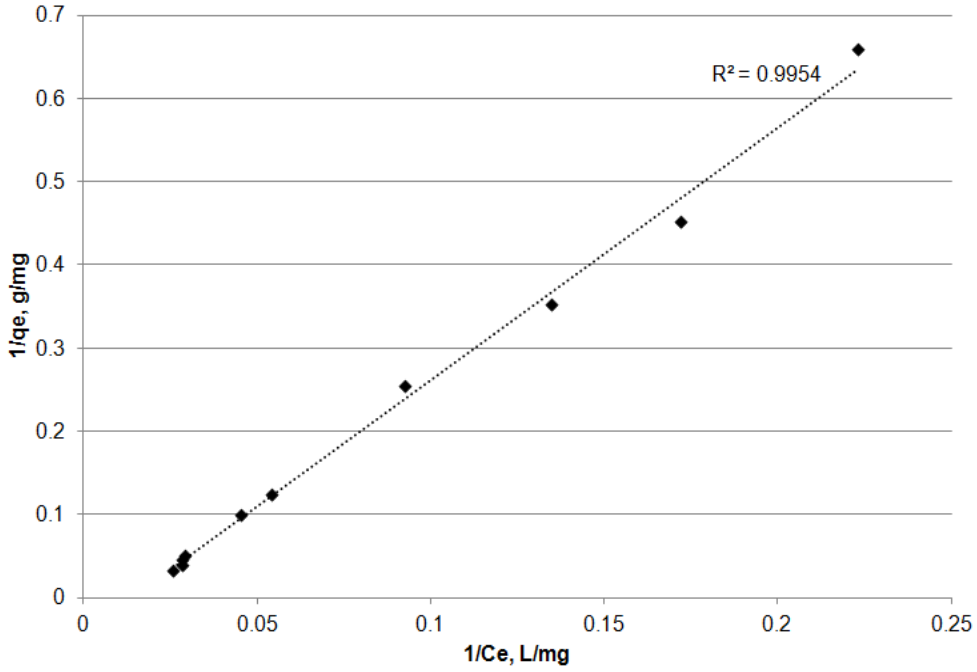

(a)

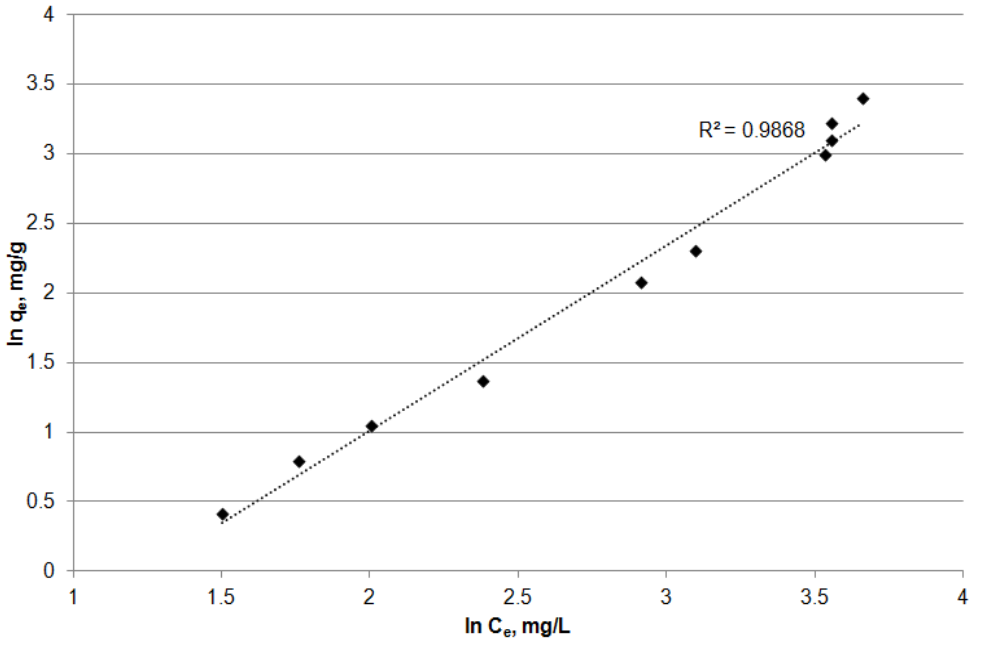

(b)

Figure 4.24 *Sargassum* experimental data curve-fit with (a) Langmuir, and (b) Freundlich model

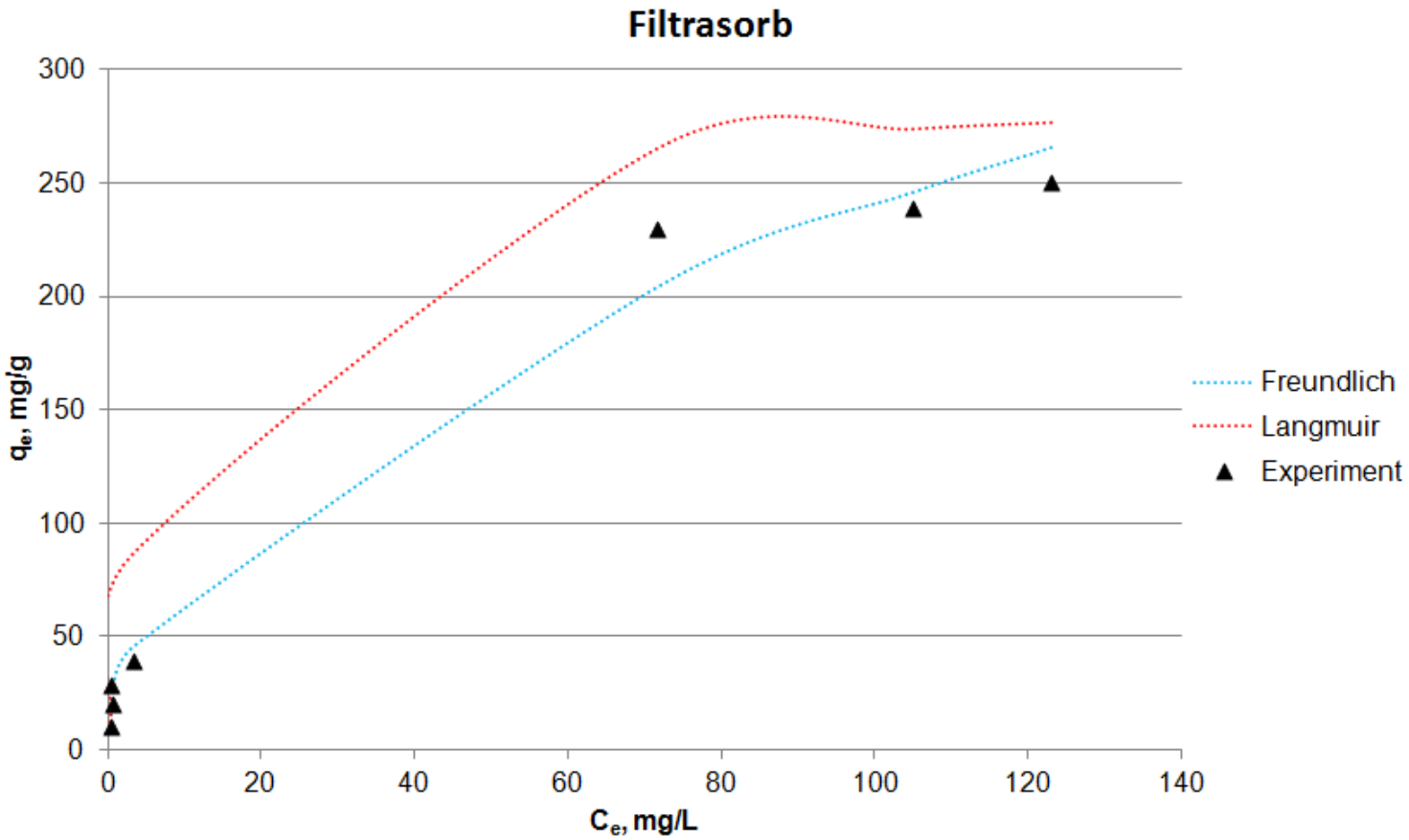

Figure 4.25 Adsorption isotherm of Filtrasorb 200

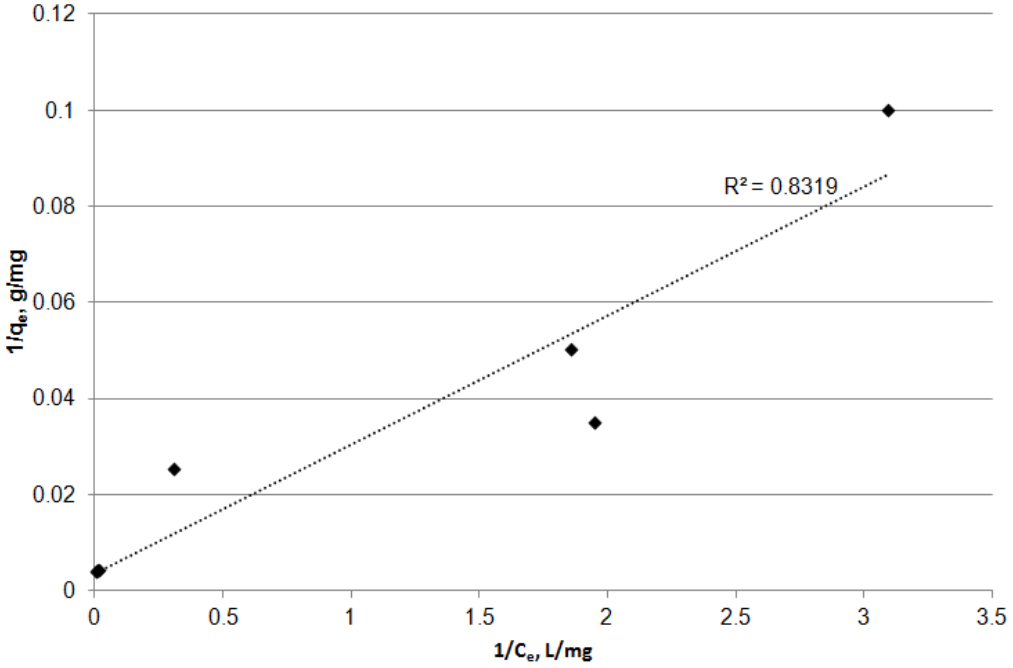

(a)

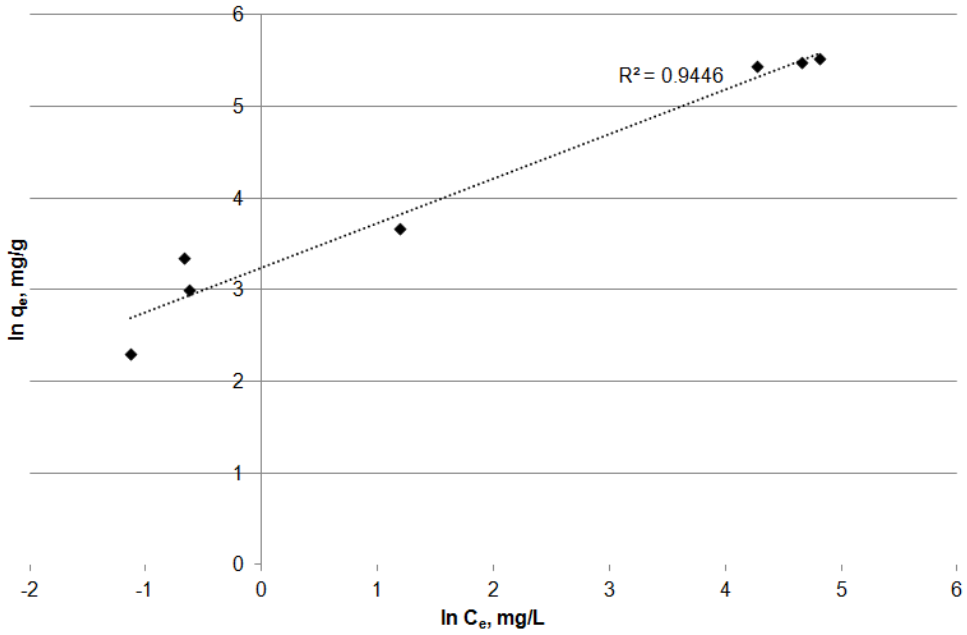

(b)

Figure 4.26 Filtrasorb 200 experimental data curve-fit with (a) Langmuir, and (b) Freundlich model.

4.5.6 Residue Metals Analysis

An additional analysis on the residue of pure seaweed was conducted using inductively coupled plasma mass spectrometry (ICP-MS) to determine the concentration of various metals, which could contribute to ecological problems if the residue is deposited in the environment. As previously mentioned, the main metals in the seaweed are alkali and alkali earth metals including Na, K, Ca, and Mg, since the seaweed comes from the marine environment. Besides, high level of Si and Al are observed, as well as some trace amounts of Sr, Ni, Cu, and Zn. The metals analysis results are listed in Table 4.25. To determine whether these concentrations pose a concern, a toxicity characteristic leaching procedure (TCLP) test would need to be conduction.

Table 4.25 Metals analysis

Metals	Concentration (ppm)	Metals	Concentration (ppm)
Na	12700	Mn	Not detected
Mg	1030	Co	Not detected
Al	2650	Ni	3.80
Si	2360	Cu	3.50
K	3160	Zn	6.75
Ca	4080	As	Not detected
Cr	Not detected	Sr	181
Fe	82	Pb	Not detected
Cd	Not detected		

4.6 Water Phase Characterization

The water phase product was analyzed by *nuclear magnetic resonance* (*NMR*) to determine structures of the compounds. According to NMR results shown in Figure 4.27, the peaks primarily come at early resonance, which possibly indicates some aliphatic or ether. Compared to Sensoz and Kaynar (2006), the main spectra is exhibited between 1.5–2.5 ppm, which possibly indicatesCH_3–, CH_2–, or CH_α–bonded to aromatic ring. Spectra between 3–4 ppm are also observed, which may represent a ring methylene group joined with two aromatic rings. A small amount of compounds at 0.5–1.5 ppm is also detected, which probably corresponds to CH_3–, CH_2–, or CH_α– that was removed from aromatic rings..

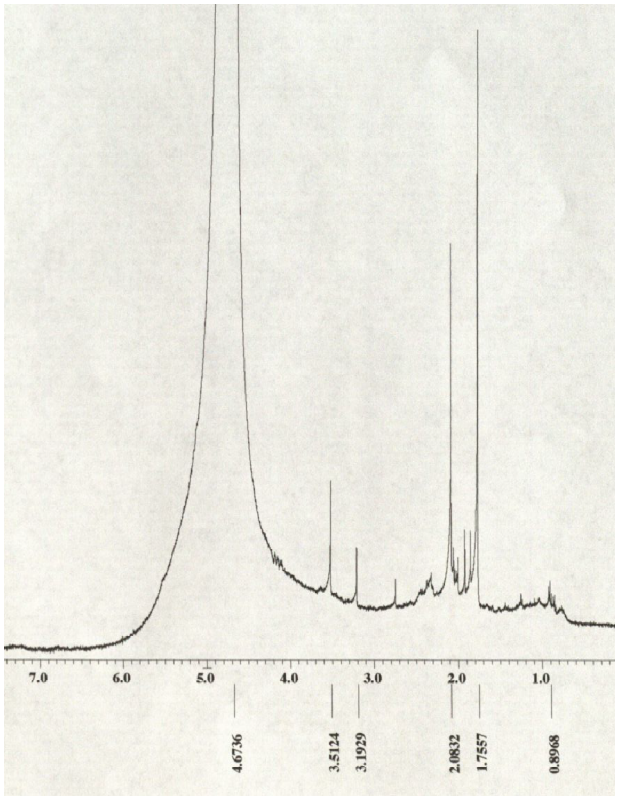

Figure 4.27 NMR spectra of water phase product

CHAPTER 5

ENERGY CALCULATION

Energy recovery is an important issue in order to specify an efficiency of a conversion process. An energy balance for the pyrolysis system used in this research is shown in Figure 5.1. Energy inputs include the energy contained in raw feedstocks, as well as electricity used to heat the pyrolysis system. Energy outputs include energy contained in products, as well as heat losses. Each of these inputs and outputs will now be discussed in turn.

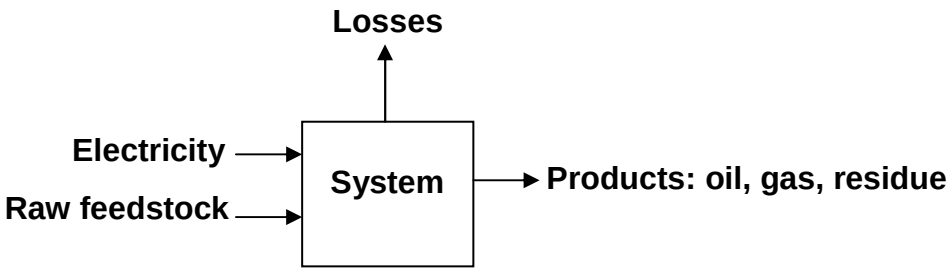

Figure 5.1 Diagram of energy balance

5.1 Energy Contained in Raw Feedstocks

Generally, a heating value of a fuel is reported as a higher heating value (HHV) or gross calorific value, which represents the heat produced from combustion of the fuel with water as a product. According to Sheng and Azevedo (2005), a standard method to evaluate the HHV of the fuel is by bomb calorimeter. This is complicated and time-consuming because of the experimental set up and calculation steps. Consequently, researchers have established another easier and cheaper method of HHV estimation by using either proximate or ultimate analysis.

A proximate analysis calculates the HHV of the fuel based on volatile matter and fixed carbon, while an ultimate analysis uses the data of main elemental compositions in the fuel including carbon, hydrogen, nitrogen, and oxygen. However, Sheng and Azevedo (2005) and Yin (2011) indicated that the ultimate analysis provides more accurate HHV than the proximate analysis after they conducted statistical studies of different HHV formulas derived from both ultimate and proximate analysis, and then compared the estimates with the actual HHV of various kinds of biomass.

There are numerous empirical equations of that related HHV to elemental compositions, which have been developed from previous studies. Sheng and Azevedo (2005) evaluated different biomass HHV equations from literatures (Dimerbas (1997), Tillman (1978), Institute of Gas Technology (1978), Graboski and Bain (1981), Annamalai et al. (1987), Channiwala and Parikh (2002), and Jenkins and Ebeling (1985)), including their own model. They compared the calculated HHV based on those equations to the observed data, then validated the equations using three statistical parameters: average error of the correlation (*AAE*), average bias error of the correlation (*ABE*), and correlation coefficient (R^2). Eventually, they suggested that their equation (Eq. 5.1) obtained the best fit with the highest R^2 of about 0.834, but the smallest *AAE* and *ABE*. They stated that the variation in biomass content significantly influences the HHV, resulting in low R^2. In addition, they noticed a relationship between the HHV and carbon and hydrogen content, with an increase in the contents leading to higher HHV. In contrast, there is insignificant trend between oxygen and the HHV.

HHV (MJ/kg) = -1.3675 + 0.3137*C* + 0.7009*H* + 0.0318*O* (Eq. 5.1, Sheng and Azevedo (2005))

Friedl et al. also (2005) proposed an HHV model (Eq. 5.2) after they applied an ordinary least squares regression (OLS) and a partial least squares regression (PLS) to estimate HHV of

122 biomass samples including energy glass, wood material, cereals, millet, sunflower, hemp, and other plant materials. Besides, they verified the model by comparing the theoretical to experimental data, and reported an R^2 of 0.935. The most recent study on HHV of biomass belongs to Yin (2011), in which he included the equations from two previous studies as well as developed his own model, shown in Eq. 5.3. The correlation between the predicted and experimental HHV was defined based on 44 biomass types, which showed a good accuracy of R^2 = 0.9976, with relatively low *AAE* and *ABE*. Consequently, Yin's HHV equation is applied in this study in order to estimate HHV of the raw feedstocks. Results are given in Table 1.

HHV (kJ/kg) = $3.55C^2 - 232C - 2230H + 51.2C \times H + 131N + 20{,}600$ (Eq. 5.2, Friedl et al. (2005))

HHV (MJ/kg) = $0.2949C + 0.8250H$ (Eq. 5.3, Yin (2011))

where HHV = higher heating value, (kJ/kg or MJ/kg)

C = carbon content, % wt.

H = hydrogen content, % wt.

O = oxygen content, % wt.

N = nitrogen content, % wt.

5.2 Energy of Input Electricity

An external electric heater supplies input energy to drive the process. In this study, a conservative assumption is used to estimate the power. It is assumed that the power supply (800 J/s) is continuously applied to the process for the entire length of time, which is 90 minutes. However, this is not precise since in the actual process the heating system is controlled by the PID controller, which sends a signal to a relay to switch the heater on or off based on a set heating rate. Thus, the actual energy input could be considerable less. Values for electricity input energy are given in Table 5.1.

5.3 Energy Output in Products

Yin's equation (5.3) was used to estimate the energy contained in the oil and residue products (HHV). For gases, only combustible gases including CH_4, H_2, and CO were taken into account for the calculation. Each gas has its own HHV, which are 141.8, 55.53, and 10.1 MJ/kg for H_2, CH_4, and CO, respectively (Bhattacharjee, 1998-2012). The total HHV of gaseous product are estimated based on an average percent weight from the whole process. The HHV values for products are shown in Table 5.1. It should be noted that the HHV of gas and residue produced from pyrolysis of the pure plastic are excluded since the amount is insignificant. Later, the HHV of each product is multiplied by its distribution fraction to obtain an overall HHV of total product as demonstrated in Eq. 5.4. As the ratio of the plastic increases, the HHV of the product is obviously higher, which mainly comes from an increase in HHV of the oil, while the gas and residue HHV remains the same.

$$HHV_{product,total} = (HHV_{oil} * \%wt._{oil}) + (HHV_{residue} * \%wt._{residue}) + (HHV_{gas} * \%wt._{gas}) \qquad \text{(Eq. 5.4)}$$

5.4 Heat Losses

Another important consideration of the energy balance is energy losses due to the heat dissipated to environment. Major heat dissipations in this process are from material used for the reactor and the insulator surrounding the system. According to the second law of thermodynamics, equilibrium between the system and its surroundings must be reached; therefore, a large portion of the power input was consumed by the reactor, insulation, and losses to the surrounding air.

5.5 Summary of Energy Inputs, Outputs, and Recovery

The total energy recovery via this process is categorized into two types. The ideal energy recovery defined as the ratio of energy contained in products to energy contained in the raw feedstock (Eq. 5.5) whereas the non ideal energy recovery defined as the ratio of energy contained in products to energy inputs (Eq. 5.6) are shown in Table 5.1, along with the energy inputs and outputs.

$$\text{Estimated Ideal Energy Recovery} = HHV_{product,\ total}/HHV_{raw\ feedstock} \quad \text{(Eq. 5.5)}$$

$$\text{Estimated Non-Ideal Energy Recovery} = HHV_{product,\ total}/(HHV_{raw\ feedstock} + \text{Electricity}) \quad \text{(Eq. 5.6)}$$

Table 5.1 Energy Inputs, Outputs, and Recovery for the Pyrolysis System

Feedstock	Energy Inputs (MJ/kg)		Energy Outputs (MJ/kg)				Estimated Ideal Energy Recovery	Estimated Non-Ideal Energy Recovery
	Raw feedstock material	Electricity	Products					
			Bio-oil	Residue	Gas	Total		
Sargassum	13.3	61.7	0.84	7.46	2.51	10.8	81.2	14.4
Recycled pellet	29.7		30.1	negligible	negligible	30.1	101	32.9
5% plastic	14.1		1.75	6.67	2.63	11.1	78.7	14.6
15% plastic	15.7		3.67	6.21	2.76	12.6	80.3	16.3
25% plastic	17.4		6.36	5.59	2.52	14.5	83.3	18.3
33% plastic	18.7		9.62	5.05	2.50	17.2	92.0	21.4

The energy recovery fraction increases as the plastic ratio increases due to higher HHV of the oil. This study exhibits much lower energy recovery compared to Lu (2007), and Mullen et al. (2005). Lu (2007) evaluated an energy performance of rice husk pyrolysis by comparing the energy consumed during the process combined with the energy of the feedstock to the energy contained in products, including gases, oil, and charcoal. He demonstrated that approximately 86% of the energy was converted into products. Mullen et al. (2005) similarly calculated the energy recovery from pyrolysis of corn cob and corn stover; the latter exhibits less efficiency (74%) than the former (76%).

One of the reasons for the low energy recovery in this study is the high surface area per volume ratio. In reactor design, it is ideal to maximize the reactor volume while keeping the surface area small. Since heat flow rate of the system is a function of the surface area, minimizing the surface area can reduce the heat flow across the reactor wall, thereby reducing the heat loss. Another reason for the heat loss is due to heat convection occurring inside the reactor. As the gas flows along the wall toward the output, some of the energy absorbed by the gas is then carried outside with the gas; according to the second law of thermodynamics, more energy intake was needed to replace this energy loss due to heat convection. Finally, energy is used to convert water from liquid phase to vapor. As the reaction created a gas water shift reaction, water was produced inside the reactor; energy was then spent to vaporize the water as the temperature was raised beyond the water boiling point.

If this pyrolysis process were to be scaled up to be applied commercially, the reactor design would be changed from the one used in the laboratory. A design that minimized heat losses would be used, which would increase the fraction of energy inputs that results in products.

.

CHAPTER 6

CONCLUSIONS AND RECOMMENDATIONS

6.1 Conclusions

- According to this study, the optimum temperature for *Sargassum* pyrolysis is 600^{o}C, because it yields the maximum oil. Therefore, the co-pyrolysis between the seaweed and the PS pellet was carried out at 600^{o}C. The pyrolysis process results in much higher carbon and hydrogen content in oil product, but lower in oxygen than the raw material. However, the process yields a relatively low amount of the oil phase, while generating a high amount of the water phase due to high oxygen content of the original feedstock.
- To illustrate the differences between terrestrial and aquatic biomass, the cedar wood was pyrolyzed to compare with the seaweed at the same condition. Even though the seaweed starts decomposing earlier, the wood yields a higher amount of oil, which corresponds to the results from thermogravimetric analysis, indicating that wood contains higher volatile matter. However, they both show a comparable oil quality.
- The polystyrene pellet alone has up to 90% conversion to oil product, which contains primarily aromatic hydrocarbons including styrene and its oligomers, as stated in other literatures. The oil is rich in carbon, but low oxygen as expected from original feedstock.
- The consequence of the interaction between the two feedstocks was observed in this study; however, instead of increasing the oil phase, co-pyrolysis increased the water phase. On the other hand, the co-pyrolysis improved the oil quality, compared to oil produced from *Sargassum* alone, by lowering the oxygen content while raising the carbon content. As a result, the heating value of the oil is higher. As the fraction of polystyrene included in the co-pyrolysis increases, the oil quality improves, and is similar to the oil from pure plastic.

- In the interaction between the biomass and the polymer, the biomass impacts the polymer, and the polymer impacts the biomass, resulting in differences in product quantity and quality. Based on the literature, the interaction can potentially be explained as follows. The biomass decomposition produces a solid residue, which is relatively reactive and becomes a source of radicals. The biomass radicals assist the chain scission process of the polymer, resulting in light liquid product and generation of hydrogen radicals. Since the seaweed has high oxygen content, the hydrogen radicals provoke water elimination from the hydroxyl group of the biomass. Thus, there is an increase in water production. In parallel, the elimination of water reduces the oxygen content of the oil phase, which improves oil quality. The water elimination reaction possibly occurs at a higher rate than the oil producing reactions; hence, there is lower oil yield, as reported by others.
- Besides, the synergistic effect is also noticed in the thermogravimetric analysis of the mixture which shift the decomposition temperature associated with the plastic to higher degree, and it is claimed to be responsible for more chain scission of the polymer which induced by the biomass.
- Methane gas production from co-pyrolysis is higher than the theoretical prediction, which possibly resulted from the water gas shift reaction, which yielded water and syngas product.
- The residues obtained from both pure seaweed and mixtures exhibit similar elemental compositions excepted for hydrogen content. There is still a large amount of oxygen observed in the residues, and a significant amount of nitrogen, which leads to low heating value and nitrogen oxide emissions, respectively. Consequently, the residue is not suitable used as a solid fuel. However, it could possibly be applied to soil as a nutrient source for plants.
- The estimated percent recovery for the laboratory pyrolysis experiments ranged from 14-32%, which increased as the plastic ratio increased since the heating value of the oil is increased. The low energy recovery is caused by various factors such as high surface area

to volume ratio of the reactor, heat convection, and the latent heat of the phase changes. An improved version of the laboratory reactor, with less heat losses, would be used in a scaled-up commercial process.

6.2 Recommendations

- According to this study, the low quality and quantity of bio-oil from macroalgae is a main problem. Besides, the algae oil contains rather high nitrogen content, which could contribute to nitrogen oxide emissions if it is used as a fuel. Even though co-pyrolysis with PS pellets improved the oil quality, the quantity did not increase as expected. This was perhaps due to the low hydrogen content of the polymer. Consequently, other co-pyrolysis studies with various types of high hydrogen content polyolefins should be carried out.
- The water phase product should be further characterized since the co-pyrolysis tends to produce more water soluble compounds which possibly are valuable.
- Seaweed pre-treatment by acid or water should be applied in further studies to investigate whether it increases oil yield, since the pre-treatment should help reduce the mineral and ash content in the seaweed.
- The process should be improved to achieve higher energy recovery. For example, a larger scale reactor should be developed to minimize the high surface area to volume ratio of the reactor which is causing a large heat loss across the surface, then resulting in low energy recovery. Moreover, the system with gas recirculation can be designed in order to diminish the heat loss carried by the exiting gas. Another reasonable way to improve the process is to utilize the energy from an exothermic reaction resulted from the decomposition of the seaweed. Therefore, further kinetic studies and the amount of heat release from the seaweed should be clearly defined in order to use it efficiently.

REFERENCES

1. Aboulkas, A., El Harfi, K., El Bouadili, A., Nadifiyine, M., Benchanaa, M., and Mokhlisse, A. (2009). “Pyrolysis kinetics of olive residue/plastic mixtures by non-isothermal thermogravimetry.” *Fuel Processing Technology, 90*, 722-728.

2. Aboulkas, A., El Harfi, K., Nadifiyine, M., and El Bouadili, A. (2008). “Thermogravimetric characteristics and kinetic of co-pyrolysis of olive residue with high density polyethylene.” *Journal of Thermal Analysis and Calorimetry, 91*(3), 737-743.

3. Adams, J.M.M., Ross, A.B., Anastasakis, K., Hodgson, E.M., Gallaher, J.A., Jones, J.M., and Donnison, I.S. (2011). “Seasonal variation in the chemical composition of the bioenergy feedstock Laminaria digitata for themochemical conversion.” *Bioresource Technology*, *102*, 226-234.

4. Aguiar, L., Marquez-Montesinos, F., Gonzalo, A., Sanchez, J.L., and Arauzo, J. (2008). “Influence of temperature and particle size on the fixed bed pyrolysis of orange peel *residues*.” *Journal of Analytical and Applied Pyrolysis, 83*, 124-130.

5. American Chemistry Council. (2005-2009). “Take a closer look at today’s polystyrene packaging.” http://www.americanchemistry.com/s_ACC/sec_article.asp?CID=65&DID= 7213& dowhat =&css=print, accessed on Januray 15, 2011

6. Anantharaman, P., Karthikaidevi, G., Manivannan, K., Thirumaran, G., and Balasubramanian, T. (2010). “Mineral composition of marine macroalgae from Mandapam coastal regions; southeast coast of India.” *Recent Research in Science and Technology*, *2*(10), 66-71.

7. Anastasakis, K., Ross, A.B., and Jones, J.M. (2011). “Pyrolysis behaviour of the main carbohydrates of brown macro-algae.” *Fuel, 90*, 598-607.

8. Andriamanantoanina, H., and Rinaudo, M. (2010). “Characterization of the alginates from five madagascan brown algae.” *Carbohydrate Polymers*, *82*, 555-560.

9. Apaydin-Varol, E., Putun, E., and Putun, A.E. (2007). “Slow pyrolysis of pistachio shell.” *Fuel, 86*, 1892-1899.

10. Arana, J.M., and Mazzoco, R.R. (2010). “Adsorption studies of methylene blue and phenol onto black stone cherries prepared by chemical activation.” *Journal of Hazardous Materials, 180*, 656-661.

11. ASTM. (2011a). “ASTM D2887-08: Standard test method for boiling range distribution of petroleum fractions by gas chromatography.” Annual book of ASTM standards section five: petroleum products, lubricants, and fossil fuels vol.05.01.

12. ASTM. (2011b). “ASTM D3860-98: Standard practice for determination of adsorptive capacity of activated carbon by aqueous phase isotherm technique.” Annual book of ASTM standards section fifteen: general products, chemical specialties, and end use products vol.15.01.

13. ASTM. (2011c). “ASTM D5291-10: Standard test methods for instrumental determination of carbon, hydrogen, and nitrogen in petroleum products and lubricants.” Annual book of ASTM standards section five: petroleum products, lubricants, and fossil fuels vol.05.02.

14. Astrup, T., and Bilitewski, B. (2011). “Pyrolysis and gasification,” *Solid waste technology & management vol.1*, Christensen, T., ed., A John Wiley and Sons, Ltd, United Kingdom.

15. Ates, F. and Isikdag, M.A. (2008). “Evaluation of the role of the pyrolysis temperature in straw biomass samples and characterization of the oils by GC/MS.” *Energy & Fuels*, *22*, 1936-1943.

16. Awad, N.E., Motawe, H.M., Selim, M., A., Matloub, A.A. (2009). “Antitumourigenic polysaccharides isolated from the brown algae, Padina pavonia (L.) Gaill. and Hydroclathrus clathratus (C. Agardh) Howe.” *Medicinal and Aromatic Plant Science and Biotechnology*, *3*(1), 6-11.

17. Aydinli, B., and Caglar, A. (2010). “The comparison of hazelnut shell co-pyrolysis with polyethylene oxide and previous ultra-high molecular weight polyethylene.” *Journal of Analytical and Applied Pyrolysis*, *87*, 263-268.

18. Azapagic, A., Emsley, A., and Hamerton, I. (2003). *Polymers, the Environment and Sustainable Development,* John Wiley & Sons, Ltd., England.

19. Bae, Y.J., Ryu, C., Jeon, J., Park, J., Suh, D.J., Suh, Y., Chang, D., and Park, Y. (2011). “The characteristics of bio-oil produced from the pyrolysis of three marine macroalgae*.” Bioresource Technology, 102*, 3512-3520.

20. Balat, M., Balat, M., Kirtay, E., and Balat, H. (2009). “Main routes for the thermo-conversion of biomass into fuels and chemicals. Part 1: pyrolysis systems.” *Energy Conversion and Management, 50*, 3147-3157.

21. Banerjee, K., Ghosh, R., Homechaudhuri, S., and Mitra, A. (2009). “Biochemical composition of marine macroalgae from Gangetic Delta at the apex of bay of Bengal.” *African Journal of Basic & Applied Sciences*, *1*(5-6), 96-104.

22. Bates, B.C., Z.W. Kundzewicz, S. Wu and J.P. Palutikof, Eds. (2008). “Climate Change and Water.” Technical Paper of the Intergovernmental Panel on Climate Change, IPCC Secretariat, Geneva.

23. Berrueco, C., Ceamanos, J., Esperanza, E., and Mastral, J.F. (2004). “Experimental study of co-pyrolysis of polyethylene/sawdust mixtures.” *Thermal Science, 8*(2), 65-80.

24. Bhattacharjee, S. (1998- 2012). “Heating values of common fuels.” http://energy.sdsu.edu/testhome/Test/solve/basics/tables/tablesComb/hhv.html, accessed on March 15, 2012.

25. Biagini, E., Barontini, F., and Tognotti, L. (2006). “Devolatilization of biomass fuels and biomass components studied by TG/FTIR technique.” *Industrial & Engineering Chemistry Research, 45*, 4486-4493.

26. Bird, M.I., Wurster, C.M., Silva, P.H., Bass, A.M., and Nys, R. (2011). “Algal biochar – production and properties.” *Bioresource Technology, 102*, 1886-1891.

27. Biron, M. (2007). *Thermoplastics and Thermoplastic Composites*, Elsevier Ltd., United Kingdom.

28. Blasi, C.D., Branca, C., and Galgano, A. (2010). “Biomass screening for the production of furfural via thermal decomposition.” *Industrial & Engineering Chemistry Research*, *49*, 2658-2671.

29. Bold, H.C., and Wynne, M.J. (1978). *Introduction to the Algae, Structure and Reproduction*, Prentice-Hall, New Jersey.

30. Brebu, M., Ucar, S., Vasile, C., and Yanik, J. (2010). “Co-pyrolysis of pine cone with synthetic polymers.” *Fuel, 89*, 1911-1918.

31. Bridgwater, A.V., Czernik, S., and Piskorz, J. (2002). “The status of biomass fast pyrolysis.” Fast pyrolysis of biomass: A handbook volume 2, A.V. Bridgwater, ed., CPL Press Liberty House, UK.

32. Bridgwater, A.V., Meier, D., and Radlein, D. (1999). “An overview of fast pyrolysis of biomass.” *Organic Geochemistry*, *30*, 1479-1493.

33. Brown, R.C., and Holmgren, J. (2000). “Fast pyrolysis and bio-oil upgrading.” http://www.ars.usda.gov/sp2UserFiles/Program/307/biomasstoDiesel/RobertBrown& JenniferHolmgrenpresentationslides.pdf, accessed on January 15, 2011

34. Caglar, A., and Aydinli, B. (2009). “Isothermal co-pyrolysis of hazelnut shell and ultra-high molecular weight polyethylene: the effect of temperature and composition on the amount of pyrolysis products.” *Journal of Analytical and Applied Pyrolysis*, *86*, 304-309.

35. Cao, Q., Jin, L., Bao, W., and Lv, Y. (2009). “Investigations into characteristics of oils produced from co-pyrolysis of biomass and tire.” *Fuel Processing Technology, 90*, 337-342.

36. Carlsson, A.S., Beilen, J.B., Moller, R., and Clayton, D. (2007). “Micro-and Macro- algae: utility for industrial applications.” Bowles, D., ed., CPL Press, United Kingdom.

37. Cho, M., Jung, S., and Kim, J. (2010). “Pyrolysis of mixed plastic wastes for the recovery of benzene, toluene, and xylene (BTX) aromatics in a fluidized bed and chlorine removal by applying various additives.” *Energy & Fuels*, *24*, 1389-1395.

38. Chun, Y., Sheng, G., Chiou, C.T., and Xing, B. (2004). “Compositions and Sorptive properties of crop residues-derived chars.” *Environmental Science & Technology, 38(17)*, 4649-4655.

39. Clarens, A.F., Resurreccion, E.P., White, M.A., and Colosi, L.M. (2010). “Environmental life cycle comparison of algae to other bioenergy feedstocks.” *Environmental Science & Technology*, *44*, 1813-1819.

40. Clean Up Australia Ltd. (2009). “Plastic Recycling Fact Sheet.” http://www.cleanup.org.au/PDF/au/cua_plastic_recycling_fact_sheet.pdf, accessed June 26, 2011.

41. Davis, T.A., Llanes, F., Volesky, B., and, Mucci, A. (2003a). “Metal selectivity of *Sargassum* spp. and their alginates in relation to their α-L-guluronic acid content and conformation.” *Environmental Science & Technology*, *37*, 261-267.

42. Davis, T.A., Volesky, B., and Mucci, A. (2003b). “A review of the biochemistry of heavy metal biosorption by brown algae.” *Water Research*, *37*, 4311-4330.

43. Demirbas, A. (2001). “Biomass resource facilities and biomass conversion processing for fuels and chemicals.” *Energy Conversion and Management*, *42*, 1357-1378.

44. Demirbas, A. (2002). “Analysis of liquid products from biomass via pyrolysis.” *Energy Source*, *24*, 337-345.

45. Demirbas, A. (2005). “Potential applications of renewable energy sources, biomass combustion problems in boiler power systems and combustion related environmental issues.” *Progress in Energy and Combustion Science*, *31*, 171-192.

46. Demirbas, A. (2006). “Effect of temperature on pyrolysis products from four nut shells.” *Journal of Analytical and Applied Pyrolysis, 76*, 285-289.

47. Demirbas, A. (2010). “Use of algae as biofuel sources.” *Energy Conversion and Management*, *51*, 2738-2749.

48. Devarenne, T. (2010). “Agrilife scientists do groundwork for genetic mapping of algae biofuel species: Botryococcus braunii algae contributed to existing petroleum deposits.” Bio/Bio news, Department of Biochemistry and Biophysics, Texas A&M University. http://biochemistry.tamu. edu/bb/chapters/news/newsletters/bbnews201004.pdf, accessed December 24, 2011.

49. European Manufacturers of Expanded Polystyrene (EUMEPS). (2002). “Building a better environment with EPS.” http://www.eumeps.org/show.php?ID=4469&psid=hmotjteo, accessed June 26, 2011.

50. Fichtner Consulting Engineers Ltd. (2004). “The viability of advanced thermal treatment of MSW in the UK.” The Environmental Services Training and Education Trust (ESTET), London, United Kingdom.

51. Fox, J.M. (2008). “Alternative Uses of *Sargassum*.” Proceedings from *Sargassum* Symposium 2008, http://www.sargassum.org/Proceedings2008/ Proceedings, accessed June 26, 2011.

52. Friedl, A., Padouvas, E., Rotter, H., and Varmuza, K. (2005). “Prediction of heating values of biomass fuel from elemental composition.” *Analytica Chimica Acta, 554*, 191-198.

53. Gani, A., and Naruse, I. (2007). “Effect of cellulose and lignin content n pyrolysis and combustion characteristics for several types of biomass.” *Renewable Energy, 32*, 649-661.

54. Gao, Y., Gregor, C., Liang, Y., Tang, D., and Tweed, C. (2009). “Algae Biodiesel: A feasibility report.” http://humanities.uchicago.edu/orgs/institute/bigproblems/Team1-1209.pdf, accessed on January 15, 2011

55. Garcia-Perez, M., Wang, X., Shen, J., Rhodes, M., Tian, F., Lee, W., Wu, H., and Li, C. (2008). “Fast pyrolysis of oil mallee woody biomass: effect of temperature on the yield and quality of pyrolysis products.” *Industrial & Engineering Chemistry Research*, *47*, 1846-1854.

56. Graham, L.E., and Wilcox, L.W. (2000). *Algae*, Prentice Hall, Inc. New Jersey.

57. Gu, R., Lee, O., and Salehzadah, Y. (2010). “An Investigation into Polystyrene Recycling at UBC.” Dawn Mills, APSC 262, The University of British Columbia.

58. Hajaligol, M., Waymack, B., and Kellogg, D. (2001). “Low temperature formation of aromatic hydrocarbon from pyrolysis of cellulosic materials.” *Fuel, 80*, 1799-1807.

59. Heo, H.S., Park, H.J., Park, Y., Ryu, C., Suh, D.J., Suh, Y., Yim, J., and Kim, S. (2010). “Bio-oil production from fast pyrolysis of waste furniture sawdust in a fluidized bed.” *Bioresource Technology*, *101*, S91-S96.

60. Hui, Z., Huaxiao, Y., Ming, L., Congwang, Z., and Song, Q. (2011). “Pyrolytic characteristics and kinetics of the marine green tide macroalgae, Enteromorpha prolifera.” *Chinese Journal of Oceanology and Limnology*, *29*(5), 996-1001.

61. Islam, M.N., Islam, M.N., Beg, M.R.A., and Islam, M.R. (2005). “Pyrolytic oil from fixed bed pyrolysis of municipal solid waste and its characterization.” *Renewable Energy*, *30*, 413-420.

62. Jakab, E., Blazso, M., and Faix, O. (2001). “Thermal decomposition of mixtures of vinyl polymers and lignocellulosic materials.” *Journal of Analytical and Applied Pyrolysis, 58-59*, 49-62.

63. Ji-lu, Z. (2007). “Bio-oil from fast pyrolysis of rice husk: yields and related properties and improvement of the pyrolysis system.” *Journal of Analytical and Applied Pyrolysis, 80*, 30-35.

64. Jung, S., Kang, B., and Kim, J. (2008). “Production of bio-oil from rice straw and bamboo sawdust under various reaction conditions in a fast pyrolysis plant equipped with a fluidized bed and char separation system.” *Journal of Analytical and Applied Pyrolysis*, *82*, 240-247.

65. Kang, B., Lee, K., Park, H., Park, Y., and Kim, J. (2006). “Fast pyrolysis of radiata pine in a bench scale plant with a fluidized bed: influence of a char separation system and reaction conditions on the production of bio-oil.” *Journal* of Analytical and *Applied Pyrolysis, 76, 32-37.*

66. Karaduman, A. (2002). “Pyrolysis of polystyrene plastic wastes with some organic compounds for enhancing styrene yield.” *Energy resource, 24*, 667-674.

67. Karaduman, A., Simsek, E.H., Cicek, B., and Bilgesu, A.Y. (2001). “Flash pyrolysis of polystyrene wastes in a free-fall reactor under vacuum.” *Journal of Analytical and Applied Pyrolysis, 60*, 179-186.

68. Kim, S., and Kim, S. (2004). “Pyrolysis characteristics of polystyrene and polypropylene in a stirred batch reactor.” *Chemical Engineering Journal, 98*, 53–60.

69. Kumar, A., Wang, L., Dzenis, Y.A., Jones, D.D., and Hanna M.A. (2008). “Thermogravimetric characterization of corn stover as gasification and pyrolysis feedstock.” *Biomass and Bioenergy, 32*, 460-467.

70. Lardon, L., Helias, A., Sialve, B., Steyer, J., and Bernard, O. (2009). “Life-cycle assessment of biodiesel production from microalgae.” *Environmental Science & Technology*, *43*(17), 6475-6481.

71. Lazarevic, D., Aoustin, E., Buclet, N., and Brandt, N. (2010). “Plastic waste management in the context of a European recycling society: Comparing results and uncertainties in a life cycle perspective. ” *Resources, Conservation and Recycling*, *55*, 246-259.

72. Lee, C., Cho, Y., Song, P., Kang, Y., Kim, J., and Choi, M. (2003). “Effects of temperature distribution on the catalytic pyrolysis of polystyrene waste in a swirling fluidized-bed reactor.” *Catalysis Today, 79-80*, 453-464.

73. Lee, K., Kang, B., Park, Y., and Kim, J. (2005). “Influence of reaction temperature, pretreatment, and a char removal system on the production of bio-oil from rice straw by fast pyrolysis, using a fluidized bed.” *Energy & Fuels*, *19*, 2179-2184.

74. Levinton, J.S. (1995). *Marine Biology Function, Biodiversity, Ecology*, Oxford University Press, Inc., New York.

75. Lev-on, M. (2009). “The future of sustainable energy technologies.” The Magazine for Environmental Manager, Air and Waste Management Association.

76. Lewis, D.H., and Smith, D.C. (1967). “Sugar alcohols (polyols) in fungi and green plants I. distribution, physiology and metabolism.” *New Phytolgist*, *66*(2), 143-184.

77. Li, D., Chen, L., Yi, X., Zhang, X., and Ye, N. (2010). “Pyrolytic characteristics and kinetics of two brown algae and sodium alginate.” *Bioresource Technology*, *101*, 7131-7136.

78. Li, D., Chen, L., Zhang, X., Ye, N., and Xing, F. (2011). “Pyrolytic characteristics and kinetic studies of three kinds of red algae.” *Biomass and Bioenergy, 35*, 1765-1772.

79. Lin, Y., and Tanaka, S. (2006). “Ethanol fermentation from biomass resources: current state and prospect.” *Applied Microbiology and Biotechnology*, *69*, 627-642.

80. Liu, Y., Qian, J., and Wang, J. (2000). “Pyrolysis of polystyrene waste in a fluidized-bed reactor to obtain styrene monomer and gasoline fraction.” *Fuel Processing Technology, 63*, 45-55.

81. Lopez, A., Marco, I., Caballero, B.M., Laresgoiti, M.F., and Adrados, A. (2010). “Pyrolysis of municipal plastic wastes: Influence of raw material composition.” *Waste Management*, *30*, 620-627.

82. Luo, Z., Wang, S., Liao, Y., Zhou, J., Gu, Y., Cen, K. (2004). “Research on biomass fast pyrolysis for liquid fuel.” *Biomass and Bioenergy*, *26*, 455-462.

83. Mahakhant, A., Chansawang, N., Kunyalung, W., Khantasopa, S., Srinorakutara, T., Burapatana, V., and Kangvansaichol, K. (2010). “R&D on microalgae for sustainable energy at TISTR.” *7th Biomass Asia Workshop*, Jakarta, Indonesia.

84. Manivannan, K., Thirumaran, G., Devi, G.K., Hemalatha, A., and Anantharaman, P. (2008). “Biochemical composition of seaweeds from Mandapam coastal regions along southeast coast of India.” *American-Eurasian Journal of Botany*, *1* (2), 32-37.

85. Mansfield, E., Kar, A., Quinn, T.P., and Hooker, S.A. (2010). “Quartz crystal microbalances for microscale thermogravimetric analysis.” *Analytical Chemistry*, *82*, 9977-9982.

86. Marano, J.J., and Ciferno, J.P. (2001). “Life-cycle greenhouse-gas emissions inventory for Fischer-Tropsch fuels.” Prepared for U.S. Department of Energy, National Energy Technology Laboratory, by Energy and Environmental Solutions, LLC.

87. Marin, N., Collura, S., Sharypov, V.I., Beregovtsova, N.G., Baryshnikov, S.V., Kuznetsov, B.N., Cebolla, V.L., and Weber, J.V. (2002). “Co-pyrolysis of wood biomass and synthetic

polymer mixtures. Part II: characterization of the liquid phases." *Journal of Analytical and Applied Pyrolysis, 65*, 41-55.

88. Marinho-Soriano, E., Fonseca, P.C., Carneiro, M.A.A., Moreira, W.S.C. (2006). "Seasonal variation in the chemical composition of two tropical seaweeds." *Bioresource Technology*, *97*, 2402-2406.

89. Mckendry, P. (2002). "Energy production from biomass (part 2): conversion technologies." *Bioresource Technology*, *83*, 47-54.

90. Miao, X., Wu, Q., and Yang, C. (2004). "Fast pyrolysis of microalgae to produce renewable fuels." *Journal of Analytical and Applied Pyrolysis*, *71*, 855-863.

91. Moreno-Pirajan, J.C., Gomez-Cruz, R., Garcia-Cuello, V.S., and Giraldo, L. (2010). "Binary system Cu(II)/(Pb(II) adsorption on activated carbon obtained by pyrolysis of cow bone study." *Journal of Analytical and Applied Pyrolysis*, *89*, 122-128.

92. Mullen, C.A., Boateng, A.A., Goldberg, N.M., Lima, I.M., Laird, D.A., and Hicks, K.B. (2010). "Bio-oil and bio-char production from corn cobs and stover by fast pyrolysis." *Biomass and Bioenergy, 34*, 67-74.

93. Murakami, K., Yamaguchi, Y., Noda, K., Fujii, T., Shinohara, N., Ushirokawa, T., Sugawa-Katayama, Y., and Katayama, M. (2011). "Seasonal variation in the chemical compostion of a marine brown alga, *Sargassum horneri* (Turner) C. Agardh." *Journal of Food Composition and Analysis*, *24*, 231-236.

94. Murugaiyan, K., and Sivakumar, K. (2008). "Seasonal variation in elemental composition of *Stoechospermum marginatum* (Ag.) Kutz and *Sargassum wightii* (Greville Mscr.) J.G. Agardh in relation to chemical composition of seawater." *Colloids and Surfaces B: Biointerfaces*, *64*, 140-144.

95. National Energy Technology Laboratory (NETL). (2006). "Fluidized bed applications and validation." R&D079, U.S. Department of Energy. http://www.netl.doe.gov/ publications/ factsheets/rd/R%26D079.pdf, accessed on December, 24, 2011.

96. Oasmaa, A., and Czernik, S. (1999). "Fuel oil quality of biomass pyrolysis oils-state of the art for the end users." , *Energy & Fuels*, *13*, 914-921.

97. Oasmaa, A., Solantausta, Y., Arpiainen, V., Kuoppala, E., and Sipila, K. (2010). "Fast pyrolysis bio-oils from wood and agricultural residues." *Energy & Fuels*, *24*, 1380-1388.

98. Onwudili, J.A., Insura, N., and Williams, P.T. (2009). "Composition of products from the pyrolysis of polyethylene and polystyrene in a closed batch reactor: effects of temperature and residence time." *Journal of Analytical and Applied Pyrolysis, 86*, 293-303.

99. Pan, P., Hu, C., Yang, W., Li, Y., Dong, L., Zhu, L., Tong, D., Qing, R., and Fan, Y. (2010). "The direct pyrolysis and catalytic pyrolysis of *Nannochloropsis* sp. Residue for renewable bio-oils." *Bioresource Technology*, *101*, 4593-4599.

100. Paradela, F., Pinto, F., Gulyurtlu, I., Cabrita, I., and Lapa, N. (2009). “Study of the co-pyrolysis of biomass and plastic wastes.” *Clean Technologies* and *Environmental Policy*, *11*, 115-122.

101. Park, H.J., Dong, J., Jeon, J., Park, Y., Yoo, K., Kim, S., Kim, J., and Kim, S. (2008). “Effects of the operating parameters on the production of bio-oil in the fast pyrolysis of Japanese larch.” *Chemical Engineering Journal, 143*, 124-132.

102. Park, H.J., Park, Y., Dong, J., Kim, J., Jeon, J., Kim, S., Kim, J., Song, B., Park, J., and Lee, K. (2009). “Pyrolysis characteristics of oriental white oak: kinetic study and fast pyrolysis in a fluidized bed with an improved reaction system.” *Fuel Processing Technology, 90*, 186-195.

103. Park, J.J., Park, K., Kim, J., Maken, S., Song, H., Shin, H., Park, J., and Choi, M. (2003). “Characterization of styrene recovery from the pyrolysis of waste expandable polystyrene.” *Energy & Fuels, 17*, 1576-1582.

104. Pena-Rodriguez, A., Mawhinney, T.P., Ricque-Marie, D., and Cruz-Suarez, L.E. (2011). “Chemical composition of cultivated seaweed Ulva clathrata (Roth) C. Agardh.” *Food Chemistry, 129*, 491-498.

105. Peng, W., Wu, Q., Tu, P., and Zhao, N. (2001). “Pyrolytic characteristics of microalgae as renewable energy source determined by thermogravimetric analysis.” *Bioresource Technology, 80*, 1-7.

106. PerkinElmer, Inc. (2005-2010a). “Award-Winning Results -- 2400 Series II CHNS/O Elemental Analysis.” http://www.perkinelmer.com/CMSResources/Images/44-74386BRO_2400Series IICHNSOelementalAnalyzer.pdf, accessed on January 14, 2012

107. PerkinElmer, Inc. (2005-2010b). “PerkinElmer 2400 Series II CHNS/O Elemental Analyzer operation manual.”

108. Pinto, F., Costa, P., Gulyurtlu, I., and Cabrita, I. (1999). “Pyrolysis of plastic wastes. 1. Effect of plastic waste composition on product yield.” *Journal of Analytical and Applied Pyrolysis, 51*, 39-55.

109. Piskorz, J., Peacocke, G.V.C., and Bridgwater, A.V. (2003). “IEA pyrolysis fundamentals review.” Fast pyrolysis of biomass: A handbook volume 1, A. Bridgwater, S. Czernik, J. Diebold, D. Meier, A. Oasmaa, C. Peacocke, J. Piskorz, and D. Radlein, eds., CPL Press Liberty House, UK.

110. Polystyrene Packaging Council (PSPC). (2011). “Polystyrene is a plastic.” http://www.polystyrenepackaging.co.za/educationalinformation.htm, , accessed December 9, 2011.

111. Purdue University, Radiological and Environmental Management. (2012). “Scanning Electron Microscope, scanning electron microscope diagram (Diagram courtesy of Iowa State University.” http://www.purdue.edu/rem/rs/sem.htm, accessed on January 14, 2012.

112. Quantachrome Corporation. (2011). “Autosorb® iQ automated gas sorption analyzer”. http://www.quantachrome.com/gassorption/autosorb_iq.html, accessed on January 14, 2012

113. Restek Corporation. (2012a). “MXT®-500 SimDist Column.” http://www.restek.com/catalog/view/599, accessed on January 14, 2012

114. Restek Corporation. (2012b). “Natural Gas ShinCarbon ST (micropacked).” http://www.restek. com/ chromatogram/view/GC_PC00672/shincarbon, accessed on January 14, 2012

115. Ringer, M., Putsche, V., and Scahill, J. (2006). “Large-scale pyrolysis oil production: A technology assessment and economic analysis.” Report No. NREL/TP-510-37779, National Renewable Energy Laboratory (NREL), U.S. Department of Energy.

116. Rioux, L.-E., Turgeon, S.L., and Beaulieu, M. (2007). “Characterization of polysaccharides extracted from brown seaweeds.” *Carbohydrate Polymers, 69*, 530-537.

117. Ross, A.B., Anastasakis, K., Kubacki, M., and Jones, J.M. (2009). “Investigation of pyrolysis behavior of brown algae before and after pre-treatment using PY-GC/MS and TGA.” *Journal of Analytical and Applied Pyrolysis, 85*, 3-10.

118. Ross, A.B., Jones, J.M., Kubachi, M.L., and Bridgeman, T. (2008). “Classification of macroalgae as fuel and its thermochemical behaviour.” *Bioresource Technology, 99*, 6494-6504.

119. Rutkowski, P. (2009). “Influence of zinc chloride addition on the chemical structure of bio-oil obtained during co-pyrolysis of wood/synthetic polymer blends.” *Waste Management, 29*, 2983-2993.

120. Rutkowski, P., and Kubacki, A. (2006). “Influence of polystyrene addition to cellulose on chemical structure and properties of bio-oil obtained during pyrolysis.” *Energy Conversion and Management, 47*, 716-731.

121. Sara Shields, S., and Boopathy, R. (2011). “ Ethanol production from lignocellulosic biomass of energy cane.” *International Biodeterioration & Biodegradation, 65*, 142-146.

122. Scott, R.P.W. (2009). “Physical chemistry resource: book 5. Thermal analysis.” http:// physicalchemistryresources.com/Book5_sections/TA_introductionHTML_1.htm, accessed on Febuary 10, 2011

123. Sensoz, S. (2003). “Slow pyrolysis of wood barks from Pinus brutia Ten. and product compositions.” *Bioresource Technology, 89*, 307-311.

124. Sensoz, S., and Kaynar, I. (2006). “Bio-oil production from soybean (Glycine max L.); fuel properties of bio-oil.” *Industrial Crops and Products, 23*, 99-105.

125. Seo, D.K., Park, S.S., Hwang, J., and Yu, T. (2010). “Study of the pyrolysis of biomass using thermo-gravimetric analysis (TGA) and concentration measurements of the evolved species.” *Journal of Analytical and Applied Pyrolysis, 89*, 66-73.

126. Sharypov, V.I., Beregovtsova, N.G., Kuznetsov, B.N., Membrado, L., Cebolla, V.L., Marin, N., and Weber, J.V. (2003). “Co-pyrolysis of wood biomass and synthetic polymers mixtures. Part III: characterization of heavy products.” *Journal of Analytical and Applied Pyrolysis, 67*, 325-340.

127. Sharypov, V.I., Marin, N., Beregovtsova, N.G., Baryshnikov, S.V., Kuznetsov, B.N., Cebolla, V.L., and Weber, J.V. (2002). “Co-pyrolysis of wood biomass and synthetic polymer mixtures. Part I: influence of experimental conditions on the evolution of solids, liquids, and gases.” *Journal of Analytical and Applied Pyrolysis, 64*, 15-28.

128. Shen, J., Wang, X., Garcia-Perez, M., Mourant, D., Rhodes, M., and Li, C. (2009). “Effects of particle size on the fast pyrolysis of oil mallee woody biomass.” *Fuel, 88*, 1810-1817.

129. Sheng, C., and Azevedo, J.L.T. (2005). “Estimating the higher heating value of biomass fuels from basic analysis data.” *Biomass and Bioenergy, 28*, 499-507.

130. Siddiqui, M.N., and Redhwi, H.H. (2009). “Pyrolysis of mixed plastics for the recovery of useful products.” *Fuel Processing Technology, 90*, 545-552.

131. Styrotrade. (2004). “polystyrene chemistry.” http://www.styrotrade.cz/en/on-polystyrene/, accessed December, 9, 2011.

132. TA Instruments. (2011). “Thermogravimetric Analysis: Q600.” http://www. tainstruments.com/ pdf/brochure/sdt.pdf, accessed on March 11, 2011.

133. Thomas, D. (2002). Seaweeds, the Smithsonian Institution Press in association with The Natural History Museum, London.

134. U.S. Department of Energy (DOE). (2011). “Is bioenergy truly renewable?” http://www1.eere. energy.gov/biomass/biomass_basics_faqs.html#biofuels, accessed on February 20, 2011.

135. U.S. Energy Information Administration (EIA). (2011a). “Renewable Energy Consumption and Electricity Preliminary Statistics 2010.” http://www.eia.gov/renewable/ annual/preliminary/, accessed on December, 24, 2011.

136. U.S. Energy Information Administration (EIA). (2011b). “What are the largest sources of total greenhouse gas emissions by sector for the United States?” http://www.eia.gov/tools/ faqs/ faq. cfm?id=75&t=11, accessed on December 24, 2011.

137. U.S. Environmental Protection Agency (EPA). (2009). “Municipal solid waste generation, recycling, and disposal in the United States: Detailed tables and figures for 2008.” Office of Resource Conservation and Recovery.

138. U.S. Environmental Protection Agency (EPA). (2011). “Plastics.” http://www.epa.gov/ epawaste/conserve/materials/plastics.htm, accessed on January 15, 2011.

139. Ucar, S., and Karagoz, S. (2009). “The slow pyrolysis of pomegranate seeds: the effect of temperature on the product yields and bio-oil properties.” *Journal of Analytical and Applied Pyrolysis, 84*, 151-156.

140. United Nations Environmental Programme (UNEP). (2009). “Converting waste plastics into a resource, Compendium of Technologies.” Division of Technology, Industry and Economics International Environmental Technology Centre Osaka/Shiga, Japan

141. Walsh, M.P. (2004-2006). “Properties of fuels.” http://www.walshcarlines.com/ pdf/fueltable.pdf, accessed on January 15, 2011.

142. Wang, J., Wang, G., Zhang, M., Chen, M., Li, D., Min, F., Chen. M., Zhang, S., Ren, Z., Yan, Y. (2006). “A comparative study of thermolysis characteristics and kinetics of seaweeds and fir wood.” *Process Biochemistry, 41*, 1883-1886.

143. Wang, L., Min, M., Li, Y., Chen, P., Chen, Y., Liu, Y., Wang, Y., and Ruan, R. (2010). “Cultivation of Green Algae Chlorella sp. in Different Wastewaters from Municipal Wastewater Treatment Plant.” *Applied Biochemistry and Biotechnology, 162*, 1174–1186.

144. Wang, P., Zhan, S., Yu, H., Xue, X., and Hong, N. (2010). “The effects of temperature and catalysts on the pyrolysis of industrial wastes (herb residue).” *Bioresource Technology, 101*, 3236-3241.

145. Wang, S., Jiang, X.M., Han, X.X., and Liu, J.G. (2009). “Combustion characteristics of seaweed biomass. 1. Combustion characteristics of Enteromorpha clathrata and *Sargassum Natans*.” *Energy & Fuels, 23*, 5173-5178.

146. Wang, S., Jiang, X.M., Wang, N., Yu, L.J., Li, Z., and He, P.M. (2007). “Research on pyrolysis characteristics of seaweed.” *Energy & Fuels, 21*, 3723-3729.

147. Weiss, T.L., Johnston, J.S., Fujisawa, K., Sumimoto, K., Okada, S., Chappell, J., and Devarenne, T. P. (2010). “Phylogenetic placement, genome size, and GC content of the liquid-hydrocarbon-producing green microalga Botryococcus braunii strain Berkeley (Showa) (Chlorophyta).” *Journal of Phycology, 46, 534-540.*

148. Westerhout, R., Koningsbruggen, M., Van Der Ham, A., Kuipers, J., and Van Swaaij, W. (1998). “Techno-economic evaluation of high temperature pyrolysis processes for mixed plastic waste.” *Trans IChemE, 76*, part A, 427-439.

149. Williams, E.A., and Williams, P.T. (1997). “The pyrolysis of individual plastics and a plastic mixture in a fixed bed reactor.” *Journal of Chemical Technology & Biotechnology, 70*, 9-20.

150. Williams, P.T. (2005). Waste Treatment and Disposal, John Wiley & Sons, Ltd., England.

151. Williams, P.T., and Bagri, R. (2004). “Hydrocarbon gases and oils from the recycling of polystyrene waste by catalytic pyrolysis.” *International Journal of Energy Research, 28*, 31-44.

152. Williams, P.T., and Slaney, E. (2007). “Analysis of products from the pyrolysis and liquefaction of single plastics and waste plastic mixtures.” *Resources, Conservation, and Recycling, 51*, 754-769.

153. Winslow, J., and Schmetz, E. (2009). “Direct Coal Liquefaction Overview.” Leonardo Technologies, Inc., presented to National Energy Technology Laboratory (NETL).

154. Yehlow, J., and Dalager, S. (2011). “Incineration: flue gas cleaning and emissions,” Solid waste technology & management vol.1, Christensen, T., ed., A John Wiley and Sons, Ltd, United Kingdom.

155. Yin, C. (2011). “Prediction of higher heating values of biomass from proximate and ultimate analysis.” *Fuel, 90*, 1128-1132.

156. Yu, L.J., Wang, S., Jiang, X.M., Wang, N., and Zhang, C.Q. (2008). “Thermal analysis studies on combustion characteristics of seaweed.” *Journal of Thermal Analysis and Calorimetry, 93*(2), 611-617.

157. Zhang, L., Xu, C., and Champagne, P. (2010). “Overview of recent advances in thermo-chemical conversion of biomass.” *Energy Conversion and Management, 51*, 969-982.

158. Zhou, L., Wang, Y., Huang, Q., and Cai, J. (2006). “Thermogravimetric characteristics and kinetic of plastic and biomass blends co-pyrolysis.” *Fuel Processing Technology, 87*, 963-969.

BIOGRAPHICAL INFORMATION

Ketwalee Kositkanawuth was born on July 28, 1983, in Bangkok, Thailand. She graduated with a Bachelor's degree in Environmental Engineering (B.Eng) from Chulalongkorn University, Thailand in 2005. Then, she decided to pursue a master's degree in Environmental Engineering at University of Texas at Arlington (UTA), and completed a Master of Engineering in Civil Engineering (M.Eng) in 2007. Later, she continued with the Doctoral degree in the same major, and the same school under the direction of Dr. Melanie L. Sattler and Dr. Brian H. Dennis at UTA. Her research focuses on developing a liquid fuel from biomass through a thermal conversion process.